_ _ _ _ _ _ _ _ _ _ _ _ _ _ _ _ _ _ _ _ _ _ _ _ _ _ _ _ _ _ _ _ _ _ _ _ _ _ _ _ _ _ _ _ _

# Zinc in diatom frustules: a proxy for bioavailable zinc in surface waters

_ _ _ _ _ _ _ _ _ _ _ _ _ _ _ _ _ _ _ _ _ _ _ _ _ _ _ _ _ _ _ _ _ _ _ _ _ _ _ _ _ _ _ _ _

Jaccard, Thomas

UNIVERSITÉ DE GENÈVE         FACULTE DES SCIENCES
Département de géologie et paléontologie    Dr. D. Ariztegui
Institut F.-A. Forel

UNIVERSITÉ DE MONTRÉAL        DÉPARTEMENT DE CHIMIE
Laboratoire de chimie biologique et analytique    Prof. K. J. Wilkinson

# Zinc In Diatom Frustules:

# A Proxy For Bioavailable Zinc In Surface Waters

## THÈSE

Présentée à la Faculté des Sciences de l'Université de Genève

pour obtenir le grade de Docteur ès sciences, mention interdisciplinaire

par

**Thomas Jaccard**

de

Les Clées (Vaud)

**Thèse No 4042**

GENÈVE

…

2008

La Faculté des sciences, sur le préavis de Messieurs, D. ARIZTEGUI, docteur et directeur de thèse (Département géologie & paléontologie, Institut F.A. Forel), K. J. WILKINSON, professeur et codirecteur de thèse (Université de Montréal, Laboratoire de chimie biologique et analytique, Montréal, Québec, Canada), W. WILDI, professeur ordinaire (Département de géologie et paléontologie, Institut F.A. Forel) et de Mesdames S. SPEZZAFERRI, docteur (Université de Fribourg, Département de géosciences, Fribourg, Suisse) et F. SYLVESTRE, docteur (Institut de Recherches pour le Développement, Centre Européen de Recherche et d'Enseignement des Géosciences de l'Environnement, Europôle Méditerranéen de l'Arbois, Aix-en-Provence, France), autorise l'impression de la présente thèse, sans exprimer d'opinion sur les propositions qui y sont énoncées.

Genève, le 12 décembre 2008

**Thèse - 4042 -**

Le Doyen Jean-Marc TRISCONE

# Table of contents

# Abstract

In spite of significant progress in the development and calibration of new proxies, major challenges still limit our ability to use these indicators to fully understand past environmental changes.

Over the past two decades, both field and laboratory experiments have shed light on the importance of trace metals in controlling –through limitation or toxicity - the growth and composition of phytoplankton communities. Nonetheless, there is still a lack of reliable tools to evaluate trace metals–phytoplankton interactions during past environmental and climatic perturbations.

In this work, we evaluated the use of the Zn content of silicate shells (frustules) of fossil diatoms to track past changes in Zn bioavailable concentrations of surface waters. This essential element is delivered to both continental and ocean waters via natural and/or anthropogenic inputs. Our approach combined laboratory and field experiments.

In the first part (Chapter 2), incorporation of Zn into the frustule of the freshwater diatom *Stephanodiscus hantzschii* was evaluated from Zn uptake experiments. Zn concentrations in the frustule were related to the $Zn^{2+}$ concentrations in the growth medium and positively correlated with intracellular concentrations of this element. The data were interpreted to indicate that the presence of Zn in the frustule might reflect encapsulation of a Zn-bearing macromolecule in the silica during frustule formation.

In a second part (Chapter 3), these results, in concert with measurements on fossil frustules isolated from a sedimentary core, were used to reconstruct changes in biovailable Zn concentrations in surface water of Lake Geneva throughout the recent past. The fair agreement between the reconstructed modern concentrations and instrumental data attested the reliability of the proxy. The downcore results indicated that the heavy anthropogenic input of Zn to the lake during the sixties and the seventies led to an increase in Zn uptake by phytoplankton. The extrapolated concentrations were nonetheless likely not high enough to have induced adverse effects on the pelagic community.

In a last effort to test the proxy, the methodology was applied to marine sediments in order to reconstruct past changes in Zn delivery and availability to phytoplankton of the Southern Ocean during last ice age (Chapter 4). The observed variations were consistent with a mechanism by which, during the last glacial maximum, massive meltwater discharges - resulting from melting icebergs - supplied Zn to surface waters. Additional data indicated that these meltwater events stimulated biological productivity and could consequently further contribute to the sequestration of $CO_2$ during ice ages.

Finally, laboratory and field data suggested that this proxy could provide a valuable tool to study past Zn-phytoplankton interactions.

# Résumé

## Introduction

L'inquiétude suscitée par les signes ubiquistes de changements environnementaux et l'appréhension d'un futur incertain dans un monde plus chaud ont éveillé un grand intérêt envers les sciences climatiques et environnementales. Cet engouement fut confirmé par l'attribution du prix Nobel de la paix au GIEC (groupe d'experts intergouvernemental sur l'évolution du climat) et à Al Gore l'année passée (2007) pour récompenser "leurs efforts visant à renforcer et propager la prise de conscience des changements climatiques dus à l'homme, et jeter les bases de mesures nécessaires pour contrer de tels changements". Une avancée significative dans la compréhension de ces changements est liée à l'utilisation de modèles numériques permettant de simuler l'évolution à long terme de la Terre. Le développement de tels outils requiert toutefois une bonne connaissance des systèmes climatiques et environnementaux et des différents phénomènes qui sont en mesure des les influencer. Comme nous disposons de données "instrumentales" seulement pour les dernières 150 années environ, les informations sur la sensibilité et la réponse de notre planète face à différents changements doivent être étudiés dans le passé géologique. En d'autres termes, une lecture attentive des archives naturelles (ou reconstructions paleo-environnementales) nous permet de tester nos hypothèses sur les causes des changements actuels.

# Les sédiments lacustres comme archives naturelles

## Enregistrements continus de haute résolution

Les sédiments lacustres accumulent du matériel produit dans la colonne d'eau (autochtone) et provenant du bassin versant (allochtone). Une carotte sédimentaire lacustre peut donc fournir des informations continues aussi bien sur les processus prenant place dans le lac que dans son bassin versant. Les taux d'accumulation de sédiment de ces systèmes terrestres (par opposition aux systèmes marins) sont en général élevés; Ils fournissent donc l'opportunité de travailler à haute résolution temporelle. Il est courant, pour obtenir des reconstructions plus robustes, de combiner ces données sédimentaires avec des archives historiques ou des données instrumentales collectées dans la région. En plus de fournir l'opportunité de travailler à haute résolution, les lacs, de par leur petite taille, sont beaucoup plus sensibles aux changements environnementaux et climatiques que les systèmes marins. Leurs sédiments offrent donc la possibilité unique de mettre en évidence et d'étudier les variations rapides et abruptes.

## Extraction de l'information contenue dans les sédiments: les "proxies"

Les mesures "directes" n'étant évidemment pas possibles dans un monde qui n'existe plus, les reconstructions paleo-environnementales reposent sur des approximations ou mesures indirectes qu'on appelle des "proxies". Ces indicateurs sont des paramètres qui peuvent êtres mesurés dans les sédiments et qui ont répondu de manière systématique aux variations d'un paramètre donné (par exemple, la température, la salinité, etc…). Ces proxies peuvent être de type biologique (influence des variables environnementales sur la succession des différentes espèces) ou géochimique (réponse des conditions physique/chimique du sédiment face à des changements environnementaux). Avant de pouvoir être utilisés, ces outils doivent avoir subi une calibration. Cette étape consiste à comprendre et à identifier les différents paramètres qui influencent le proxy. En d'autres termes, avant d'utiliser un proxy, il est essentiel de

comprendre et d'évaluer comment – et jusqu'à quel point – le signal mesuré traduit les variations d'un paramètre environnemental donné. Cette étape est en général accomplie à partir d'observations effectuées dans l'environnement moderne.

### Défis futurs

En dépit de progrès significatifs dans le développement et la calibration de nouveaux proxies, nos connaissances ne nous permettent toujours pas, à l'heure actuelle, de reconstruire de manière adéquate certains paramètres environnementaux clés. Ceci est par exemple le cas pour l'évaluation du rôle joué par les métaux traces sur le phytoplancton.

## Phytoplancton et métaux traces

Les métaux traces jouent un rôle important sur la composition et la croissance de la communauté du phytoplancton (Morel et al., 2003). Ces métaux peuvent être essentiels (Fe, Mn, Zn, Cu, Co, Mo et Ni) ou, au contraire, inhibiteurs (Pb, Ag, Hg,…). Parmis les nutriments, certains deviennent toutefois toxiques à concentrations élevées (Cu, Zn et Ni).

### Prise en charge des métaux traces et spéciation chimique

Les membranes cellulaires étant pratiquement imperméables aux composés chargés ou polaires, la prise en charge de métal par la cellule doit être effectuée via des transporteurs spécialisés. Pour interagir avec l'organisme, le métal doit d'abord être transporté vers la cellule, puis, dans un deuxième temps, réagir avec les sites présents sur la surface extérieure de la membrane. À ce stade, l'ion métallique peut soit se dissocier du transporteur et réintégrer le milieu, soit être transporté à l'intérieur de la

cellule (ces processus sont mis en évidence dans la figure A). Ce phénomène complexe de prise en charge a été étudié en appliquant des modèles cinétiques et thermodynamiques aux données récoltées lors d'expériences en laboratoire durant lesquelles la spéciation des métaux est contrôlée de manière rigoureuse et systématique. Ces expériences ont montré qu'en général, le phénomène de prise en charge n'est pas gouverné par la concentration totale de métal, mais par la fraction de l'ion libre ou d'espèces labiles inorganiques (pour plus de détails, se référer à Slaveykova and Wilkinson, 2005). Par conséquent, la spéciation chimique des métaux joue un rôle important dans leur interaction avec les micro-organismes.
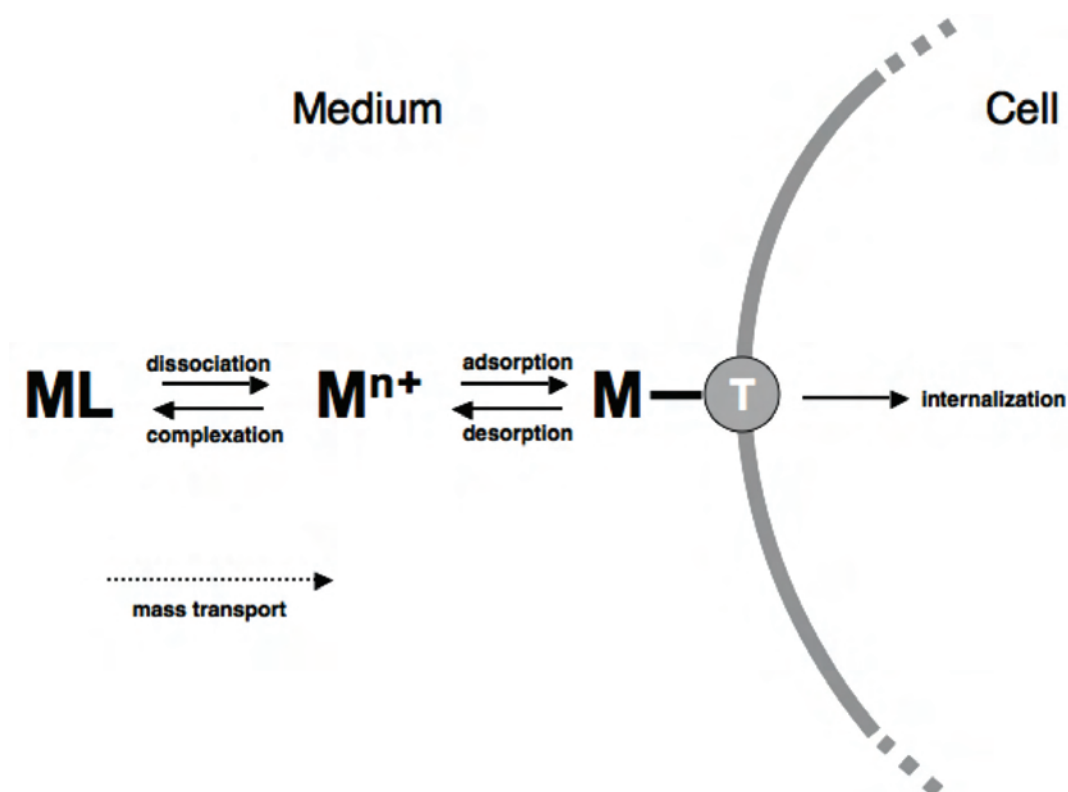


**Figure A** Modèle conceptuel mettant en évidence les principaux processus physico-chmiques impliqués dans la prise en charge d'un métal par un micro-organisme aquatique (d'après Slaveykova et Wilkinson 2005).

**Reconstruction des interactions phytoplancton-métaux traces**

En dépit d'un intérêt croissant dans le domaine de la "chimie aquatique bio-inorganique", nous n'avons toujours pas, à l'heure actuelle, d'outil adéquat pour étudier les interactions métaux traces – phytoplancton dans le passé. La complexité du processus de prise en charge (discuté ci-dessus) limite fortement l'utilisation de la concentration totale en métal du sédiment pour évaluer ces interactions. Le défi consiste à pouvoir relier des analyses faites sur le sédiment aux concentrations biodisponibles passées.

## Objectifs et vue d'ensemble de l'étude

Dans cette étude, nous avons évalué la possibilité d'utiliser de la teneur en Zn des tests siliceux (frustules) de diatomées fossiles pour reconstruire les concentrations de Zn biodisponible des eaux de surface. L'approche utilisée se décline en trois parties et combine calibration en laboratoire avec une diatomée d'eau douce (chapitre 2) et reconstructions à partir de diatomées fossiles isolées de carottes sédimentaires lacustre (chapitre 3) et marine (chapitre 4).

**Incorporation de Zn dans le frustule de la diatomée d'eau douce *Stephanodiscus hantzschii***

Des expériences de prise en charge de Zn ont été conduites avec la diatomée d'eau douce *Stephanodiscus hantzschii* pour étudier le phénomène d'incorporation de Zn dans les frustules. Les données mettent en évidence la relation entre la concentration de $Zn^{2+}$ (ion libre) dans le milieu expérimental et le Zn incorporé dans les frustules - donné sous la forme du rapport molaire Zn/Si du frustule - (figure B). Ces données confirment les résultats obtenus par Ellwood et Hunter (2000) sur la diatomée marine *Thalassiosira pseudonana*.
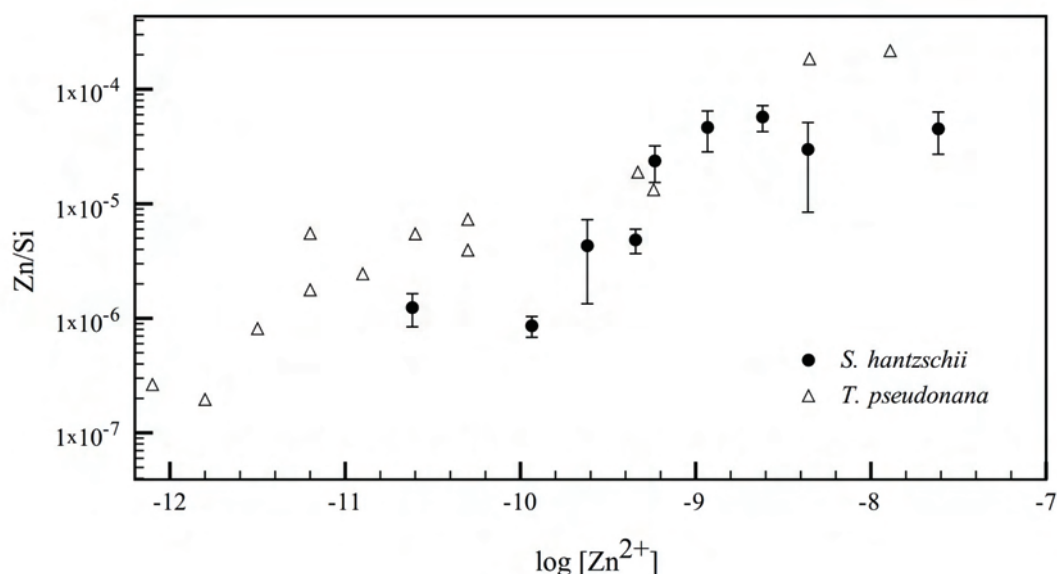
**Figure B** Rapport molaire Zn/Si des frustules en fonction de la concentration de $Zn^{2+}$ du milieu expérimental pour la diatomée d'eau douce *S. hantzschii* (cercles remplis). Les barres d'erreur représentent des intervalles de confiance à 95%. Les données des expériences menées sur la diatomée marine *T. pseudonana* (Ellwood and Hunter 2000) sont représentées par les triangles.

La forte corrélation obtenue entre la teneur en Zn des frustules, Zn/Si, et le Zn intracellulaire, $Zn_{cell}$, indique que le Zn est transféré au frustule à partir de compartiments internes (figure C). Les résultats obtenus lors d'expériences supplémentaires étudiant le rôle de Si et de Mn sur l'incorporation de Zn nous ont amenés à proposer un nouveau mécanisme: l'incorporation de Zn dans les frustules se ferait via l'association du Zn avec une macromolécule qui serait co-précipitée avec la silice lors de la formation du frustule.
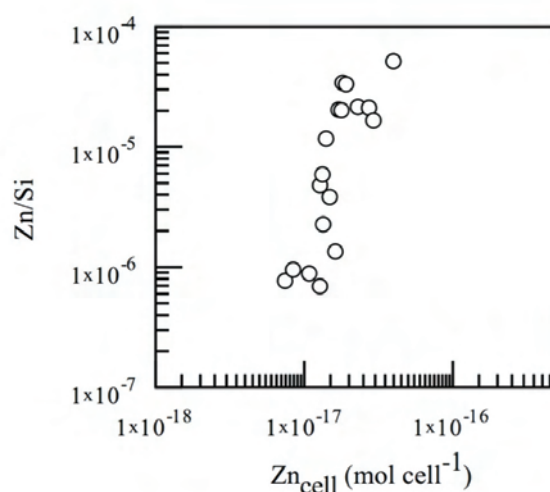


**Figure C** Rapport molaire Zn/Si des frustules en fonction du Zn intracellulaire $Zn_{cell}$. L'association de ces deux variables est caractérisée par un coefficient de spearman, rs, de 0.87.

## Évaluation des variations historiques de Zn biodisponible à partir d'un enregistrement terrestre de $(Zn/Si)_{opal}$
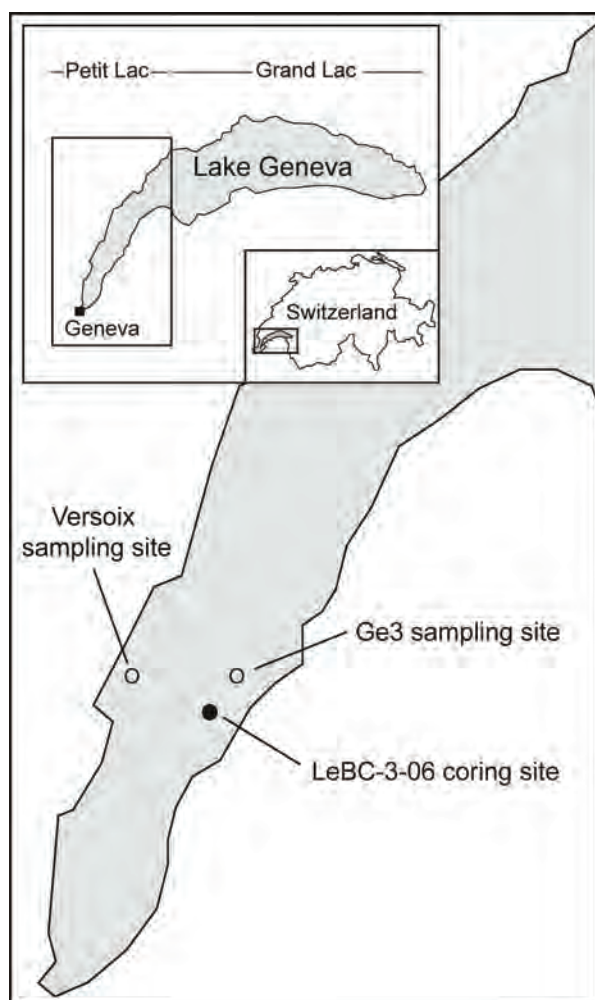


**Figure D** Emplacement du site de carottage LEBC-3-06

Dans ce deuxième volet, les résultats de l'expérience de prise en charge, combinés avec des mesures sur des échantillons de diatomées fossiles isolées d'une carotte sédimentaire (carte dans la figure D), nous ont permis de reconstruire les variations de Zn biodisponible des eaux de surface du Léman pour le passé récent. Les valeurs de $(Zn/Si)_{opal}$ mesurées sur les échantillons fossiles (où l'indice "opal" fait référence à la forme de silice hydratée constituant les frustules fossiles) sont en accord avec les valeurs obtenues en laboratoire sur *Stephanodiscus hantzschii* (1er volet de l'étude; discuté ci-dessus), une diatomée représentative des assemblages du Léman (figure E) ainsi qu'avec les données instrumentales disponibles.

Les reconstructions indiquent que l'augmentation anthropique des apports de Zn au cours des années soixante et septante s'est traduite par une prise en charge plus élevée de ce métal par le phytoplancton. Les concentrations n'étaient toutefois pas assez élevées pour induire des effets néfastes sur la communauté pélagique.
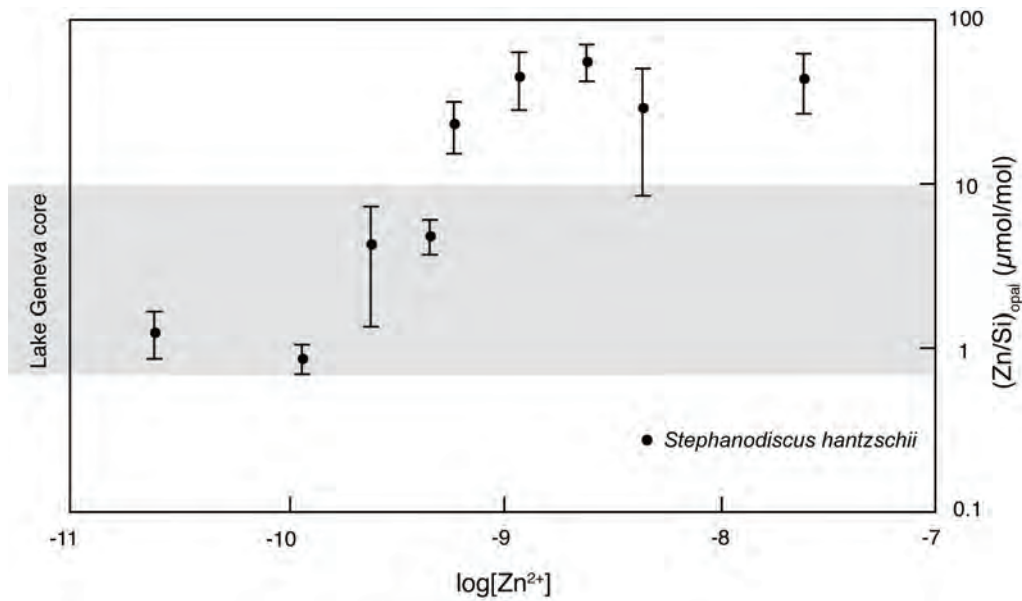
**Figure E** (Zn/Si)$_{opal}$ en fonction de la concentration de Zn$^{2+}$ du milieu expérimental pour la diatomée d'eau douce *S. hantzschii*. La surface grise indique la gamme de valeurs mesurées dans les diatomées fossiles du Léman (carotte LEBC-3-06).

## Productivité biologique et biodisponibilité des micronutriments dans les eaux de l'Océan Austral durant la dernière période glaciaire.

Dans cette dernière partie, nous avons appliqué notre indicateur à des sédiments marins provenant du secteur antarctique de l'Océan Austral (site RC13-259; figure F) recouvrant la dernière période glaciaire.
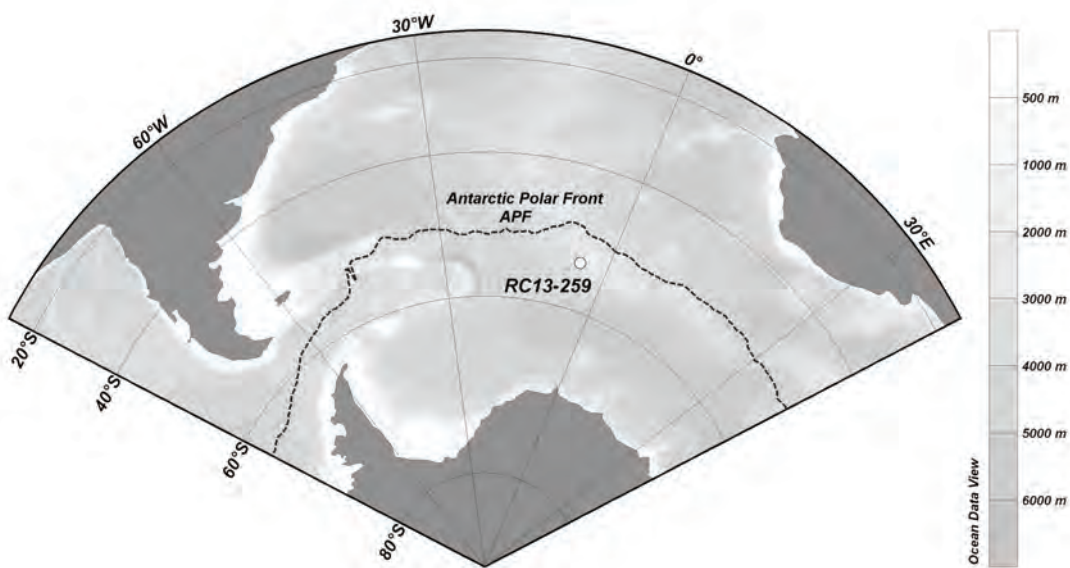


**Figure F** Carte de l'Atlantique Austral avec l'emplacement du site RC13-259. La ligne en traitillés délimite le front polaire antarctique (APF; Antarctic Polar Front).

Nos résultats, combinés avec d'autres indicateurs, (Figure G) nous ont permis de mettre en évidence un mécanisme par lequel, durant le dernier maximum glaciaire, des débâcles massives d'icebergs ont, via leurs eaux de fontes, relâché du Zn dans les eaux de surface. De plus, les données indiquent que ces événements ont stimulé la productivité biologique et auraient, par conséquent, pu contribuer à séquestrer du $CO_2$ dans l'océan durant les périodes glaciaires.
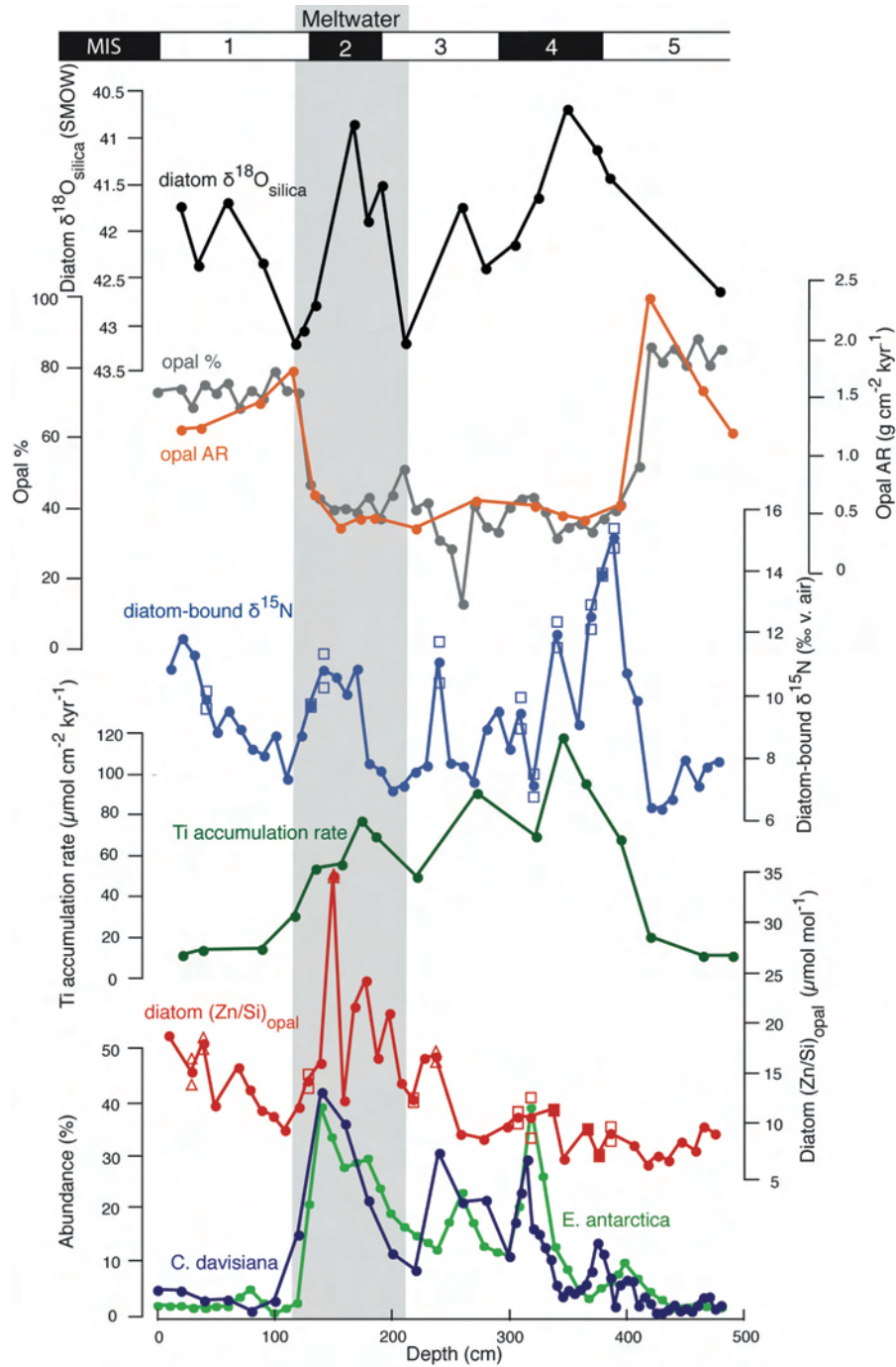
## Conclusion

La possibilité d'utiliser la concentration en Zn des frustules de diatomées fossiles pour reconstruire les variations passées de Zn biodisponible dans les eaux de surface a été évaluée au cours de ce travail.

Les mécanismes contrôlant l'incorporation de Zn dans les frustules ont été étudiés lors d'expériences de prise en charge de Zn par la diatomée d'eau douce *Stephanodiscus hantzschii*. Les résultats indiquent que la concentration de Zn dans les frustules est corrélée de manière positive à la concentration intracellulaire et représentative de la concentration en $Zn^{2+}$ du milieu expérimental. La présence de Zn dans les frustules a été interprétée comme émanant de l'association du Zn avec une macromolécule qui serait co-précipitée avec la silice lors de la formation du frustule.

Les concentrations de Zn biodisponible des eaux de surface du Léman reconstruites à partir d'analyses sur des échantillons fossiles sont en accord avec les données instrumentales disponibles et indiquent que les apports anthropiques élevés de Zn durant les années soixante et septante ont donné lieu à une augmentation de prise en charge de ce métal par le phytoplancton.

Finalement, des mesures sur des échantillons de l'Océan Austral, nous ont permis de mettre en évidence, pour la première fois, une augmentation de la biodisponibilité de micronutriments durant le dernier maximum glaciaire. Ces mesures associées à d'autres indicateurs suggèrent que des débâcles massives d'icebergs ont, via leurs eaux de fontes, relâché du Zn dans les eaux de surfaces. Ces événements ont vraisemblablement stimulé la productivité biologique et auraient, par conséquent, pu contribuer à séquestrer du $CO_2$ dans l'océan durant les périodes glaciaires.

Au final, cette étude qui combine données de laboratoire et de terrain, montre que le proxy étudié peut fournir un outil adéquat pour étudier les interactions entre le zinc et le phytoplancton dans le passé.

---

◁ **Figure G** Profils de la carotte sédimentaire RC13-259: $\delta^{18}O_{silica}$(Shemesh *et al.,* 1994) en noir, concentration d'opal (Charles et al., 1991) en gris et taux d'accumulation d'opal normalisé (avec Th) en orange, "diatom-bound $\delta^{15}N$" en bleu, taux d'accumulation de Ti normalisé (avec Th) en vert foncé (Latimer and Filippelli, 2001), $(Zn/Si)_{opal}$ en rouge et abondances de *C. davisiana* et *E. antarctica* (Shemesh *et al.*, 1994) en bleu foncé et vert clair respectivement en fonction de la profondeur. Le modèle d'âge (MIS; Marine Isotopic Stages) est basé sur les données de Charles *et al.* (1991). La période durant laquelle les eaux de surfaces ont subi des injections massives d'eau de fontes est mise en évidence en gris.

# Références

Charles C. D., Froelich P. N., Zibello M. A., Mortlock R. A., and Morley J. J. (1991) Biogenic opal in Southern Ocean sediments over the last 450,000 years: Implications for surface water chemistry and circulation. *Paleoceanography* **6**, 697-728.

Ellwood M. J. and Hunter k. A. (2000) The incorporation of zinc and iron into the frustule of the marine diatom *Thalassiosira pseudonana. Limnol. Oceanogr.* **45**(7), 1517-1524.

Latimer J. C. and Filippelli G. M. (2001) Terrigenous input and paleoproductivity in the Southern Ocean. *Paleoceanography* **16**(6), 627-643.

Morel F. M. M., Milligan A. J., and Saito M. A. (2003) Marine bioinorganic chemistry: The role of trace metals in the oceanic cycles of major nutrients. In *Treatise on Geochemistry*, Vol. 6 (ed. K. K. Turekian and H. D. Holland), Elsevier Ltd., Cambridge. pp. 113-143.

Shemesh A., Burckle L. H., and Hays J. D. (1994) Meltwater input to the Southern Ocean during the Last Glacial Maximum. *Science* **266**(5190), 1542-1544.

Slaveykova V. I. and Wilkinson K. J. (2005) Predicting the bioavailability of metals and metal complexes: critical review of the biotic ligand model. *Environmental Chemistry* **2**, 9-24.

# Chapter 1

## Introduction

## 1.1 Global change and paleoenvironmental reconstruction

### 1.1.1 Introduction

Today's concern for our future in a warming and changing world has led to an increasing interest in climate and environmental sciences and their related projections. One example of this interest was clearly demonstrated when the 2007 Nobel peace prize was awarded to the IPCC (Intergovernmental Panel on Climate Change) and Al Gore for "their efforts to build up and disseminate greater knowledge about man-made climate change, and to lay the foundations for the measures that are needed to counteract such change". In their efforts to provide a reliable basis to assess and discuss global climate change, scientists have turned to computer models to simulate the long-term evolution of the planet's climate and environment. The development of such tools requires a good understanding of planetary biogeochemical processes and their associated environmental feedbacks. Because instrumental data have only been available for *ca*. the past 150 years, data about earth's sensitivity to changing conditions needs to be evaluated from evidence obtained from the geological past. In other words, paleoenvironmental data derived from natural archives provides much of the basis for testing hypotheses about the causes of global change.

### 1.1.2 Lake sediments as natural archives

*Continuous and high resolution records*

Lake sediments accumulate autochthonous (produced within the lake) and allochthonous (originating from the surrounding environment) materials and so sediment cores from lakes can provide continuous records of environmental change, both, within the lake and within catchments. Since sediment accumulation rates are often high in lakes, sediments can offer the potential for high resolution records. These data can often be blended with historical and instrumental records to provide a robust reconstruction of past conditions. In addition to a higher resolution, due to their smaller size, lakes are more sensitive to environmental changes than marine systems. Indeed,

whereas marine records provide insight into long-term, past climatic records, lake sediments offer a unique opportunity for assessing rapid environmental changes.

*Extracting information from lake sediments: the proxies*

Since direct measurements are not possible in a world that no longer exists, paleoenvironmental reconstructions rely on indirect analyses or proxies. The latter are parameters that can be measured in the sediments and that have responded to systematic changes of environmental variables (*e.g*., temperature, salinity, *etc*.). Proxies rely either on biology (how environmental variables influenced species compositions and successions) or on geo-chemistry/physics (how did the physicochemical properties of the sediment respond to changing conditions).

To extract paleoenvironmental signals from proxy data, the record must first be calibrated. Calibration involves understanding and identification of the different processes controlling the proxy. Stated another way, it is necessary to asses how and to what extent the proxy signal records changes in the environmental parameters of interest. This critical issue is generally achieved through observations in the modern environment.

### 1.1.3 Future challenges

In spite of significant progress in the development and calibration of new proxies, major challenges still limit our ability to use these indicators to fully understand the past environment. This is especially clear when trying to develop reliable paleochemical proxies to study the interactions between phytoplankton and trace metals.

## 1.2 Phytoplankton and trace metals

### 1.2.1 Introduction

Trace metals play a significant role in regulating the growth and species composition of phytoplankton (for a review, see Morel et al., 2003). These elements include essential

metals (Fe, Mn, Zn, Cu, Co, Mo and Ni) and biological inhibitors (such as Pb, Ag and Hg). Additionally, some nutrients have been shown to become toxic at elevated concentrations (Cu, Zn and Ni).

### 1.2.2 Trace metal uptake and chemical speciation

Because cellular membranes are virtually impermeable to charged or polar compounds, trace metal uptake by phytoplankton must be mediated by specialized transporters. Indeed, in order to interact with the organism, the metal must first be transferred from the bulk medium to the organism (mass transport) and then react with sensitive sites on the outer membrane. At this stage, the metal ion can either dissociate back into the medium or be transported across the membrane (these processes are summarized in Fig. 1.1).
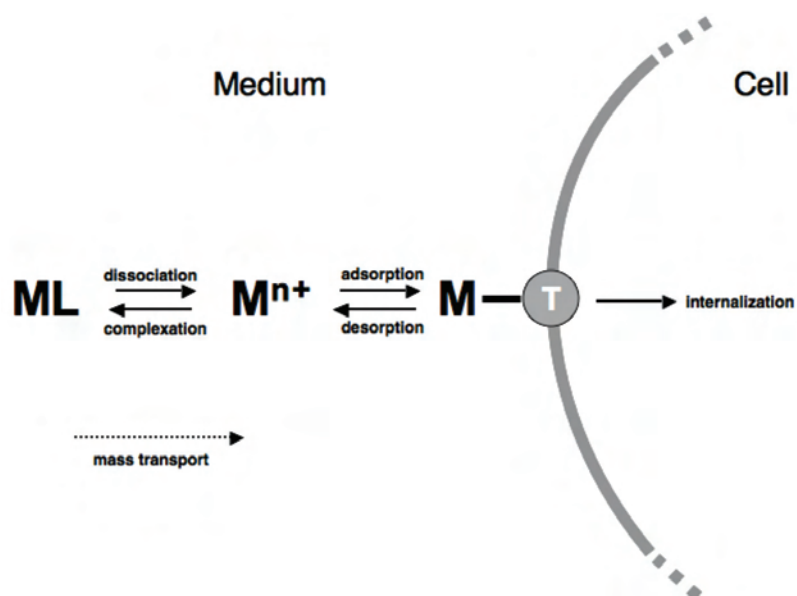


**Figure 1.1** Conceptual model of the important physiochemical processes leading to uptake of a trace metal by an aquatic microorganism (adapted from Slaveykova and Wilkinson, 2005).

This complex issue of trace metal speciation and biological availability has been addressed through the application of thermodynamic and kinetic models combined with experiments in which speciation chemistry was rigorously varied and controlled (for a review, see Slaveykova and Wilkinson, 2005). This approach demonstrated that the biological uptake of a given trace metal was, in general, not controlled by its total concentration, but by the fraction of aqueous free ions or kinetically labile inorganic

species (Sunda and Guillard, 1976; Anderson et al., 1978; Hudson and Morel, 1990). Indeed, since the chemical forms of trace metals will greatly influence their biological effects, chemical speciation is an important issue when dealing with trace metal – phytoplankton interactions.

### 1.2.3 Reconstruction of the interactions between trace metals and phytoplankton

In spite of growing interest in the field of "aquatic bioinorganic chemistry", there is still a lack of reliable tools to evaluate the influence of trace elements on phytoplankton growth and community composition during past environmental and climatic perturbations. The complexity of the uptake process (as discussed above) limits the use of total sedimentary metal concentrations to evaluate past metal-phytoplankton interactions. The main challenge is therefore to relate sediment analyses with past concentrations of bioavailable or intracellular metals.

## 1.3   Objectives and thesis overview

In this work, we evaluated the possibility of using the Zn content of silicate shells (frustules) of fossil diatoms to track historical changes in the bioavailable concentrations of Zn in surface waters. An integrated field and laboratory approach was used. In the first part of the dissertation, we studied the mechanism of Zn uptake to the frustule of the freshwater diatom *Stephanodiscus hantzschii* under controlled laboratory conditions (Chapter 2). These results, in concert with measurements on diatoms isolated from a sedimentary core, were used to reconstruct changes in bioavailable Zn concentrations in the surface waters of Lake Geneva over the past several decades (Chapter 3). By comparing the predicted concentrations of bioavailable Zn against the available field data, it was possible to assess the reliability of the dataset. Finally, the proxy was applied to marine sediments in order to reconstruct past changes in Zn delivery and availability to phytoplankton of the Southern Ocean during the last ice age (Chapter 4).

## 1.4　Environmental relevance of the study

### 1.4.1　Diatoms in paleoenvironmental reconstructions

Diatoms are unicellular algae that are among the main contributors to phytoplankton blooms in both lakes and oceans. They feature a characteristic ability to generate a highly patterned external wall composed of amorphous silica ($SiO_2 \cdot nH_2O$): the frustule. The good preservation of the frustules in sediments, the ubiquity of diatoms (they are able to colonize almost all aquatic microhabitat) and the high sensitivity of the diatoms with respect to external environmental parameters has made these algae extremely attractive for both terrestrial and marine paleoenvironmental reconstructions. Since diatom species have usually quite narrow optima and tolerances for environmental conditions, studies of fossil diatom assemblages (and the subsequent development of transfer functions for the reconstruction of environmental variables including, temperature, pH, conductivity, *etc*.) has been, and still is, a major source of paleoenvironmental information. In addition to these taxonomy related indicators, more recently, geochemical investigations of fossil frustules (isotopic silicon and oxygen composition, trace metal content, isotopic nitrogen and carbon composition of frustule-bound organic matter) have yielded new proxies (Shemesh et al., 1993; De La Rocha et al., 1998; Ellwood and Hunter, 1999).

In spite of recent advances in the development of opal-based indicators, most of the existing lacustrine and marine proxies are based on carbonate materials (*i.e.* corals, foraminifera, ostracods, *etc*.). These organisms can be very scarce in some lakes and important areas of the ocean - such as the Southern Ocean and the North Pacific, which are key regions in terms of oceanic $CO_2$ regulation (Sarmiento and Toggweiler, 1984; Siegenthaler and Wenk, 1984). Therefore, there is an urgent need to develop new diatom-based indicators of past environmental conditions.

### 1.4.2　Zinc and phytoplankton

Zn is an essential micronutrient for phytoplankton but can also become inhibitory at elevated concentrations (Anderson et al., 1978; Sunda and Huntsman, 1992, 1995, 2000). It acts as co-factor in many cellular enzymes (Da Silva and Williams, 1991). The

principal use of Zn by phytoplankton remains unclear, although an important role is as a cofactor in carbonic anhydrase (CA). This enzyme is required for the uptake and fixation of inorganic carbon and its ability to catalyze the interconversion of bicarbonate ions and $CO_2$ (Morel *et al.*, 1994) makes it very precious when $CO_2$ concentrations at cell surface are low (Badger and Price, 1994; Lane and Morel, 2000; Burkhardt et al., 2001; Sunda and Huntsman, 2005). Indeed, algal growth under low $pCO_2$ needs high CA and Zn cellular concentrations and carbon-zinc co-limitation may consequently occur (Morel et al., 1994). In addition to being a co-factor in CA, Zn has been shown to play important functions in DNA metabolism (Da Silva and Williams, 1991) and is thought to take part in frustule formation in diatoms (Rueter and Morel, 1981; De La Rocha et al., 2000; Ellwood and Hunter, 2000).

Zn toxicity is thought to be related to Zn-P interactions (Bates et al., 1985; Kuwabara, 1985; Paulsson et al., 2002): low levels of phosphorus generally increase Zn toxicity to algae, while high phosphorus concentrations are able to decrease the adverse effects. In phytoplankton, high Zn concentrations have been shown to decrease cell division rates (Tadros et al., 1990) and decouple cell division and photosynthesis (Fisher et al., 1981; Stauber and Florence, 1990; Rijstenbil et al., 1994).

### 1.4.3  Zinc in the environment

*Zinc contamination of aquatic systems*

Due to its widespread use in industry, anthropogenic Zn loading to freshwaters (via wastewaters or atmospheric deposition) generally dominates over natural inputs. Since Zn toxicity occurs through Zn-P interactions and may indeed be increased in environments where phytoplankton growth is P-limited, freshwater systems may be particularly sensitive to human-induced increasing Zn loadings.

*Zinc limitation in the Ocean*

There is evidence that Zn limits phytoplankton growth in some regions of the ocean, such as the sub-Arctic Pacific (Coale, 1991; Crawford et al., 2003) and coastal waters

off California and Costa Rica (Franck et al., 2003). In addition, because differences of Zn requirements among phytoplankton species occur, Zn limitation can affect the composition and structure of planktonic communities (Brand et al., 1983; Sunda and Huntsman, 1995). It has also been argued that Zn-C co-limitation might have large impact on the carbon cycle (Morel et al., 1994). This is because low Zn concentrations would chiefly reduce the growth of organisms that use a CA dependent bicarbonate ion transport system, as opposed to coccolithophores, which exhibit little or no CA activity and can use $CO_2$ from $HCO_3$ via the calcification reaction ($2HCO_3^- + Ca^{2+} \rightarrow CaCO_3 + CO_2 + H_2O$). Thus low Zn concentrations would promote both low productivity and a high rain ratio ($CaCO_3$ / organic C export) and induce the biological pump into an inefficient mode (because $CaCO_3$ regenerates $CO_2$). According to Morel and co-workers (1994), high Zn (and Fe) inputs to the open oceans that resulted from high levels of terrigeneous dust during glacial times may have resulted in a low rain ratio as well as increased productivity, potentially contributing to $CO_2$ sequestering.

In oligotrophic ocean regions, where concentrations of inorganic phosphate are low, phytoplankton are able to use organic phosphate through the use of Zn-dependent enzymes (Shaked et al., 2006). Consequently, at low Zn concentrations or availability, the synthesis of these enzymes might be limited, leading to a Zn-P co-limitation of phytoplankton growth.


### 1.4.4 Potential applications of the proxy

The reconstruction of historical changes of bioavailable Zn concentrations will allow for a better understanding of key questions concerning interactions between Zn and phytoplankton and indeed interactions between trace metals and phytoplankton. This will range from reconstructions of "paleopollution" (examination of questions dealing with the impact of anthropogenic Zn on the phytoplankton community and its bioavailability under changing trophic conditions) to the study of Zn limitation in the ocean and its associated feedbacks on climate.

## 1.5   References

Anderson M. A., Morel F. M. M., and Guillard R. R. L. (1978) Growth limitation of a coastal diatom by low zinc ion activity. *Nature* **276**, 70-71.

Badger M. R. and Price G. D. (1994) The Role of Carbonic Anhydrase in Photosynthesis. *Annual Review of Plant Physiology and Plant Molecular Biology* **45**(1), 369-392.

Bates S. S., Tessier A., Campbell P. G. C., and Letourneau M. (1985) Zinc-phosphorous interactions and variation in zinc accumulation during growth of *Chlamydomonas variabilis* (Chlorophyceae) in batch culture. *Can. J. Fish. Aquat. Sci.* **42**(1), 86-94.

Brand L. E., Sunda W. G., and Guillard R. R. L. (1983) Limitation of marine-phytoplankton reproductive rates by zinc, manganese, and iron. *Limnol. Oceanogr.* **28**, 1182-1198.

Burkhardt S., W., Amoroso G., Riebesell U., and Sültenmeyer D. (2001) $CO_2$ and $HCO_3^-$ uptake in marine diatoms acclimated to different $CO_2$ concentrations. *Limnol. Oceanogr.* **46**(6), 1378-1391.

Coale K. H. (1991) Effects of iron, manganese, copper, and zinc enrichments on productivity and biomass in the subarctic Pacific. *Limnol. Oceanogr.* **36**, 1851-1864.

Crawford D. W., Lipsen M. S., Purdie D. A., Lohan M. C., Statham P. J., Whitney F. A., Putland J. N., Johnson W. K., Sutherland N., Peterson T. D., Harrison P. J., and Wong C. S. (2003) Influence of zinc and iron enrichments on phytoplankton growth in the northeastern subarctic Pacific. *Limnol. Oceanogr.* **48**(4), 1583-1600.

Da Silva J. J. R. and Williams R. J. P. (1991) *The biological chemistry of the elements*. Oxford University Press.

De La Rocha C. L., Brzezinski M. A., DeNiro M. J., and Shemesh A. (1998) Silicon-isotope composition of diatoms as an indicator of past oceanic change. *Nature* **395**(6703), 680-683.

De La Rocha C. L., Hutchins D. A., Brzezinski M. A., and Zhang Y. (2000) Effects of iron and zinc deficiency on elemental composition and silica production by diatoms. *Mar. Ecol. Prog. Ser.* **195**, 71-79.

Ellwood M. J. and Hunter K. A. (1999) Determination of the Zn/Si ratio in diatom opal: a method for the separation, cleaning and dissolution of diatoms. *Mar. Chem.* **66**(3-4), 149-160.

Ellwood M. J. and Hunter k. A. (2000) The incorporation of zinc and iron into the frustule of the marine diatom *Thalassiosira pseudonana*. *Limnol. Oceanogr.* **45**(7), 1517-1524.

Fisher N. S., Jones G. J., and Nelson D. M. (1981) Effects of copper and zinc on growth, morphology, and metabolism of *Asterionella japonica (Cleve)*. *J. Exp. Mar. Biol. Ecol.* **51**, 37-56.

Franck V. M., Bruland K. W., Hutchins D. A., and Brzezinski M. A. (2003) Iron and zinc effects on silicic acid and nitrate uptake kinetics in three high-nutrient, low-chlorophyll (HNLC) regions. *Mar. Ecol. Prog. Ser.* **252**, 15-33.

Hudson R. J. M. and Morel F. M. M. (1990) Iron transport in marine phytoplankton: Kinetics of cellular and medium coordination reactions. *Limnol. Oceanogr.* **35**, 1002-1020.

Kuwabara J. S. (1985) Phosphorus-zinc interactive effects on growth by *Selenastrum capricornutum* (chlorophyta). *Environ. Sci. Technol.* **19**, 417-421.

Lane T. W. and Morel F. M. M. (2000) A biological function for cadmium in marine diatoms. *Proc. Natl. Acad. Sci. USA* **97**(9), 4627-4631.

Morel F. M. M., Milligan A. J., and Saito M. A. (2003) Marine bioinorganic chemistry: The role of trace metals in the oceanic cycles of major nutrients. In *Treatise on Geochemistry*, Vol. 6 (ed. K. K. Turekian and H. D. Holland), Elsevier Ltd., Cambridge. pp. 113-143.

Morel F. M. M., Reinfelder J. R., Roberts S. B., Chamberlain C. P., Lee J. G., and Yee D. (1994) Zinc and carbon co-limitation of marine phytoplankton. *Nature* **369**, 740-742.

Paulsson M., Mansson V., and Blanck H. (2002) Effects of zinc on the phosphorus availability to periphyton communities from the river Gota Alv. *Aquat. Toxicol.* **56**(2), 103-113.

Rijstenbil J. W., Derksen J. W. M., Gerringa L. J. A., Poortvliet T. C. W., Sandee A., van Den Berg M., van Drie J., and Wijnholds J. A. (1994) Oxidative stress induced by copper: Defense and damage in the marine planktonic diatom *Dytilum brightwellii* grown in continous culture with high and low zinc levels. *Mar. Biol.* **119**, 583-590.

Rueter J. G. J. and Morel F. M. M. (1981) The interaction between zinc deficiency and copper toxicity as it affects the silicic acid uptake mechanisms in *Thalssiosira pseudonana*. *Limnol. Oceanogr.* **26**(1), 67-73.

Sarmiento J. L. and Toggweiler J. R. (1984) A new model for the role of the oceans in determining atmospheric $pCO_2$. *Nature* **308**(5960), 621-624.

Shaked Y., Xu Y., Leblanc K., and Morel F. M. M. (2006) Zinc availability and alkaline phosphatase activity in Emiliania huxleyi: Implications for Zn–P co-limitation in the ocean. *Limnol. Oceanogr.* **51**(1), 299-309.

Shemesh A., Macko S. A., Charles C. D., and Rau G. H. (1993) Isotopic evidence for reduced productivity in the glacial Southern Ocean. *Science* **262**(5132), 407-410.

Siegenthaler U. and Wenk T. (1984) Rapid atmospheric CO2 variations and ocean circulation. *Nature* **308**(5960), 624-626.

Slaveykova V. I. and Wilkinson K. J. (2005) Predicting the bioavailability of metals and metal complexes: critical review of the biotic ligand model. *Environmental Chemistry* **2**, 9-24.

Stauber J. L. and Florence T. M. (1990) Mechanism of toxicity of zinc to the marine diatom *Nitzschia closterium*. *Mar. Biol.* **105**, 519-524.

Sunda W. G. and Guillard R. R. L. (1976) The relationship between cupric ion activity and the toxicity of copper to phytoplankton. *J. Mar. Res.* **34**, 511-529.

Sunda W. G. and Huntsman S. A. (1992) Feedback interactions between zinc and phytoplankton in seawater. *Limnol. Oceanogr.* **37**(1), 25-40.

Sunda W. G. and Huntsman S. A. (1995) Cobalt and zinc interreplacement in marine phytoplankton: biological and geochemical implications. *Limnol. Oceanogr.* **40**(8), 1404-1417.

Sunda W. G. and Huntsman S. A. (2000) Effect of Zn, Mn, and Fe on Cd accumulation in phytoplankton: implications for oceanic Cd cycling. *Limnol. Oceanogr.* **45**, 1501-1516.

Sunda W. G. and Huntsman S. A. (2005) Effect of CO2 supply and demand on zinc uptake and growth limitation in a coastal diatom. *Limnol. Oceanogr.* **50**(4), 1181-1192.

Tadros G. M., Mbuthia P., and Smith W. (1990) Differential response of marine diatoms to trace metals. *Bull. Environ. Contam. Toxicol.* **44**, 826-831.

# Incorporation of zinc into the frustule of the freshwater diatom *Stephanodiscus hantzschii*

Thomas Jaccard, Daniel Ariztegui and Kevin J. Wilkinson

## Abstract

Zinc incorporation into the frustule (siliceous cell wall) of the freshwater diatom *Stephanodiscus hantzschii* was studied for $Zn^{2+}$ concentrations ranging from 25 pmol $L^{-1}$ to 25 nmol $L^{-1}$. A sigmoidal dependency was observed between $Zn^{2+}$ concentrations in the culture medium and the concentration of Zn in the frustule. Intracellular and frustule Zn concentrations were positively correlated, indicating that intracellular pools were used to supply the Zn that was incorporated into the frustule. The mechanism behind Zn incorporation was examined by determining the role of Si and Mn on Zn uptake to the cell wall via competition experiments. Results were consistent with a mechanism by which Zn and Mn competed for an intracellular site that leads to incorporation into the frustule. The study suggests that the Zn content of fossil frustules could be a valuable tool to study past levels of bioavailable Zn based upon Zn-phytoplankton interactions.

## 2.1 Introduction

Zn is an essential micronutrient for phytoplankton but can become inhibitory at elevated concentrations (Anderson et al., 1978; Sunda and Huntsman, 1992, 1995, 2000). Due to its widespread use in industry, anthropogenic Zn loading to freshwaters (via wastewaters or atmospheric deposition) generally dominates over natural inputs. Consequently, there is a great interest in evaluating the effects of these changes on Zn concentrations in the pelagic community. Since there is a consensus that total metal concentrations in the water are poor predictors of toxicological effects, several models have been developed to relate the chemical speciation of the metals to their bioavailability (for a review, see Slaveykova and Wilkinson, 2005).

Nonetheless, there is still a lack of reliable tools to evaluate the influence of Zn – and other trace metals - on phytoplankton growth and community composition during past environmental and climatic perturbations. One major obstacle is the difficulty in relating sediment analyses with past concentrations of bioavailable or intracellular metals.

Ellwood and Hunter (2000a) have investigated the incorporation of Zn and Fe into the frustule (siliceous cell wall) of the marine diatom, *Thalassiosira pseudonana*. Zn levels in the cell wall generally increased over a wide range of free $Zn^{2+}$ concentrations in culture media, leading the authors to suggest that Zn content in fossil frustules could be used to track historical changes in oceanic concentrations of free $Zn^{2+}$. This novel proxy was subsequently applied to Southern Ocean samples spanning the last interglacial-glacial transition (Ellwood and Hunter, 2000b) where the authors did not find any evidence to support the "zinc hypothesis" (*i.e.*, Zn stimulation of export production during the ice ages; Morel et al., 1994).

The goal of this study was to investigate further whether Zn concentrations of the frustules could be employed as a paleolimnological indicator of bioavailable Zn. Since a good physiological understanding of the uptake process is required in order to correctly interpret fossil samples, the mechanisms leading to Zn uptake to the cell wall were studied for the common freshwater diatom, *Stephanodiscus hantzschii*. Specifically, the influence of $Zn^{2+}$ concentrations and the role of $Mn^{2+}$ and Si on Zn incorporation by the frustule were systematically evaluated.

## 2.2   Methodology

### 2.2.1   Zn uptake experiments

Zn uptake by *Stephanodiscus hantzschii* (UTCC 267) was evaluated in a modified CHU-10 medium (see appendix1; Nichols, 1973). Free $Zn^{2+}$ ion concentrations were systematically varied by concomitant addition of Zn and EDTA (ethylene diamine tetra-acetic acid) over a $Zn^{2+}$ concentration range ($10^{-10.6}$ -$10^{-7.6}$ mol $L^{-1}$) that is characteristic of natural freshwaters (Xue and Sigg, 1994; Xue et al., 1995). Calculated free ion concentrations (MINTEQA2; Allison et al., 1991) are reported in Table 2.1. All experiments were carried out at pH = 6.4 at 20 °C in acid-cleaned polycarbonate flasks and with 100 rpm rotary shaking. Lighting was provided on a 12:12 hour light:dark cycle using 50 µmol photons $m^{-2}$ $s^{-1}$ of white fluorescent lighting. Cells were cultured in our modified CHU-10 medium with a pZn of 9.62 prior to transfer – at mid-exponential growth - to 50 mL of experimental medium containing the desired $Zn^{2+}$ concentration to get an initial cell density of *ca*. 2 x $10^{4}$ cells $mL^{-1}$. Finally, when mid exponential growth phase was attained, the cells were then transferred to 300 mL of experimental medium. Experiments were performed under laminar flow and other precautions in order to avoid both biological and chemical contaminations. Cell numbers were measured daily using an electronic particle counter (Coulter Multisizer 2). The specific growth rate was calculated from the linear regression of a natural logarithmic plot of cell number as a function of time. *S. hantzschii* was grown for 6 or more generations and harvested at the end of the exponential growth phase. A 50 mL aliquot was collected from the final *ca.* 300 mL of cell culture for analyses of intracellular metal content. In that case, cells were centrifuged and washed with 10 mL of a metal-free medium containing $10^{-3}$ mol $L^{-1}$ EDTA (Hassler et al., 2004). Intracellular metal contents were determined by ICP-MS (inductively coupled plasma mass spectrometer; Hewlett Packard, 4500; detection limits for Zn and Mn of 0.1 ppb) following digestion of the pellet for 1 hour in 1 mL of ultrapure concentrated $HNO_3$ at 80°C. The remaining 250 mL of cell culture were filtered over a 3 µm nitrocellulose membrane that was subsequently digested for 1 hour in 2mL of concentrated $HNO_3$ at 80°C. The residual silica was then washed 4 times with 10 mL of MilliQ water and dissolved in 8 mL of a 0.1 mol $L^{-1}$/0.1 mol $L^{-1}$ HCl/HF solution for 4 hours at 80°C. We preferred hot HCl/HF rather than an NaOH dissolution

(Paasche, 1973) since with the latter, silica polymerization was occasionally observed when samples were cooled down to room temperature. The possible loss of Si from solution due to the formation of volatile $SiF_4$ was investigated. Under the conditions used in this experiment, Si recovery was, within error, 100%, attesting to the reliability of the dissolution process. After dissolution, samples were centrifuged and visually inspected to ensure complete dissolution of the silica. In the solution containing the dissolved silica, Zn and Mn concentrations were measured by ICP-MS (detection limits for Zn and Mn of 0.1 ppb) while Si was determined in diluted samples (100 times) using a molybdate-blue spectrophotometric method (Merck, Spectroquant 14794) at 820 nm (Perkin Elmer Lambda 35 spectrophotometer). Blank $HNO_3$ and HF/HCl digests were systematically verified for metal contamination. For a limited number of samples, intracellular and frustule metal concentrations could not be measured on the same 300 mL aliquot of sample. In those cases, additional experiments were prepared under identical conditions in order to analyze intracellular metal content.

**Table 2.1** Composition of the experimental medium used for Zn uptake experiments.

| Macro-nutrients | total concentrations |
|---|---|
| $NO_3^-$ | 488 $\mu$mol $L^{-1}$ |
| $PO_4^{3-}$ | 57 $\mu$mol $L^{-1}$ |
| $Si(OH)_4$ | 207 $\mu$mol $L^{-1}$ |

| Metals | $\log [M^{n+}]$ |
|---|---|
| $Na^+$ | -3.08 |
| $Mg^{2+}$ | -4.00 |
| $K^+$ | -3.94 |
| $Ca^{2+}$ | -3.62 |
| $Mn^{2+}$ | -6.18 |
| $Fe^{3+}$ | -18.99 |
| $Co^{2+}$ | -10.44 |
| $Cu^{2+}$ | -12.56 |
| $Zn^{2+}$ | varied between -10.62 and -7.61 |

| Chelator | total concentration |
|---|---|
| EDTA | varied between 12.4 and 89.3 $\mu$mol $L^{-1}$ |

### 2.2.2 Role of Mn and Si on Zn incorporation

In some experiments designed to determine the role of Si and Mn on Zn incorporation, $Si(OH)_4$ and $Mn^{2+}$ concentrations were 10 times higher than were generally used in the experimental medium (Table 2.2). These competition experiments were performed at pZn levels of 8.93 and 9.23. In spite of $Si(OH)_4$ concentrations approaching saturation in the more concentrated media, no silica precipitation was observed.

**Table 2.2** $Zn^{2+}$, $Mn^{2+}$ and $Si(OH)_4$ concentrations of the experimental media used for the experiments in which the role of $Mn^{2+}$ and Si on Zn incorporation were evaluated.

| Experiment | $\log[Zn^{2+}]$ | $\log[Mn^{2+}]$ | $[Si(OH)_4]$ (mmol $L^{-1}$) |
|---|---|---|---|
| Zn uptake experiment (control) | -9.23 | -6.18 | 0.21 |
| | -8.93 | -6.18 | 0.21 |
| Role of $Mn^{2+}$ on Zn incorporation | -9.23 | -5.21 | 0.21 |
| | -8.93 | -5.20 | 0.21 |
| Role of Si on Zn incorporation | -9.23 | -6.18 | 2.10 |
| | -8.93 | -6.18 | 2.10 |

## 2.3 Results

### 2.3.1 Specific growth rate

Maximal growth rates were observed over the entire range of examined $Zn^{2+}$ concentrations, except at a pZn of 7.61, where the growth decreased (Fig. 2.1). No significant effect ($p>0.05$, $t$-test) on the specific growth rate was observed for a 10 fold increase of $[Mn^{2+}]$ (pZn=9.23, $p=0.054$, df=8, $t$-test; pZn=8.93, $p=0.320$, df=7, $t$-test) or $[Si(OH)_4]$ (pZn=9.23, $p=0.139$, df=7, $t$-test; pZn=8.93, $p=0.217$, df= 6, $t$-test).
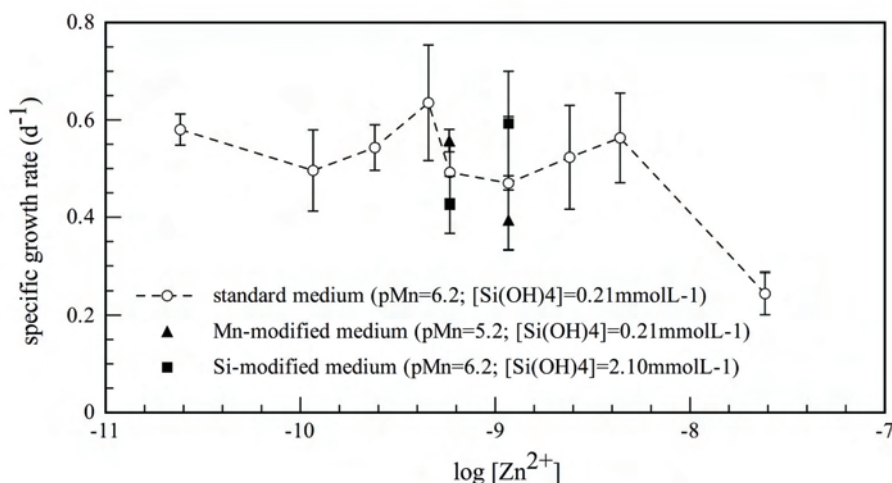
**Figure 2.1** Specific growth rate ($d^{-1}$) of *Stephanodiscus hantzschii* as a function of $\log[Zn^{2+}]$ for Zn uptake experiments (open circles and dashed line, pMn = 6.2, $[Si(OH)_4]$ = 0.21 mmol $L^{-1}$) or for experiments examining the role of a modification in $Mn^{2+}$ (filled triangles, pMn = 5.2, $[Si(OH)_4]$ = 0.21 mmol $L^{-1}$ ) or $Si(OH)_4$ concentrations (filled squares, pMn = 6.2, $[Si(OH)_4]$ = 2.10 mmol $L^{-1}$). Error bars indicate the 95% confidence interval (CI). No significant differences ($p>0.05$, *t*-test) were found between specific growth rates for Zn uptake experiment and those obtained when $[Si(OH)_4]$ or $[Mn^{2+}]$ were varied.

## 2.3.2 Zn uptake

For Zn uptake experiments, intracellular Zn concentrations, $Zn_{cell}$, generally increased as a function of the $Zn^{2+}$ concentration in the medium (Fig. 2.2). Nonetheless, $Zn_{cell}$ had only a weak dependence on $Zn^{2+}$ concentrations in the medium: an approximately 200 fold increase in free Zn led to only a four-fold increase of intracellular Zn. Intracellular Zn determinations for pZn values of 8.62 and 7.61 were discarded because blank samples were contaminated by Zn.
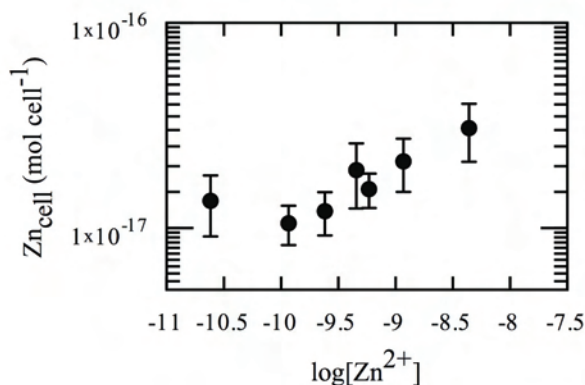


**Figure 2.2** Intracellular zinc, $Zn_{cell}$, as a function of $\log[Zn^{2+}]$ for *Stephanodiscus hantzschii*. Error bars indicate 95% CI.
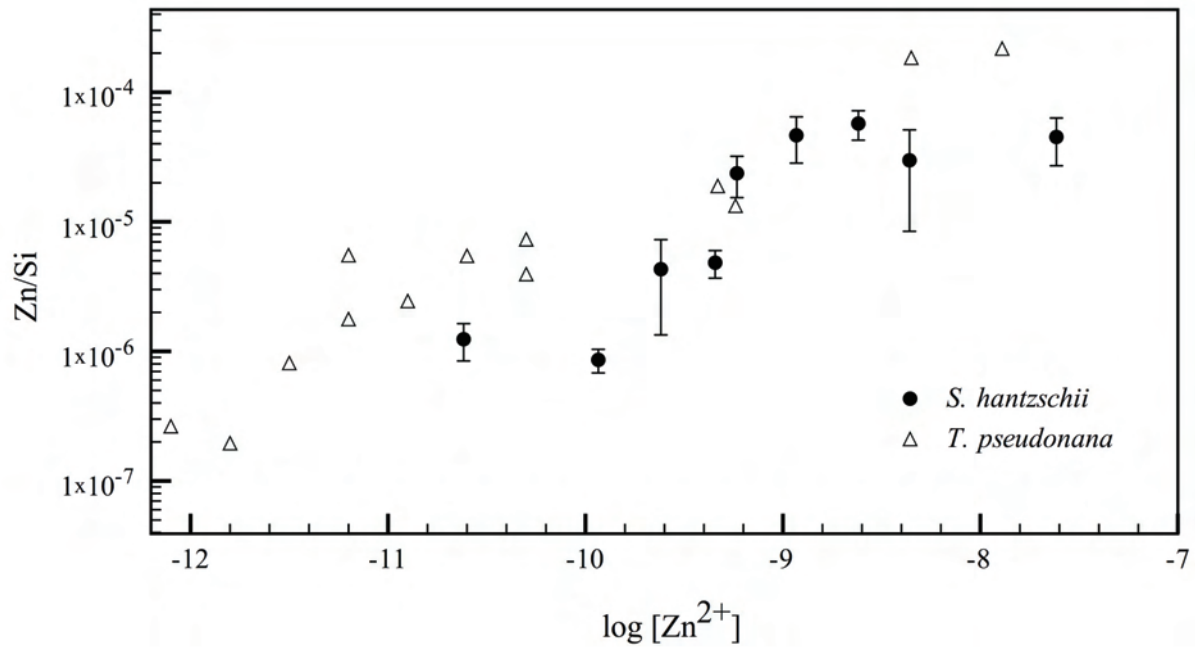
**Figure 2.3** Frustule Zn/Si molar ratio as a function of log[$Zn^{2+}$] for *Stephanodiscus hantzschii* (filled circles). Error bars indicate 95% CI. The results of Ellwood and Hunter (2000a) for *Thalassiosira pseudonana* are reported by the open triangles.

A sigmoidal relationship was observed between the molar Zn/Si ratio of the frustule when plotted as a function of the $Zn^{2+}$ concentration in the medium. A maximal slope was observed for pZn values between 9.9 and 8.9 (Fig. 2.3). Similar Zn/Si data, obtained for the marine diatom *Thalassiosira pseudonana* (Ellwood and Hunter, 2000a), are reported for comparison. To assess the dependency of the Zn in the frustule on the intracellular Zn, these parameters were reported in a log-log plot (Fig. 2.4). Only data from experiments for which Zn concentrations were measured on identical samples for both the frustule and the cell have been reported. Zn contents of the frustule were not normalized to the Si content, but rather provided on a per cell basis (Si = (2.0±0.2)x$10^{-13}$ mol Si cell$^{-1}$ did not vary over the course of the experiment and are consistent with the values found by Twining et al. (2003) for the same *S. hantzschii* clone). A strong positive correlation (Spearman correlation coefficient, $r_s$=0.87) was observed between the Zn associated with the cell wall, $Zn_{frust}$, and the intracellular Zn, $Zn_{cell}$.
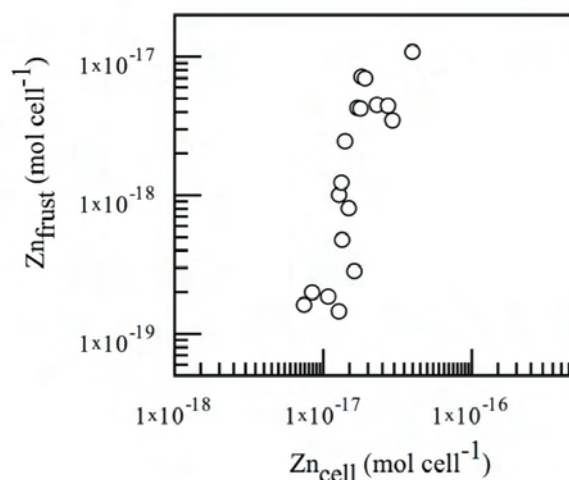
**Figure 2.4** Zn frustule content, $Zn_{frust}$, as a function of the intracellular Zn concentration, $Zn_{cell}$, for *Stephanodiscus hantzschii*. A Spearman correlation coefficient of $r_s=0.87$ was obtained for the association of these two variables.

### 2.3.3 Role of Mn and Si on Zn incorporation

For the Zn uptake experiments, neither the intracellular Mn nor the normalized molar Mn/Si cell wall ratio varied greatly over the range of studied $[Zn^{2+}]$ (data not shown). Nonetheless, the addition of $Mn^{2+}$ significantly ($p<0.05$, $t$-test) decreased the Zn/Si ratio (Fig. 2.5a; pZn=9.23, $p=0.026$, df=6, $t$-test; pZn=8.93, $p=0.011$, df=8, $t$-test) even though intracellular Zn concentrations were not affected (Fig. 2.5b; pZn=9.23, $p=0.479$, df=5, $t$-test; pZn=8.93, $p=0.699$, df=4, $t$-test). Quite expectedly, higher $[Mn^{2+}]$ in the medium also led to higher values of Mn in the frustule (Fig. 2.5c; pZn=9.23, $p=0.001$, df=6, $t$-test; pZn=8.93, $p=0.005$, df=8, $t$-test) and inside the cell (Fig. 2.5d; pZn=9.23, $p=0.007$, df=5, $t$-test; pZn=8.93, $p=0.004$, df=4, $t$-test).

**Figure 2.5** Values of (a) frustule Zn/Si molar ratio, (b) intracellular Zn, $Zn_{cell}$, (c) frustule Mn/Si molar ratio and (d) intracellular Mn, $Mn_{cell}$ of *Stephanodiscus hantzschii* for two concentrations of $Zn^{2+}$ (x-axis) and two $Mn^{2+}$ concentrations (white bars or control: pMn=6.2; grey bars: pMn=5.2). The stars denote significant differences ($p<0.05$, *t*-test) with respect to the control.

Increased concentrations of $Si(OH)_4$ in the medium resulted in an increased accumulation of intracellular Zn (Fig. 2.6b; pZn=9.23, $p=0.047$, df=6, *t*-test; pZn=8.93, $p=0.011$, df=7, *t*-test), with a greater effect observed at pZn = 8.93. A Significant effect on the concentration in the frustule was only observed for Zn at pZn=8.93 (Fig. 2.6a; pZn=9.23, $p=0.662$, df=7, *t*-test; pZn=8.93, $p=0.003$, df=9, *t*-test), in which case a higher Zn/Si value was observed. A higher concentration of $Si(OH)_4$ in the medium lead to higher values of intracellular Mn (Fig.2.6d; pZn=9.23, $p=0.006$, df=6, *t*-test; pZn=8.93, $p=0.006$, df=7, *t*-test), even though no significant effect on the Mn/Si ratio in the frustule was observed (Fig. 2.6c; pZn=9.23, $p=0.185$, df=7, *t*-test; pZn=8.93, $p=0.568$, df=9, *t*-test).
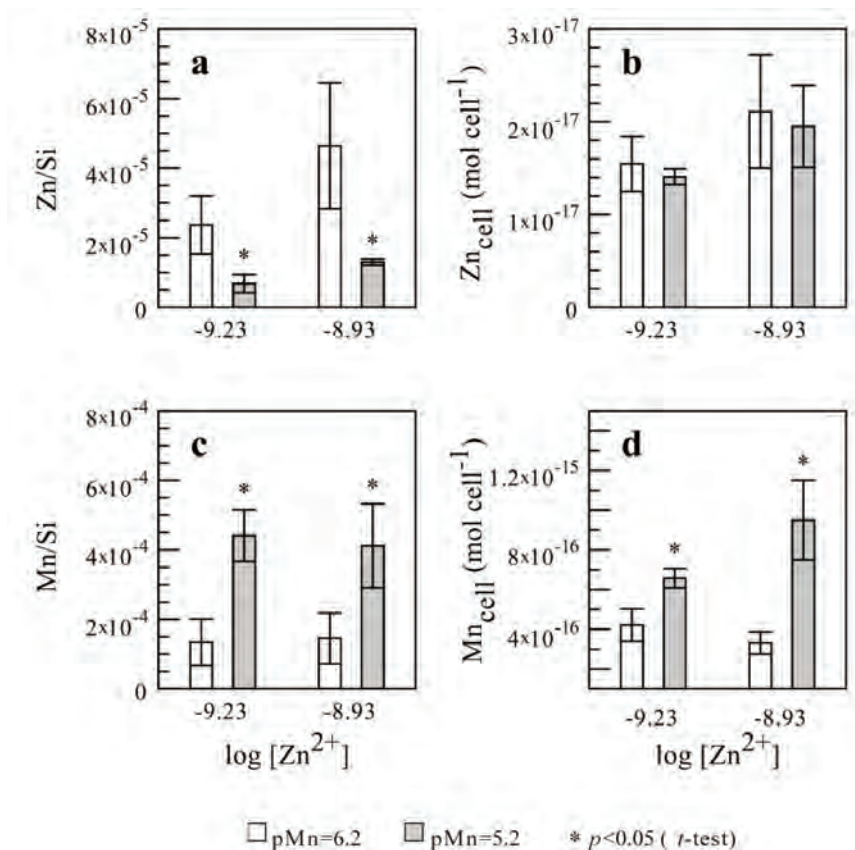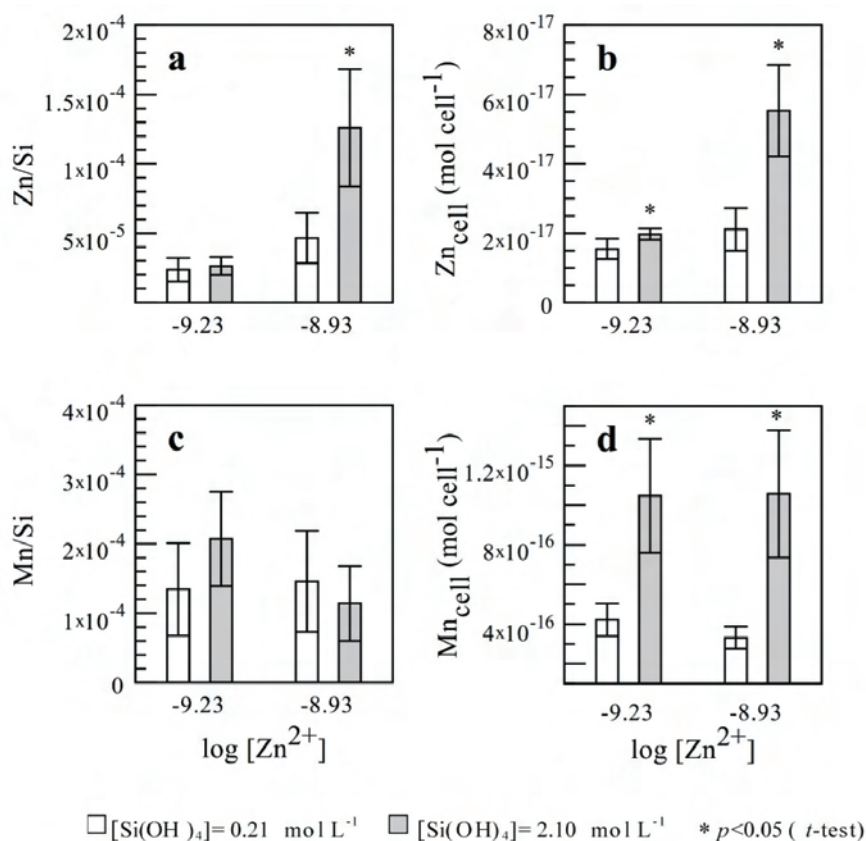
**Figure 2.6** Values of (a) frustule Zn/Si molar ratio, (b) intracellular Zn, $Zn_{cell}$, (c) frustule Mn/Si molar ratio and (d) intracellular Mn, $Mn_{cell}$ of *Stephanodiscus hantzschii* for two concentrations of $Zn^{2+}$ (x-axis) and two $Si(OH)_4$ concentrations (white bars or control: $[Si(OH)_4]$=0.21 mmol $L^{-1}$; grey bars: $[Si(OH)_4]$=2.10 mmol $L^{-1}$). The stars denote significant differences ($p<0.05$, *t*-test) with respect to the control.

## 2.4   Discussion

### 2.4.1  Zn uptake experiment

From the weak slope in Fig. 2.2, it was clear that intracellular Zn concentrations, $Zn_{cell}$, were highly regulated over the studied range of $Zn^{2+}$ concentrations for this diatom. Values of cellular Zn were consistent with those found by Twining et al. (2003) for the same *S. hantzschii* clone grown in the WCL-1 medium (Guillard, 1975). In addition, a similar trend was observed for Zn uptake by phytoplankton in seawater where Sunda and Huntsman (1992) obtained a sigmoidal dependency between intracellular Zn and $Zn^{2+}$ concentrations in seawater. In that study, which examined several species of diatoms and a coccolithophore, minimal slopes were consistently observed in the pZn

range of 10.5 -9.5 while larger slopes were determined above and below this range. The shape of the curves has been interpreted to indicate that there were at least two separate uptake systems for Zn with widely different affinity constants. In that case, the minimal slopes at intermediate $[Zn^{2+}]$ were attributed to a negative feedback regulation of the high affinity Zn uptake system whereas the increased slope at higher Zn concentrations corresponded to Zn uptake by the low-affinity site. In this paper, no evidence for a second uptake system was obtained, albeit the examined concentration range was smaller than that studied by Sunda and Huntsman.

The shape of the Zn/Si vs. $[Zn^{2+}]$ curve for *S. hantzschii* (Fig. 2.3) was very similar to that obtained for the marine diatom, *T. pseudonana* (Ellwood and Hunter, 2000a), even though slightly lower Zn/Si ratios were observed here. The similarity in the shape of the two Zn/Si datasets suggests a common mechanism of Zn incorporation into the frustule of the two diatom species. The discrepancy between the absolute values of the Zn/Si ratios for the two diatoms can be explained by a number of factors including the different media used in the two studies. For example, the medium employed here contained nearly 200 times more $Mn^{2+}$ than the experimental medium used to grow *T. pseudonana*. Recall that in our Mn variation experiments, higher concentrations of $Mn^{2+}$ in the medium significantly lowered the Zn/Si ratio (Fig. 2.5a). Other factors such as a species-specific variability cannot be excluded.
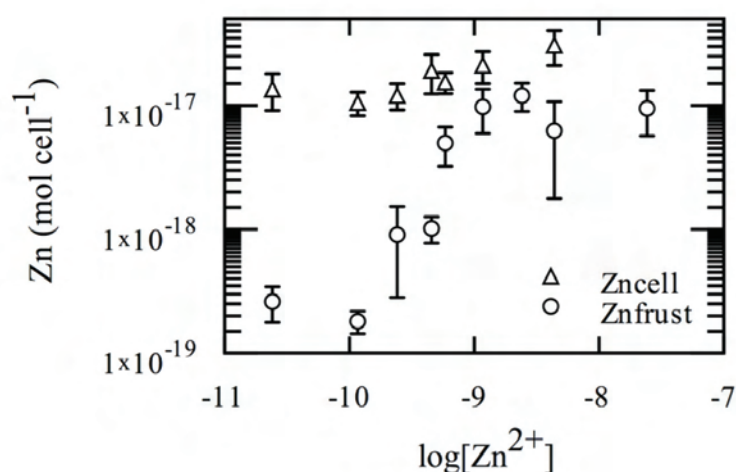


**Figure 2.7** Intracellular zinc, $Zn_{cell}$, and zinc in the frustule, $Zn_{frust}$, as a function of $\log[Zn^{2+}]$ for *Stephanodiscus hantzschii*. Error bars indicate 95% CI.

The strong positive correlation between Zn in the frustule and that in the cell (Fig. 2.4) is consistent with a mechanism in which the internal intracellular Zn pools are used to supply Zn to the cell wall (Ellwood and Hunter, 2000a). A plot of $Zn_{frust}$ and $Zn_{cell}$ against $[Zn^{2+}]$ (Fig. 2.7) demonstrated that $Zn_{frust}$ represented between 1 and 27% of the cell's Zn reserves (*i.e.* $Zn_{frust}$ + $Zn_{cell}$). The leveling off in the Zn/Si curve for $Zn^{2+}$ concentrations exceeding *ca.* $10^{-9}$ mol $L^{-1}$, which did not appear to occur for the intracellular Zn data (intracellular concentration for a pZn of 8.36 is significantly higher than for a pZn of 9.23; $p$=0.019, df=5, *t*-test) provides some evidence for a saturable system of Zn incorporation into the frustule.

### 2.4.2  Role of Mn on Zn incorporation

As discussed earlier, it is thought that at least two transport systems control Zn entry into the cell. In addition to these two primary Zn transporters, in the green alga, *Chlamydomonas* sp., Zn is able to use the Mn transporter at low $Mn^{2+}$ concentrations (Sunda and Huntsman, 1998). For the relatively high range of Zn concentrations examined in this study, Zn was likely taken up by the low-affinity system since intracellular Zn did not change significantly with variable $[Mn^{2+}]$, suggesting that either this pathway is not used in *S. hantzschii* or that only relatively small concentrations of Zn entered the cell by the Mn uptake pathway. Indeed, while higher concentrations of $Mn^{2+}$ did not affect intracellular Zn levels, they increased both intracellular Mn and Mn/Si while decreasing Zn/Si. These variations suggested that Mn and Zn could compete for an intracellular site that leads to metal incorporation by the frustule. This hypothesis is consistent with the positive linear correlation that was observed between the Zn/Mn ratio in the cell and that in the frustule ($R^2$=0.82). These data also suggest that the intracellular uptake site had a higher affinity for Zn than for Mn. Indeed, given the dependency between $(Zn/Mn)_{frust}$ and $(Zn/Mn)_{cell}$, for a similar intracellular concentration of Zn and Mn, approximately 15 times more Zn than Mn was found in the cell wall (Fig. 2.8). Note that over the range of studied $Zn^{2+}$, no Cu was detected in the cell wall (Cu/Si molar ratio detection limits = $10^{-7}$) in spite of the presence of a significant quantity of intracellular Cu (($1.4\pm0.4$)x$10^{-14}$ mol cell$^{-1}$, data not shown). Under the assumption that the same metal uptake site is employed for all 3 metals and that the intracellular Zn, Mn

and Cu are equally available, these data can be interpreted to suggest that Mn and Cu have a lower affinity than Zn for the metal uptake site.
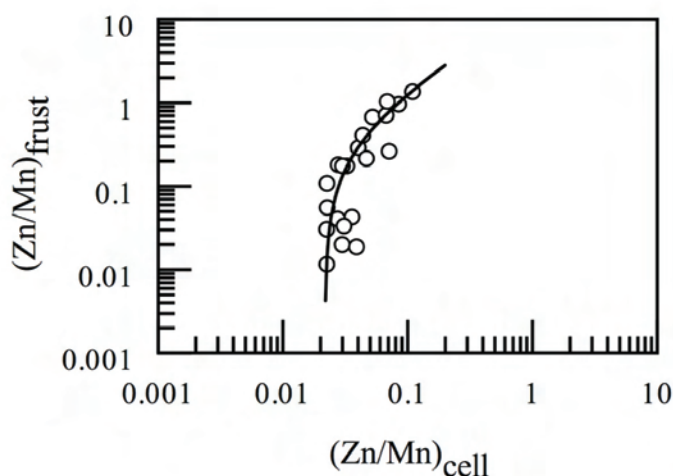


**Figure 2.8** Frustule Zn/Mn molar ratio, $(Zn/Mn)_{frust}$, as a function of the intracellular Zn/Mn molar ratio, $(Zn/Mn)_{cell}$, for *Stephanodiscus hantzschii*. A correlation coefficient of $R^2=0.82$ with a slope of 15.2 is obtained for the linear regression of these data.

### 2.4.3 Mechanism of Zn incorporation

Previous long-term incubation studies have shown that silicic acid $(Si(OH)_4)$ uptake by *T. pseudonana* was reduced for Zn deficient cultures and by Cu toxicity (Rueter and Morel, 1981). These same authors observed that Zn-limited *T. weissflogii* morphologically resembled Cu-inhibited or Si-starved *T. pseudonana*. Fisher et al. (1981) could not distinguish between Cu-treated cells and Si-limited cells of the diatom *Asterionella japonica*. These results led to the hypothesis that silicic acid uptake was mediated by a Zn-dependent system that could be inactivated by copper. Nonetheless, a recent study showed that Zn concentrations had no influence on short-term Si uptake kinetics (Thamatrakoln and Hildebrand, 2007). This suggests that previous long-term studies were reflecting the influence of Zn on Si cell wall incorporation kinetics rather than on biological uptake. This alternative explanation is supported by a recent investigation of the effect of Zn deficiency on silica production (De La Rocha et al., 2000) and is consistent with our hypothesis of a Zn-dependent system that is modulated by Mn - and possibly Cu - competitive interactions.

Some proteins or peptides have been shown to be tightly associated with the frustules and could only be released by complete dissolution of the silica. It is possible that Zn

incorporation into the frustule might be via one of these HF- or NH$_4$F-extractable organic macromolecules. These compounds include some of the major components involved in silica polymerization: silaffins (Kroger et al., 2001; Kroger et al., 2002; Frigeri et al., 2006) and long-chain polyamines (LCPA; Kroger et al., 2000 ; also identified in fossil frustules by Ingalls et al. (2004)) in addition to pleuralins (protein present in the overlap region between the two halves of the cell wall; Kroger et al., 1997; Kroger and Wetherbee, 2000) and several other unidentified molecules (Swift and Wheeler, 1992; Frigeri et al., 2006). Whereas the association of pleuralins with the frustule is due to their high affinity for silica, LCPAs and silaffins, because of to their small size, are expected to become fully encapsulated in the silica spheres (Vrieling et al., 2002). Indeed, studies have shown that organic molecules of 8-15 kDa could be irreversibly encapsulated in silica (Gill and Ballesteros, 2000 and references therein). Recently, Schroder et al. (2003) identified a new Zn-dependent enzyme (silicase) involved in the biomineralization of silica in sponges. Although silicase has not been found in diatoms, its homologue carbonic anhydrase (CA) is present. Because the Zn in CA can be substituted by Mn (Okrasa and Kazlauskas, 2006), this enzyme – or a homologue -, if associated with the silica of the frustule could provide a good candidate for the Zn-bearing organic macromolecule involved in cell wall incorporation. In the freshwater diatom *Navicula pelliculosa*, ferredoxin-NADP reductase (FNR), a homologue of CA that is also capable of binding Zn (Catalano Dupuy et al., 2004) has been shown to have a strong affinity for silica (Hazelaar, 2006).

In addition to this mechanism, there are at least three other potential explanations for Zn incorporation into diatom cell walls. Aluminum and germanium have been found in diatom frustules (Azam et al., 1973; Gehlen et al., 2002) and investigation of the atomic structure of this biogenic silica revealed a structural association between Al and Si (Gehlen et al., 2002). This was interpreted as Al being incorporated during the biosynthesis of the frustule (Gehlen et al., 2002). Since Al, Ge and Si have the same coordination numbers with oxygen and similar atomic diameters, they can easily substitute Si. In contrast, the atomic radius of Zn in tetrahedral geometry is almost twice that of Si and thus, association with Si is less likely to occur for Zn. Nonetheless, Lal et al. (2006) have suggested that the substantial interstitial spaces in the polymerizing silica structure could easily accommodate metal ions. Finally, recent work by Vrieling et

al. (2007) on diatom biosilification could provide an alternative extracellular mechanism for Zn incorporation into the frustules. In order to explain the important effect of ionic strength on diatom biosilica formation, these authors proposed that the simultaneous uptake of silicic acid and other external ions could take place by (macro)pinocytosis - a form of nonspecific endocytosis in which extracellular fluids are brought into the cell within vesicles. Although these would be reasonable mechanisms for Zn incorporation into the cell wall, the tight relationship between $Zn_{cell}$ and $Zn_{frust}$, the "saturable" nature of the Zn deposition process and the observed competition between Mn and Zn incorporation into the frustule suggest that for *S. hantzschii*, Zn incorporation into the frustule through a Zn-bearing organic macro-molecule is the most likely explanation.

### 2.4.4  Role of Si on Zn incorporation

The addition of silicic acid to the medium increased the intracellular contents of both the Zn and Mn (Fig. 2.6b, 2.6d). The reason for the increased accumulation under the higher silicic acid regime is not clear. In the frustule, a significant difference was only obtained for Zn at pZn levels of 8.93 (Fig. 2.6a, 2.6c), in which case higher Zn/Si ratios were measured. Because the addition of silicic acid had no significant effect on the Si content of the frustules (pZn=9.23, *p*=0.724, df=5, *t*-test; pZn=8.93, *p*=0.844, df=5, *t*-test; data not shown), these changes must reflect higher Zn uptake to the cell wall rather than modifications to Si deposition.

Consistent with our previously discussed hypothesis of Zn incorporation, the observed decoupling between the Mn concentrations in the cell and the frustule (higher intracellular concentrations but no change in the frustule content) likely reflects the competition of Zn and Mn for the site leading to cell wall incorporation. Indeed, high intracellular Zn concentrations prevented Mn from being incorporated into the cell wall. The Zn/Si ratio found for the experiment performed at a pZn of 8.93 (Fig. 2.6a) was the highest measured in this study and indeed higher than the apparent maximum found during the Zn uptake experiment (Fig. 2.3), suggesting that an additional effect was associated with the higher silicic acid concentrations in the medium. For example, Si could be postulated to regulate the production of the hypothetical Zn-dependent

macromolecule responsible for metal incorporation into the frustule, which would consequently influence both Zn/Si and Mn/Si ratios in the cell wall.


## 2.5   Conclusion

Our investigations showed that Zn is incorporated into the frustule of the freshwater diatom *Stephanodiscus hantzschii*. The sigmoidal relationship between $Zn^{2+}$ concentrations in the growth medium and the Zn incorporated into the cell wall, Zn/Si, is consistent with previous results on *Thalassiosira pseudonana*, suggesting a common mechanism of Zn incorporation into the frustule of these two diatoms. In addition, the strong dependency of the Zn frustule content on the intracellular concentration of Zn indicates that the Zn that was incorporated into the cell wall was from an intracellular source. Experiments examining the effects of Mn and Si on Zn uptake to the frustule were consistent with a mechanism in which Zn and Mn would compete for an intracellular site leading to cell wall incorporation. These investigations also demonstrated that measurements of the Zn/Si ratio of fossil frustules from sediments could be a useful proxy for intracellular Zn concentrations, which are themselves strongly dependant on $Zn^{2+}$ concentrations of the water. This approach can therefore provide a suitable tool to study past Zn-phytoplankton interactions. Field and laboratory data, however, are still required to obtain a better biological and chemical understanding of the processes that control Zn incorporation into the frustules and potential diagenetic overprints.

## 2.6   References

Allison J. D., Brown D. S., and Novo-Gradac K. J. (1991) MINTEQA2/ PRODEFA2, a geochemical assessment model for environmental systems: Version 3.0 Users manual. *US Environmental Protection Agency, Athens, GA.* EPA/600/3-91/021.

Anderson M. A., Morel F. M. M., and Guillard R. R. L. (1978) Growth limitation of a coastal diatom by low zinc ion activity. *Nature* 276, 70-71.

Azam F., Hemmingsen B. B., and Volcani B. E. (1973) Germanium incorporation into the silica of diatom cell walls. *Arch. Microbiol.* 92(1), 11-20.

Catalano Dupuy D. L., Rial D. V., and Ceccarelli E. A. (2004) Inhibition of pea ferredoxin-NADP(H) reductase by Zn-ferrocyanide. *Eur. J. Biochem.* 271(22), 4582-4593.

De La Rocha C. L., Hutchins D. A., Brzezinski M. A., and Zhang Y. (2000) Effects of iron and zinc deficiency on elemental composition and silica production by diatoms. *Mar. Ecol. Prog. Ser.* 195, 71-79.

Ellwood M. J. and Hunter k. A. (2000a) The incorporation of zinc and iron into the frustule of the marine diatom *Thalassiosira pseudonana*. *Limnol. Oceanogr.* 45(7), 1517-1524.

Ellwood M. J. and Hunter K. A. (2000b) Variations in the Zn/Si record over the last interglacial glacial transition. *Paleoceanography* 15(5), 506-514.

Fisher N. S., Jones G. J., and Nelson D. M. (1981) Effects of copper and zinc on growth, morphology, and metabolism of *Asterionella japonica (Cleve)*. *J. Exp. Mar. Biol. Ecol.* 51, 37-56.

Frigeri L. G., Radabaugh T. R., Haynes P. A., and Hildebrand M. (2006) Identification of proteins from a cell wall fraction of the diatom *Thalassiosira pseudonana*. *Mol. Cell. Proteomics* 5.1, 182-193.

Gehlen M., Beck L., Calas G., Flank A.-M., Van Bennekom A. J., and Van Beusekom J. E. E. (2002) Unraveling the atomic structure of biogenic silica: evidence of the structural association of Al and Si in diatom frustules. *Geochim. Cosmochim. Acta* 66(9), 1601-1609.

Gill I. and Ballesteros A. (2000) Bioencapsulation within synthetic polymers (Part 1): sol-gel encapsulated biologicals. *Trends Biotechnol.* 18(7), 282-296.

Guillard R. R. L. (1975). In *Culture of marine invertebrate animals* (ed. W. L. Smith and M. H. Chanley), Plenum, New York. pp. 29-60.

Hassler C. S., Slaveykova V. I., and Wilkinson K. J. (2004) Discriminating between intra- and extracellular metals using chemical extractions. *Limnol. Oceanogr. Meth.* **2**, 237-247.

Hazelaar S. (2006) Nanoscale architecture: the role of proteins in diatom silicon biomineralization. PhD thesis, Groningen Univ.

Ingalls A. E., Anderson R. F., and Pearson A. (2004) Radiocarbon dating of diatom-bound organic compounds. *Mar. Chem.* **92**(1-4), 91-105.

Kroger N. and Wetherbee R. (2000) Pleuralins are involved in theca differentiation in the diatom *Cylindrotheca fusiformis*. *Protist* **151**(3), 263-273.

Kroger N., Deutzmann R., and Sumper M. (2001) Silica-precipitating peptides from diatoms: The chemical structure of silaffin-1A from *Cylindrotheca fusiformis*. *Journal of Biological Chemistry* **276**(28), 26066-26070.

Kroger N., Lehmann G., Rachel R., and Sumper M. (1997) Characterization of a 200-kDa Diatom Protein that is Specifically Associated with a Silica-Based Substructure of the Cell Wall. *Eur J Biochem* **250**(1), 99-105.

Kroger N., Deutzmann R., Bergsdorf C., and Sumper M. (2000) Species-specific polyamines from diatoms control silica morphology. *Proc. Natl. Acad. Sci. USA* **97**(26), 14133-14138.

Kroger N., Lorenz S., Brunner E., and Sumper M. (2002) Self-assembly of highly phosphorylated silaffins and their function in biosilica morphogenesis. *Science* **298**(5593), 584-586.

Lal D., Charles C., Vacher L., Goswami J. N., Jull A. J. T., McHargue L., and Finkel R. C. (2006) Paleo-ocean chemistry records in marine opal: Implications for fluxes of trace elements, cosmogenic nuclides ($^{10}$Be and $^{26}$Al), and biological productivity. *Geochim. Cosmochim. Acta* **70**, 3275-3289.

Morel F. M. M., Reinfelder J. R., Roberts S. B., Chamberlain C. P., Lee J. G., and Yee D. (1994) Zinc and carbon co-limitation of marine phytoplankton. *Nature* **369**, 740-742.

Nichols H. W. (1973) Growth media - freshwater. In *Handbook of Phycological Methods-Culture Methods and Growth Measurements* (ed. J. R. Stein), Cambridge University Press, Cambridge. pp. 7-24.

Okrasa K. and Kazlauskas R. J. (2006) Manganese-substituted carbonic anhydrase as a new peroxidase. *Chem. Eur. J.* **12**(6), 1587-1596.

Paasche E. (1973) Silicon and the ecology of marine plankton diatoms. I. *Thalassiosira pseudonana* (*Cyclotella nana*) grown in a chemostat with silicate as limiting nutrient. *Mar. Biol.* **19**(2), 117-126.

Rueter J. G. J. and Morel F. M. M. (1981) The interaction between zinc deficiency and copper toxicity as it affects the silicic acid uptake mechanisms in *Thalssiosira pseudonana*. *Limnol. Oceanogr.* **26**(1), 67-73.

Schroder H. C., Krasko A., Le Pennec G., Adell T., Hassanein H., Muller I. M., and Muller W. E. G. (2003) Silicase, an enzyme which degrades biogenous amorphous silica: contribution to the metabolism of silica deposition in the demosponge *Suberites domuncula*. *Prog. Mol. Subcell. Biol.* **33**, 249-268.

Slaveykova V. I. and Wilkinson K. J. (2005) Predicting the bioavailability of metals and metal complexes: critical review of the biotic ligand model. *Environmental Chemistry* **2**, 9-24.

Sunda W. G. and Huntsman S. A. (1992) Feedback interactions between zinc and phytoplankton in seawater. *Limnol. Oceanogr.* **37**(1), 25-40.

Sunda W. G. and Huntsman S. A. (1995) Cobalt and zinc interreplacement in marine phytoplankton: biological and geochemical implications. *Limnol. Oceanogr.* **40**(8), 1404-1417.

Sunda W. G. and Huntsman S. A. (1998) Interactions among $Cu^{2+}$, $Zn^{2+}$, and $Mn^{2+}$ in controlling cellular Mn, Zn, and growth rate in the coastal alga *Chlamydomonas*. *Limnol. Oceanogr.* **43**(6), 1055-1064.

Sunda W. G. and Huntsman S. A. (2000) Effect of Zn, Mn, and Fe on Cd accumulation in phytoplankton: implications for oceanic Cd cycling. *Limnol. Oceanogr.* **45**, 1501-1516.

Swift D. M. and Wheeler A. P. (1992) Evidence of an organic matrix from diatom biosilica. *J. Phycol.* **28**, 202-209.

Thamatrakoln K. and Hildebrand M. (2007) Silicon uptake in diatoms revisited: a model for saturable and nonsaturable uptake kinetics and the role of silicon transporters. *Plant Physiol.*, pp.107.107094.

Twining B. S., Baines S. B., Fisher N. S., Maser J., Vogt S., Jacobsen C., Tovar-Sanchez A., and Sañudo-Wilhelmy S. A. (2003) Quantifying trace elements in individual aquatic protist cells with a synchrotron x-ray fluorescence microprobe. *Anal. Chem.* **75**, 3806-3816.

Vrieling E. G., Beelen T. P. M., van Santen R. A., and Gieskes W. W. C. (2002) Mesophases of (bio)polymer-silica particles inspire a model for silica biomineralization in diatoms. *Angew. Chem. Int. Ed.* **41**(9), 1543-1546.

Vrieling E. G., Sun Q., Tian M., Kooyman P. J., Gieskes W. W. C., van Santen R. A., and Sommerdijk N. A. J. M. (2007) Salinity-dependent diatom biosilification implies an important role of external ionic strength. *Proc. Natl. Acad. Sci. USA* **104**(25), 10441-10446.

Xue H. B. and Sigg L. (1994) Zinc speciation in lake waters and its determination by ligand exchange with EDTA and differential pulse anodic stripping voltammetry. *Anal. Chim. Acta* **284**(3), 505-515.

Xue H. B., Kistler D., and Sigg L. (1995) Competition of copper and zinc for strong ligands in a eutrophic lake. *Limnol. Oceanogr.* **40**(6), 1142-1152.

# Assessing past changes in bioavailable zinc from a terrestrial (Zn/Si)$_{opal}$ record

Thomas Jaccard, Daniel Ariztegui and Kevin J. Wilkinson

## Abstract

Historical changes in bioavailable Zn concentrations of the surface waters of Lake Geneva were assessed by analyzing the zinc content of fossil diatoms. The measured ratios of Zn to Si in the opal ($(Zn/Si)_{opal}$) were consistent with both data obtained for cultured freshwater diatoms that were representative of lake Geneva and with field data. Reconstructed variations suggested that increased Zn uptake by phytoplankton occurred in the period from 1960-1980 resulting from an increased loading of Zn to the lake. Nonetheless, observed concentrations were sufficiently low that no adverse effects were expected on the pelagic community. The data presented here suggest that $(Zn/Si)_{opal}$ records may become a valuable tool to assess past changes in bioavailable Zn concentrations in freshwater systems.

## 3.1 Introduction

Zn is an essential metal for phytoplankton that becomes toxic at elevated concentrations (Anderson et al., 1978; Sunda and Huntsman, 1992). Due to its widespread use in industry, anthropogenic Zn loading to freshwaters (via wastewaters or atmospheric deposition) generally dominates over natural inputs. In phytoplankton, high Zn concentrations have been shown to decrease cell division rates (Tadros et al., 1990) and decouple cell division and photosynthesis (Fisher et al., 1981; Stauber and Florence, 1990). Nonetheless, Zn toxicity is very much dependent upon the physicochemistry of the freshwater, including chemical speciation. For example, low levels of phosphorus generally increase Zn toxicity to algae, while high phosphorus concentrations are able to decrease the adverse effects (Bates et al., 1985; Kuwabara, 1985; Paulsson et al., 2002). Consequently, waters in which phytoplankton growth is P-limited (most freshwaters) are likely to be more susceptible to Zn toxicity. The fate, bioaccumulation and biological effects of Zn in natural waters is generally more closely related to concentrations of the free ion rather than total metal (Anderson et al., 1978). $Zn^{2+}$ concentrations are regulated by a number of complex interactions between trace metal ions, major ions and ligands, including particles.

In the context of paleolimnological studies, these complex processes controlling Zn bioavailability may prevent the use of bulk Zn sedimentary concentrations to study past Zn-phytoplankton interactions. Recent laboratory studies on the freshwater diatom *Stephanodiscus hantzschii* have demonstrated that the Zn content of diatom siliceous cell-walls (frustules) reflects intracellular concentrations and is related to bioavailable Zn concentrations in water (Jaccard et al., in review-a; Chapter 2). Indeed, analyses of the Zn contents of fossil frustules may allow reconstruction of past changes in bioavailable Zn surface water concentrations.

Here, we applied this novel freshwater proxy to Lake Geneva sediments. Results were discussed in light of instrumental data and field observations available for the recent past.
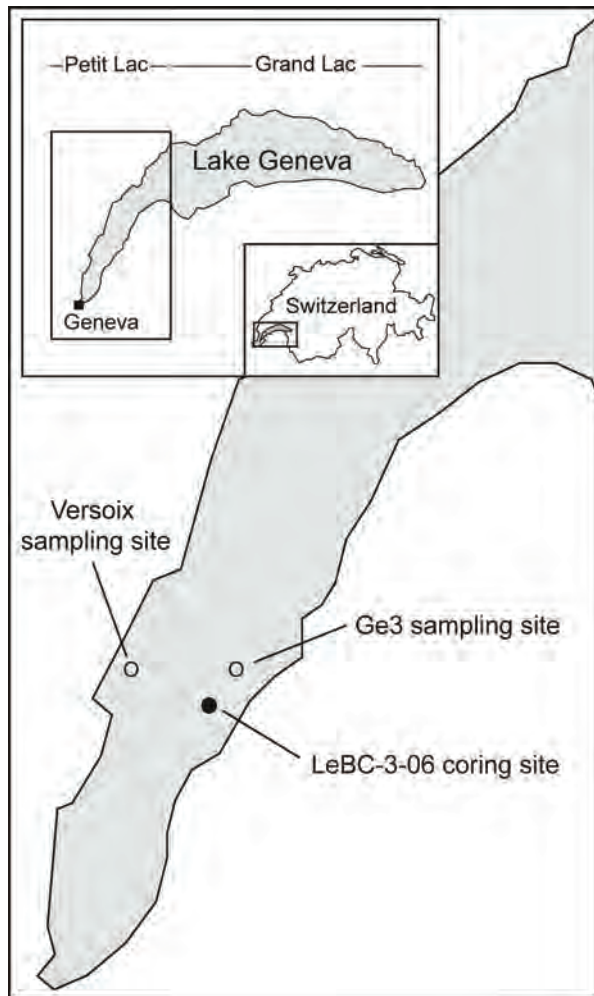
## 3.2 Geographical and ecological settings



**Figure 3.1** Location of Lake Geneva LeBC-3-06, Ge3 and Versoix coring and sampling sites.

Lake Geneva is the largest freshwater basin in Western Europe (surface area 580 $km^2$, volume 89 $km^3$) and is located in the Alps between France and Switzerland (Fig. 3.1). The lake is subdivided into two sub-basins: the "*Grand Lac*" and the "*Petit Lac*". The *Petit Lac* is a medium-sized basin (volume 3 $km^3$) with an average depth of 41 m.

Starting in the 1960s, heavy phosphorus inputs to the lake led to its eutrophication with a maximum of 90 µg P $L^{-1}$ attained in the late seventies. A subsequent decrease to the current concentration of *ca.* 30 µg P $L^{-1}$ is the result of a lake restoration program initiated in the early seventies. A long-term study (1974-1998) of the seasonal changes in the phytoplankton communities revealed that the Plankton Ecology Group (PEG) model (Sommer et al., 1986) was successful for predicting the dynamics of the first half of the year (Anneville et al., 2002a; Anneville et al., 2002b). Summer communities differed from those predicted by the PEG model and were subject to significant changes over the 24 year period. These shifts were interpreted as having resulted from gradual changes to parameters such as the deepening of the phosphorus-depleted layer and the timing of the depletion. According to these data, diatoms, which represented *ca.* 25% of the annual biomass, were mainly present in the autumn to the spring with about half of the total diatom biomass produced in springtime. Spring diatom assemblages were dominated by *Fragilaria crotonensis*, *Asterionella formosa*, *Stephanodiscus minutulus*, *Aulacoseira islandica* su *helvetica*, *Fragiliaria ulna* v. *angustissima* and *Stephanodiscus*

*alpinus*, summer assemblages by *Fragilaria crotonensis*, autumn assemblages by *Diatoma tenius*, *Stephanodiscus binderianus* and *Aulacoseira granulata* v. *angustissima*, and winter assemblages included *Stephanodiscus neoastraea* and *Cymatopleura solea* (Anneville et al., 2002a). These seasonal changes, while observed in the *Grand-Lac* basin, are not thought to differ greatly from the *Petit-Lac* basin (S. Lavigne, pers. comm.).

## 3.3  Methodology

The gravity core LeBC-3-06 was retrieved from the *Petit Lac* (6.21 °E / 46.28 °N; depth 57 m; Fig. 3.1) in February 2006. The core was split into two halves and magnetic susceptibility (Bartington MS2E sensor for high resolution surface measurements) was measured on the split core. One core-half was sampled with a centimeter resolution. These samples were dried (water content was measured), crushed and dated using $^{137}$Cs. Additionally, to ensure the recovery of the most recent sediments, $^{7}$Be (half-life of 53 d) was measured in the top of the core. $^{137}$Cs and $^{7}$Be analyses were performed by gamma spectroscopy using a high purity germanium well detector (Ortec).

The variation in biogenic opal content of these samples was determined by alkaline leaching (method adapted from Ohlendorf and Sturm, 2007). Briefly, 10 mL of 1 M NaOH were added to *ca*. 50 mg of dried, homogenized sediment. Samples were sonicated and then heated at 100 °C for 3 hours. A 5 mL sub-sample was collected from the hot solution, diluted in 40 mL of MilliQ water, neutralized with 5 mL of $HNO_3$ 1 M and analyzed for Si and Al contents. Si was determined from spectrophotometry (Spectronic 1201 spectrophotometer) at 820 nm using a molybdate-blue method (Merck, Spectroquant 14794). Al was quantified using inductively coupled plasma mass spectrometry (ICP-MS, Agilent, HP 4500). In order to correct for possible losses due to evaporation, samples were precisely weighted before and after digestion.

Total organic carbon (TOC), the Hydrogen index (HI, mass ratio of hydrocarbons to organic carbon) and the mineral carbon content (MinC) were measured with a Rock-

Eval (Re6) analyzer at the Geological Institute of the University of Neuchâtel, Switzerland (for more details, see Steinmann et al., 2003).

The second half of the core was sampled at half-centimeter intervals from the top of the core to 15 cm and then at each centimeter for the rest of the core. These samples were homogenized and an aliquot was collected for metal analyses. In this case, aliquots were dried and metals extracted overnight with 2 M $HNO_3$ (5 mL for 100 mg of dried sediment) at 100 °C (Osol, 1998). Metal concentrations were measured by ICP-MS. To ensure the reliability of the procedure, certified sediment material (STSD-1 and LKSD-1, Lynch, 1990) was extracted and measured simultaneously.

In the remaining wet samples, carbonate and organic matter were removed by addition of HCl (37%) and $H_2O_2$ (30%). Following a 63 μm filtering step, diatoms were separated from the <63 μm fraction using a heavy liquid separation (methodology adapted from Morley et al., 2004). In a 50 mL centrifuge tube, 25 mL of sodium polytungstate (SPT), at a density of 2.2 g $mL^{-1}$, were added to the wet sediment prior to homogenization (vortex) and sonication of the samples for 20 min. The supernatant was collected following a 20 minute centrifugation at 1500 x g. The entire procedure (*i.e.* sonication, centrifugation and collection of the supernatant) was repeated (3 times) using successive supernatants in order to improve the separation. By the end of the extraction procedure, the samples contained only diatoms and phytoclasts (revealed by microscopic inspection). Samples were collected on a 3 μm nitrocellulose filter. A concentrated $HNO_3$ / $KClO_3$ (8:1) solution (slightly heated if needed) was used to dissolve the filter and remove the phytoclasts (G. E. Gorin, pers. comm.).
Some samples, containing low quantities of opal were merged with their adjacent sample in order to have sufficient opal for Zn determinations. Diatom separations were performed in samples from the top of the sediment core to a depth of 17 cm. The opal fraction was then chemically cleaned using a methodology developed by Shemesh et al. (1988) and subsequently modified by Ellwood and Hunter (1999). This involved a reductive cleaning step (1h at 90°C in 2mL of a 0.1% w/w hydroxylamine hydrochloride – acetic acid solution), followed by etching of the frustules with NaF (30 min at 90°C in 2 mL of a 0.1% NaF solution) and a final oxidative cleaning with an $HNO_3$/HCl mixture (2h

at 90°C in 3.5 mL of a 8 M/2 M $HNO_3$/HCl solution). The residual cleaned silica was then washed 4 times with 10 mL of MilliQ water and dissolved in 8 mL of a 0.1 M/0.1 M HCl/HF solution for 4 hours at 80°C. We preferred a digestion with hot HCl/HF rather than NaOH (Paasche, 1973) since with the latter, silica polymerization was occasionally observed when samples were cooled down to room temperature. On the other hand, the possible loss of Si from solution due to the formation of volatile $SiF_4$ was investigated for the conditions used here. Within experimental error, Si recovery was 100%, attesting to the reliability of the dissolution process. Following dissolution, samples were centrifuged and visually inspected to ensure their complete dissolution. Zn concentrations were measured by ICP-MS (detection limits for Zn of 0.1 $\mu g\ L^{-1}$) while Si was determined in (100 times) diluted samples using spectrophotometry (see above). In order to assess the reliability of the overall procedure, two sediment samples (34 and 40 cm) were merged, homogenized, separated into four sub-samples and subject to full procedural replication beginning with the sediment separation.

Additionally, optical and electronic microscopic investigations were abundantly applied throughout the procedure. Some metals like Al, Ti or Mn, which are indicative of clay or oxide contamination, were measured in parallel with the Zn in the dissolved opal solution.

## 3.4 Results and discussion

### 3.4.1 Dating and bulk sediment analyses

Two distinct $^{137}$Cs peaks were observed at 5.5 and 11.5 cm (Fig. 3.2) and were attributed to the 1986 Chernobyl explosion and to the 1963 nuclear bomb tests respectively. Ages and sediment accumulation rates were interpolated between these peaks and the core-top. Detection of $^{7}$Be in the top of the core suggested that the most recent sediments were being recovered. TOC showed a constant increase from *ca*. 20 cm to the top of the core, with exception of the two uppermost samples, which had low organic carbon contents. A drop in mineral carbon content and an increase in magnetic susceptibility accompanied these low TOC values. These results strongly suggested a re-working of surface sediments.
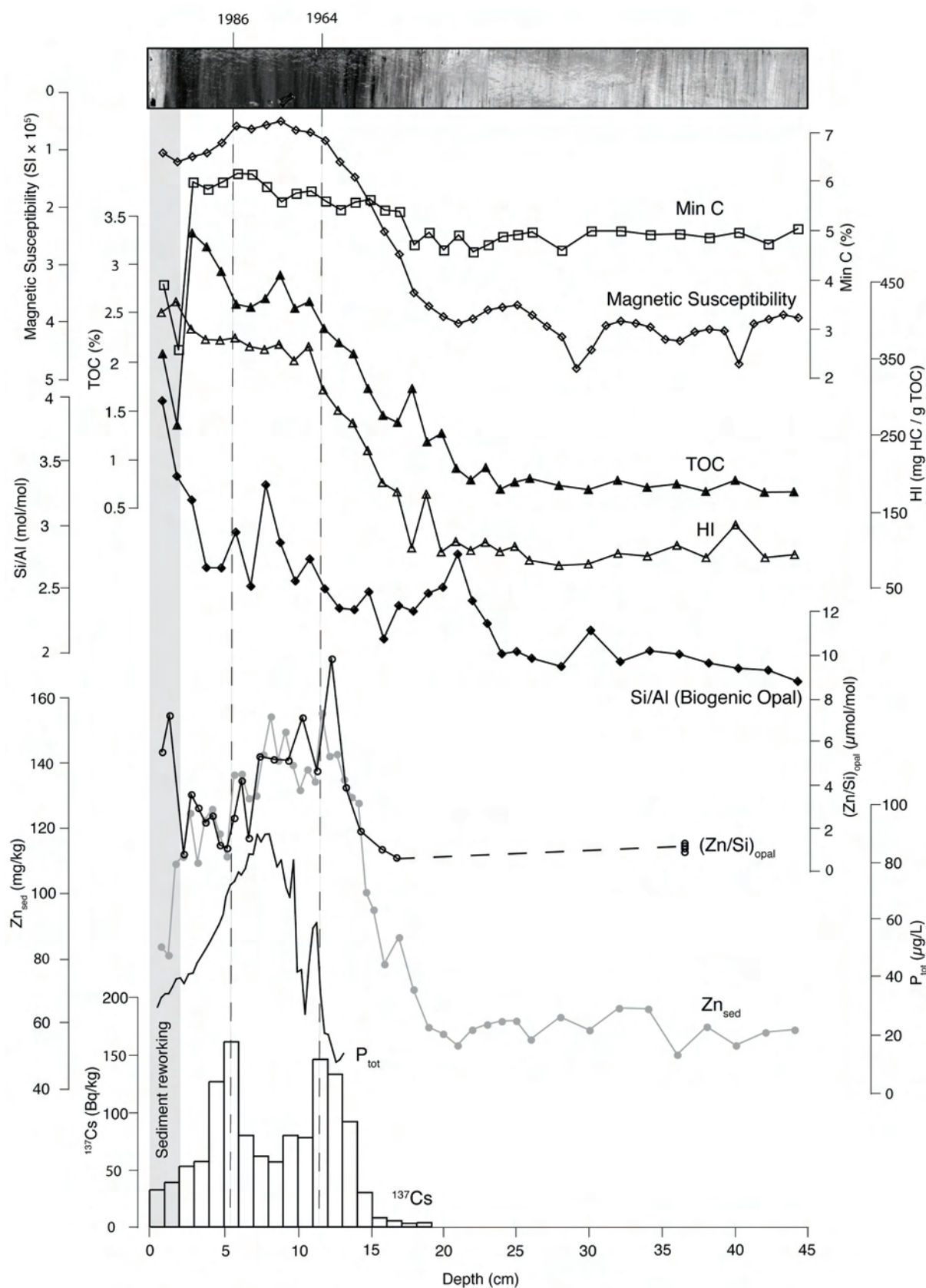
**Figure 3.2** LeBC-3-06 photography and downcore profile of magnetic susceptibility (open diamonds), mineral carbon (Min C, open squares), total organic carbon (TOC, filled triangles), hydrogen index (HI, open triangles), Si/Al (biogenic opal, filled diamonds), $(Zn/Si)_{opal}$ (open circles), $Zn_{sed}$ (filled grey circles) and $^{137}Cs$ (open bars) as a function of depth. Historical P concentrations in the lake are reported by the black line (CIPEL, 1957-2007). The shaded area indicates sediment reworking.

42

The observed decrease in TOC with depth is likely to reflect an increasing productivity with time resulting from the increasing phosphorus inputs to the lake. This result is consistent with both the observation of a decreasing HI with depth (indicative of a higher content of authigenic (algal) organic matter in the recent sediments) and with documented phosphorous concentrations in the lake (CIPEL, 1957-2007). Consistent with field observations (CIPEL, 1957-2007), our data suggest that algal productivity did not decrease in spite of a significant reduction in P.

This observation is attributed to changes in the phytoplankton community composition with the appearance of species with different mixotrophy and different growth and loss rates (Anneville and Pelletier, 2000). The variations in biogenic opal content of the sediment, presented as Si/Al molar ratios, could not be explained solely by the productivity trend or the annual variations in the trophic status of the lake. Since diatoms were mainly present in the period from autumn to spring (Anneville et al., 2002a), it is likely that they rarely experienced P-limiting conditions, which occurred mainly in the summer. Indeed, diatom growth would have been more affected by external factors, such as temperature and lighting than by nutrient status.
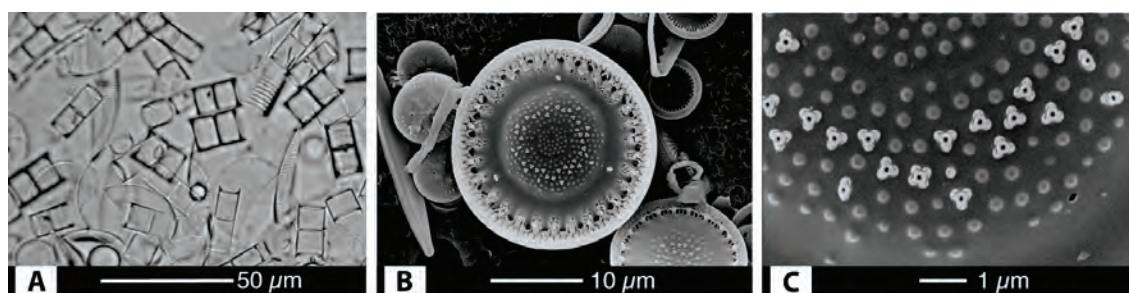


**Figure 3.3** Optical (A) and scanning electron (B and C) microscopic images of the opal samples.

### 3.4.2 Reliability of the $(Zn/Si)_{opal}$ analyses

Al, Ti and Mn were detected in the dissolved opal samples, potentially indicating contamination by a mineral phase such as aluminosilicates. Nonetheless, several lines of evidence suggest that Zn concentrations were due to biogenic contributions rather than contamination by the mineral phase. First, in culture experiments, Al and Mn have

been shown to be incorporated into the frustules (Gehlen et al., 2002; Jaccard et al., in review-a; Chapter 2), suggesting that at least a fraction of these metals resulted from biological uptake. Secondly, if the measured Zn originated from mineral contamination rather than direct uptake from the water column, correlations between Zn and Al, Ti or Mn would be expected in the dissolved opal. In fact, only weak correlations were obtained among these metals ($R^2$ =0.15 for Zn vs. Al; $R^2$ =0.03 for Zn vs. Ti and $R^2$ <0.01 for Zn vs. Mn; data not shown) suggesting different sources for Zn and the other metals. Finally, microscopic investigations (Fig. 3.3) did not reveal the presence of any contamination phase in the cleaned opal samples. Evaluations of the method precision (n=4) on full procedural replicates gave values that were within 15% of the expected mean.
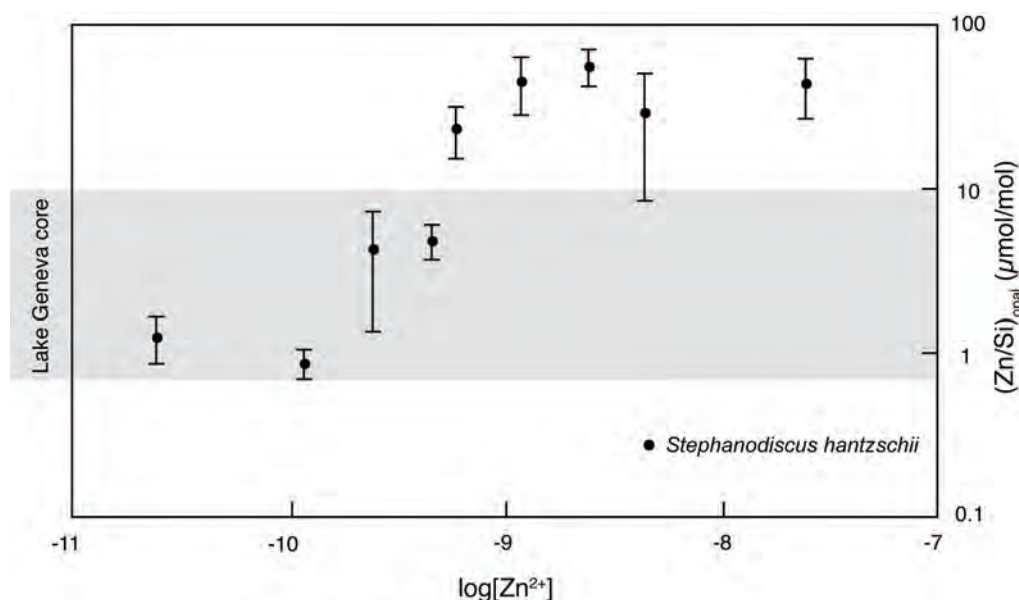


**Figure 3.4** $(Zn/Si)_{opal}$ molar ratios as a function of $[Zn^{2+}]$ for the cultured freshwater diatom *Stephanodiscus hantzschii* (Jaccard et al., in review-a; Chapter 2). Error bars indicate 95% confidence intervals. The shaded area represents the range of $(Zn/Si)_{opal}$ measured in diatoms extracted from the Lake Geneva LeBC-3-06 sediment core.

### 3.4.3 $(Zn/Si)_{opal}$ downcore variations

Values of $(Zn/Si)_{opal}$ ranged from 0.6 to 9.8 µmol mol$^{-1}$ and were in fair agreement with data from marine cores, which vary between 1.2 and 34 µmol/mol (Ellwood and Hunter, 2000; Hendry and Rickaby, 2008; Jaccard et al., in review-b; Chapter 4). These data

were also consistent with Zn/Si ratios found in the cultured freshwater diatom *S. hantzschii* (Fig. 3.4, Jaccard et al., in review-a; Chapter 2) , which is a diatom that was abundantly found in Lake Geneva in the seventies and the eighties (CIPEL, 1957-2007). According to this dataset, maximum $Zn^{2+}$ concentrations were in the neighborhood of 5 $\times$ $10^{-10}$ M with the lowest values, below or near *ca.* 2 $\times$ $10^{-10}$ M (see Fig. 3.4). Furthermore, a monthly survey of dissolved Zn concentrations in surface waters (collected at 3 and 5 m) of the Ge3 sampling site (Fig. 3.1) between 2000 and 2007 revealed no clear seasonal pattern with average concentrations of *ca.* 5 nM (data from P. Nirel, pers. comm.). Based upon the assumption that only a small fraction of dissolved Zn is in its free ionic form, the value is in the range of those estimated from the $(Zn/Si)_{opal}$ data and agrees well with $Zn^{2+}$ concentrations reported for other Swiss lakes, ranging from 0.3 to 15 $\times$ $10^{-10}$ M (Knauer et al., 1998). In addition, *in situ* voltametric data collected in the *Petit Lac* near Versoix (Fig. 3.1) showed that dynamic Zn concentrations ranged from 2 nM for nearshore values (harbor) to 0.1 nM for offshore (2 km) values (Tercier-Waeber and Buffle, 2000). These concentrations are slightly higher than those reconstructed from the $(Zn/Si)_{opal}$ ratios. Since the mobile Zn fraction accounts for the free ion and small labile complexes (Tercier-Waeber et al., 1998), the latter, if not bioavailable, could explain the observed differences.

We observed a strong positive correlation (Spearman correlation coefficient, $r_s$=0.76; df=16, *p*<0.01) between the Zn content of the sediment, $Zn_{sed}$, and the $(Zn/Si)_{opal}$ ratio between 2 and 14 cm. On the other hand, in surface sediments, the signals were decoupled: Zn concentrations in sediments decreased while $(Zn/Si)_{opal}$ increased. This result might be due to the sediment re-working of the recent core depths (see above). In the older parts of the sediment core (below 15 cm), increases in $(Zn/Si)_{opal}$ lagged behind increases in the Zn content of the sediment, $Zn_{sed}$. For example, $Zn_{sed}$ increased below depths of 19 cm while $(Zn/Si)_{opal}$ increased from 16 cm. A threshold effect observed in laboratory culture experiments at low $Zn^{2+}$ concentrations (Fig. 3.4) might explain these differences: variations in $Zn^{2+}$ water concentrations in the $10^{-10}$-$10^{-11}$ M range are not expected to influence the $(Zn/Si)_{opal}$ ratio whereas they might lead to changes in Zn deposition to the sediments.

Al has been shown to become incorporated into fossil frustules through a diagenetic process where an aluminosilicate layer is formed on the surface of the opal (Koning et

al., 2007). This process, if also active for Zn, might explain the strong relationship obtained between $Zn_{sed}$ and $(Zn/Si)_{opal}$. The good agreement between the field and laboratory data and the lack of coupling between Zn and Al (and other metals) in the frustules suggests, however, that the $(Zn/Si)_{opal}$ signal recorded primarily surface water conditions and was little affected by post-depositional processes.

If we assume that $Zn_{sed}$ reflects the total Zn loaded to surface waters (*i.e.*, most of the Zn input is incorporated in the sediments, Sigg et al., 1996), the downcore variations in $Zn_{sed}$ and $(Zn/Si)_{opal}$ suggest that the anthropogenic loading of Zn - with a maximum during the sixties and the seventies - was accompanied by higher Zn uptake by phytoplankton.

In freshwaters, most of the dissolved Zn is present as organic complexes (Xue and Sigg, 1994). The organic ligands likely result from the exudation of microorganisms or from the degradation of the organisms themselves. If we assume thermodynamic control of Zn uptake, the bioavailability of Zn will be mainly controlled by the quantity of dissolved Zn and the amount of metal-binding ligands (Morel and Hering, 1993; Campbell, 1995). The observed positive correlation between $Zn_{sed}$ and $(Zn/Si)_{opal}$ suggests that, here, changes in Zn uptake to diatom were likely mainly controlled by variations of dissolved Zn concentration.

Comparison of these data with laboratory data and known field $Zn^{2+}$ concentrations suggests that maximum $Zn^{2+}$ concentrations of surface waters were in the sub-nanomolar range. These values of $Zn^{2+}$, which are in the range of optimal growth conditions for freshwater phytoplankton (Knauer et al., 1997; Hassler et al., 2005; Jaccard et al., in review-a; Chapter 2), are not expected to have any negative influence on phytoplankton development.In addition, these high concentrations are associated with the highest P concentrations in the lake, which could contribute to decrease the Zn toxicity.


## 3.5   Conclusion

A $(Zn/Si)_{opal}$ record has been produced for recent lake Geneva sediments and is, to our knowledge, the first freshwater $(Zn/Si)_{opal}$ record. It was consistent with data obtained from culture studies and with data collected from the surface waters. The downcore

results indicated that the heavy anthropogenic input of Zn during the sixties and the seventies led to an increase in Zn uptake by phytoplankton. The extrapolated concentrations were nonetheless likely not high enough to have induced adverse effects on the pelagic community. According to this study, the zinc content of the frustules of fossil diatoms is likely to be a valuable tool to reconstruct past concentrations of bioavailable Zn in freshwater systems. Such a tool would be particularly relevant for assessing the impact of past events of anthropogenic loading of Zn to the biological communities.

## 3.6    References

Anderson M. A., Morel F. M. M., and Guillard R. R. L. (1978) Growth limitation of a coastal diatom by low zinc ion activity. *Nature* **276**, 70-71.

Anneville O. and Pelletier J.-P. (2000) Recovery of Lake Geneva from eutrophication: quantitative response of phytoplankton. *Arch. Hydrobiol.* **148**(4), 607-624.

Anneville O., Ginot V., Druart J.-C., and Angeli N. (2002a) Long-term study (1974-1998) of seasonal changes in the phytoplankton in Lake Geneva: a multi-table approach. *J. Plankton Res.* **24**(10), 993-1008.

Anneville O., Souissi S., Ibanez F., Ginot V., Druart J.-C., and Angeli N. (2002b) Temporal mapping of phytoplankton assemblages in Lake Geneva: annual and interannual changes in their patterns of succession. *Limnol. Oceanogr.* **47**(5), 1355-1366.

Bates S. S., Tessier A., Campbell P. G. C., and Letourneau M. (1985) Zinc-phosphorous interactions and variation in zinc accumulation during growth of *Chlamydomonas variabilis* (Chlorophyceae) in batch culture. *Can. J. Fish. Aquat. Sci.* **42**(1), 86-94.

Campbell P. G. C. (1995) Interactions between trace metals and aquatic organisms: a critique of the free-ion activity model. In *Metal speciation and bioavailability in aquatic systems* (ed. A. Tessier and D. R. Turner), John Wiley and Sons, Chichester. pp. 45-102.

CIPEL. (1957-2007) Commission internationale pour la protection des eaux du Leman (CIPEL): rapports annuels de campagnes (ed. CIPEL).

Ellwood M. J. and Hunter K. A. (1999) Determination of the Zn/Si ratio in diatom opal: a method for the separation, cleaning and dissolution of diatoms. *Mar. Chem.* **66**(3-4), 149-160.

Ellwood M. J. and Hunter K. A. (2000) Variations in the Zn/Si record over the last interglacial glacial transition. *Paleoceanography* **15**(5), 506-514.

Fisher N. S., Jones G. J., and Nelson D. M. (1981) Effects of copper and zinc on growth, morphology, and metabolism of *Asterionella japonica (Cleve)*. *J. Exp. Mar. Biol. Ecol.* **51**, 37-56.

Gehlen M., Beck L., Calas G., Flank A.-M., Van Bennekom A. J., and Van Beusekom J. E. E. (2002) Unraveling the atomic structure of biogenic silica: evidence of the structural association of Al and Si in diatom frustules. *Geochim. Cosmochim. Acta* **66**(9), 1601-1609.

Hassler C. S., Behra R., and Wilkinson K. J. (2005) Impact of zinc acclimation on bioaccumulation and homeostasis in *Chlorella kesslerii*. *Aquat. Toxicol.* **74**(2), 139-149.

Hendry K. R. and Rickaby R. E. M. (2008) Opal (Zn/Si) ratios as a nearshore geochemical proxy in coastal Antarctica. *Paleoceanography* **23**(PA2218), , doi:10.1029/2007PA001576.

Jaccard T., Ariztegui D., and Wilkinson K. J. (in review-a) Incorporation of zinc into the frustule of the freshwater diatom *Stephanodiscus hantzschii*. *Chem. Geol.*

Jaccard T., Robinson R. S., Ariztegui D., and Wilkinson K. J. (in review-b) Changes in micronutrient bioavailability and biological productivity in the glacial Southern Ocean. *Geophys. Res. Lett.*

Knauer K., Behra R., and Sigg L. (1997) Effects of free $Cu^{2+}$ and $Zn^{2+}$ ions on growth and metal accumulation in freshwater algae. *Environ. Toxicol. Chem.* **16**(2), 220-229.

Knauer K., Ahner B. A., Xue H. B., and Sigg L. (1998) Metal and phytochelatin content in phytoplankton from freshwater lakes with different metal concentrations. *Environmental Toxicology and Chemistry* **17**(12), 2444-2452.

Koning E., Gehlen M., Flank A. M., Calas G., and Epping E. (2007) Rapid post-mortem incorporation of aluminum in diatom frustules: Evidence from chemical and structural analyses. *Mar. Chem.* **106**(1-2), 208-222.

Kuwabara J. S. (1985) Phosphorus-zinc interactive effects on growth by *Selenastrum capricornutum* (chlorophyta). *Environ. Sci. Technol.* **19**, 417-421.

Lynch J. (1990) Provisional elemental values for eight new geochemical lake sediment and stream sediment reference materials LKSD-1, LKSD-2, LKSD-3, LKSD-4, STSD-1, STSD-2, STSD-3 and STSD-4. *Geostandard Newslett.* **14**(1), 153-167.

Morel F. M. M. and Hering J. G. (1993) *Principles and applications of aquatic chemistry*. Wiley Interscience.

Morley D. W., Leng M. J., Mackay A. W., Sloane H. J., Rioual P., and Battarbee R. W. (2004) Cleaning of lake sediment samples for diatom oxygen isotope analysis. *J. Paleolimnol.* **31**(3), 391-401.

Ohlendorf C. and Sturm M. (2007) A modified method for biogenic silica determination. *J. Paleolimnol.* **39**(1), doi:10.1007/s10933-007-9100-7.

Osol. (1998) Ordonnance du 1er juillet 1998 sur les atteintes portées aux sols (Osol), Vol. 814.12. Office federal de la protection de l'environnement.

Paasche E. (1973) Silicon and the ecology of marine plankton diatoms. I. *Thalassiosira pseudonana* (*Cyclotella nana*) grown in a chemostat with silicate as limiting nutrient. *Mar. Biol.* **19**(2), 117-126.

Paulsson M., Mansson V., and Blanck H. (2002) Effects of zinc on the phosphorus availability to periphyton communities from the river Gota Alv. *Aquat. Toxicol.* **56**(2), 103-113.

Shemesh A., Mortlock R. A., Smith R. J., and Froelich P. N. (1988) Determination of Ge/Si in marine siliceous microfossils: Separation, cleaning and dissolution of diatoms and radiolaria. *Mar. Chem.* **25**, 305-323.

Sigg L., Kistler D., and Ulrich M. M. (1996) Seasonal variations in a eutrophic lake. *Aquat. Geochem.* **1**, 313-328.

Sommer U., Gliwicz Z. M., Lampert W., and Duncan A. (1986) The PEG-model of seasonal succession of planktonic events in fresh waters. *Arch. Hydrobiol.* **106**, 433-471.

Stauber J. L. and Florence T. M. (1990) Mechanism of toxicity of zinc to the marine diatom *Nitzschia closterium*. *Mar. Biol.* **105**, 519-524.

Steinmann P., Adatte T., and Lambert P. (2003) Recent changes in sedimentary organic matter from Lake Neuchâtel (Switzerland) as traced by rock-eval pyrolysis. *Eclogae Geol. Helv.* **96**(suppl. 1), 109-116.

Sunda W. G. and Huntsman S. A. (1992) Feedback interactions between zinc and phytoplankton in seawater. *Limnol. Oceanogr.* **37**(1), 25-40.

Tadros G. M., Mbuthia P., and Smith W. (1990) Differential response of marine diatoms to trace metals. *Bull. Environ. Contam. Toxicol.* **44**, 826-831.

Tercier-Waeber M. L. and Buffle J. (2000) Submersible online oxygen removal system coupled to an in situ voltammetric probe for trace element monitoring in freshwater. *Environ. Sci. Technol.* **34**(18), 4018-4024.

Tercier-Waeber M. L., Belmont-Hebert C., and Buffle J. (1998) Real-time continuous Mn(II) monitoring in lakes using a novel voltammetric in situ profiling system. *Environ. Sci. Technol.* **32**(10), 1515-1521.

Xue H. B. and Sigg L. (1994) Zinc speciation in lake waters and its determination by ligand exchange with EDTA and differential pulse anodic stripping voltammetry. *Anal. Chim. Acta* **284**(3), 505-515.

# Changes in micronutrient bioavailability and biological productivity in the glacial Southern Ocean

Thomas Jaccard, Rebecca S. Robinson, Daniel Ariztegui and Kevin J. Wilkinson

## Abstract

The Southern Ocean plays an important role in the $CO_2$ air-sea balance and has regulated atmospheric $CO_2$ concentrations over glacial-interglacial cycles. Increased productivity resulting from higher dust deposition over Antarctica could have contributed to lower the atmospheric $CO_2$ content during ice ages. Although Fe-fertilization has been observed in waters of present Southern Ocean, there is still a lack of convincing evidence for such events in the past. Nutrients supply and consumption were reconstructed by analyzing the Zn content of diatom frustules and diatom-bound $\delta^{15}N$ from sediments of the South Atlantic. The data evidence for the first time a greater availability of micronutrients to phytoplankton during the LGM. These changes, in concert with higher nitrate consumption, likely resulted from massive meltwater discharge to the Southern Ocean. The widespread presence of meltwaters and free-drifting icebergs may have stimulated nutrient drawdown that would have contributed to the sequestration of additional $CO_2$ during glacials.

## 4.1 Introduction

In the contemporary Southern Ocean, the presence of $CO_2$-rich waters at the surface, together with an incomplete (macro-)nutrient consumption, result in a net transfer of $CO_2$ from the ocean to the atmosphere. Nutrient and $CO_2$ drawdown is restricted by the paucity of the micronutrient Fe and the low light levels in the Southern Ocean. An increase in nutrient consumption and the delivery of carbon to the deep sea (*i.e.* the biological pump) in the Antarctic could affect the air-sea balance of $CO_2$. This mechanism has been proposed to explain the substantially reduced atmospheric carbon dioxide concentrations estimated during ice ages (Knox and McElroy, 1984; Sarmiento and Toggweiler, 1984; Siegenthaler and Wenk, 1984), when higher dust-borne Fe input would have significantly enhanced export productivity (Martin, 1990). Although Fe stimulation of productivity and carbon sequestration has been widely documented in the high nutrient low chlorophyll (HNLC) waters of present Southern Ocean (Blain et al., 2007; Boyd et al., 2007), there is still a lack of convincing evidence for such events in the past.

Glacial meltwater input and free-drifting icebergs appear to exert a major influence on the pelagic ecosystem of the Southern Ocean. The presence of meltwater in the coastal waters west of the Antarctic peninsula was correlated to phytoplankton blooms that extended spatially over 100 km offshore (Dierssen et al., 2002). Meltwater and biomass production are linked by the physical stratification of the water column: input of freshwater creates a stable and shallow surface layer that favors phytoplankton growth. In addition to this physical stabilization, the presence of limiting nutrients in these waters, such as Fe, may also have a positive effect on bloom development in offshore regions. Observations of high microphytoplankton biomass associated with two free-drifting icebergs in the northwest Weddell Sea during the austral spring led to the hypothesis that the release of trace elements and Fe from the melting icebergs, into the surrounding waters stimulated the local productivity (Smith et al., 2007). Phytoplankton culturing experiments confirmed that micronutrients associated with the iceberg-borne terrigenous material were bioavailable: addition of this terrigenous fraction to a media containing no other metals fully supported the growth of the coastal diatom *Thalassiosira weissflogii* (Smith et al., 2007). Free-drifting icebergs and their associated

communities may indeed enhance the sequestration of carbon in the deep sea. This process may have been even more important during the last ice age when iceberg discharge and meltwater inputs were higher. Oxygen isotope analyses of planktonic and benthic foraminifers combined with diatom transfer function showed that from 35 to 17 kyr BP, the Southern Ocean polar front was covered by a meltwater lid containing a significant contribution from melting icebergs calved from Antarctic ice shelves (Labeyrie et al., 1986). Oxygen isotopes in biogenic silica from the Atlantic and Indian sector of the Southern Ocean are low during the Last Glacial Maximum (LGM). This runs counter to the global ice volume signal observed in planktonic foraminifera and has been interpreted to be the result of meltwater in surface waters during diatom growth season (Shemesh et al., 1994).

To study the potential impact of these meltwater input events - and their associated micronutients delivery - on productivity, we assessed changes in Zn availability to phytoplankton by measuring the Zn content of diatom opal (Ellwood and Hunter, 1999; Ellwood and Hunter, 2000a; Jaccard et al., submitted; Chapter 2) and in relative nitrate consumption by isotopic measurements of diatom-bound nitrogen (Shemesh et al., 1993). These indicators were integrated in a multi-proxy approach and combined with oxygen isotope data of biogenic silica and other proxies available for sedimentary core RC13-259 from the Antarctic sector of the South Atlantic (54°S, 5°W; Fig. 4.1).

## 4.2 Methodology

The physical separation of the fossil diatom frustules from the sediments and the procedure for diatom-bound $\delta^{15}N$ analyses was performed at the Geosciences Department of the University of Princeton, USA, and followed Robinson and Sigman (2008). For the $(Zn/Si)_{opal}$ analyses, *ca.* 8 mg of the purified opal fraction were chemically cleaned following a methodology adapted from Ellwood and Hunter (1999). This involved a reductive cleaning step (1h at 90°C in 2mL of a 0.1% w/w hydroxylamine hydrochloride – acetic acid solution), followed by etching of the frustules with NaF (30 min at 90°C in 2 mL of a 0.1% NaF solution) and a final oxidative cleaning with an $HNO_3/HCl$ mixture (2h at 90°C in 3.5 mL of a 8 M/2 M $HNO_3/HCl$ solution). The cleaned opal was dissolved in 10 mL of a 0.1M/0.1M HF/HCl solution (4 hours, 90°C). We

preferred hot HCl/HF rather than an alkaline dissolution since with the latter, silica polymerization was occasionally observed when samples were cooled down to room temperature. On the other hand, the possible loss of Si from solution due to the formation of volatile $SiF_4$ was investigated for the conditions used here. Within experimental error, Si recovery was 100%, attesting to the reliability of the dissolution process. After dissolution, samples were centrifuged and visually inspected to ensure complete dissolution of the silica. In the solution containing the dissolved silica, Zn concentrations were measured by inductively coupled plasma mass spectrometry (ICP-MS, Agilent, HP 4500, detection limits for Zn of 0.1 ppb) while Si was determined in diluted samples (100 x) using a molybdate-blue spectrophotometric method at 820 nm (Merck Spectroquant 14794 reagents and Perkin Elmer Lambda 35 spectrophotometer). Blank HF/HCl digests were systematically verified for metal contamination. For both, $\delta^{15}N$ and $(Zn/Si)_{opal}$ analyses, a full procedural replication was employed that began with separate sediment separations.

Opal and Ti accumulation rates have been interpolated and normalized with Th data from R. Anderson (pers. comm. to R.S. Robinson, 2005).
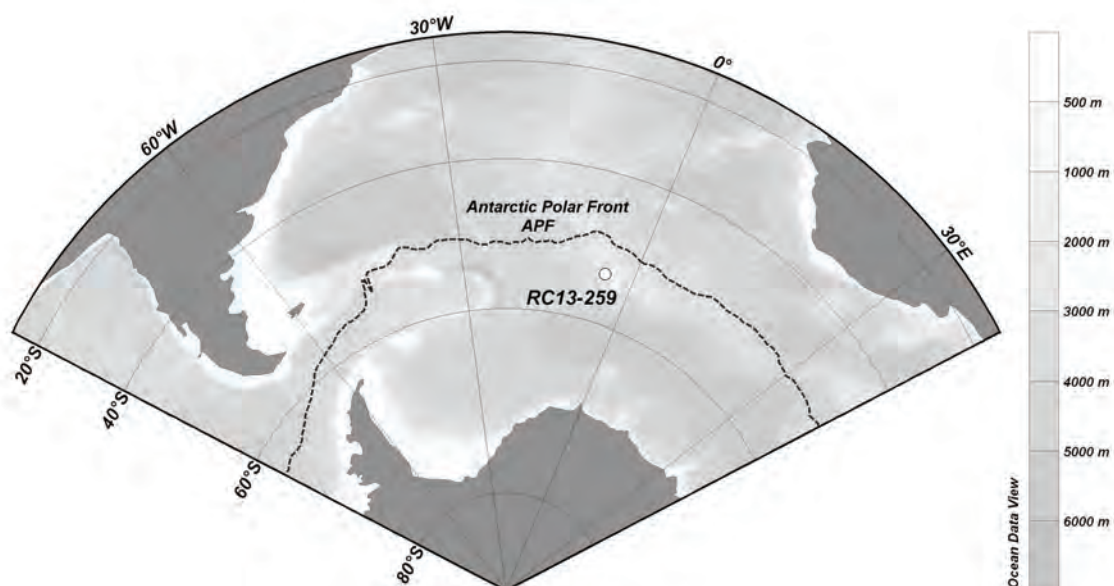


**Figure 4.1** Map of the South Atlantic showing the RC13-259 site location. The position of the Antarctic Polar Front (APF) is delineated by the dashed line (Orsi et al., 1995).

## 4.3  Results and discussion

Based upon the light values of $\delta^{18}O$ in biogenic silica (Shemesh et al., 1994), the site RC13-259 experienced high freshwater inputs to surface waters during the ice age, with distinct minima associated with the beginning of the glacial episode and the LGM (Fig. 4.2). The $\delta^{18}O_{silica}$ minima correspond to maxima in dust deposition over Antarctica (Petit et al., 1999), as interpreted from the Titanium accumulation rates (Latimer and Filippelli, 2001). Zn concentrations in diatom opal, $(Zn/Si)_{opal}$, are also at a maximum during the LGM but stay low during most of the ice age. These values are somewhat higher than reported in a previous record from the same core (Ellwood and Hunter, 2000b). This was likely due to different methodologies that were applied in these two studies. Since we observed Si polymerization for samples dissolved in alkaline solutions, we slightly modified Ellwood and Hunter's methodology (Ellwood and Hunter, 1999) so as to employ a weak HF solution for the dissolution of diatom opal (see methodological section). This modification resulted in a high reproducibility among samples that underwent full separate analytical procedures (*i.e.*, beginning with separate sediment separations) and is evidence for a reliable dataset. Two lines of evidence indicate that the observed $(Zn/Si)_{opal}$ variations are mainly related to changes in bioavailable Zn conditions rather than changes in Zn deposition mechanisms among diatom species. First, laboratory studies conducted with the marine diatom *Thalassiosira pseudonana* (Ellwood and Hunter, 2000a) and the freshwater diatom *Stephanodiscus hantzschii* suggested a common mechanism of Zn incorporation into the frustule of these two diatoms (for more details about the mechanism, see Jaccard et al., in review; Chapter 2). Secondly, we found only weak correlation (Spearman correlation coefficient of 0.38; data not shown) between the $(Zn/Si)_{opal}$ ratio and the percentage of *E. Antarctica* (Fig. 4.2), the dominant species in glacial assemblages, suggesting that the diatom composition of the samples had no or little effect on the observed $(Zn/Si)_{opal}$ variations.

▷**Figure 4.2** RC13-259 downcore profile of diatom $\delta^{18}O_{silica}$ (Shemesh et al., 1994) (black), opal concentration (Charles et al., 1991) (grey) and opal Th-normalized accumulation rate (orange), diatom-bound $\delta^{15}N$ (Robinson and Sigman, 2008) (light blue), Th-normalized Ti accumulation rate (Latimer and Filippelli, 2001) (green), $(Zn/Si)_{opal}$ (red) and abundance of *C. davisiana* and *E. antarctica* (Shemesh et al., 1994) (dark blue and light green respectively) as a function of depth. In diatom-bound $\delta^{15}N$ and $(Zn/Si)_{opal}$ profiles open squares and open triangles indicate respectively "full replicate" and "partial replicate" analyses (beginning with separate sediment separations and separate cleaning respectively). When several replicates have been analyzed, filled circles represent the average value. MIS timings (Martinson et al., 1987) are based on Charles et al. age model (Charles et al., 1991). The apparent period of massive meltwater discharge to surface waters is highlighted in grey.
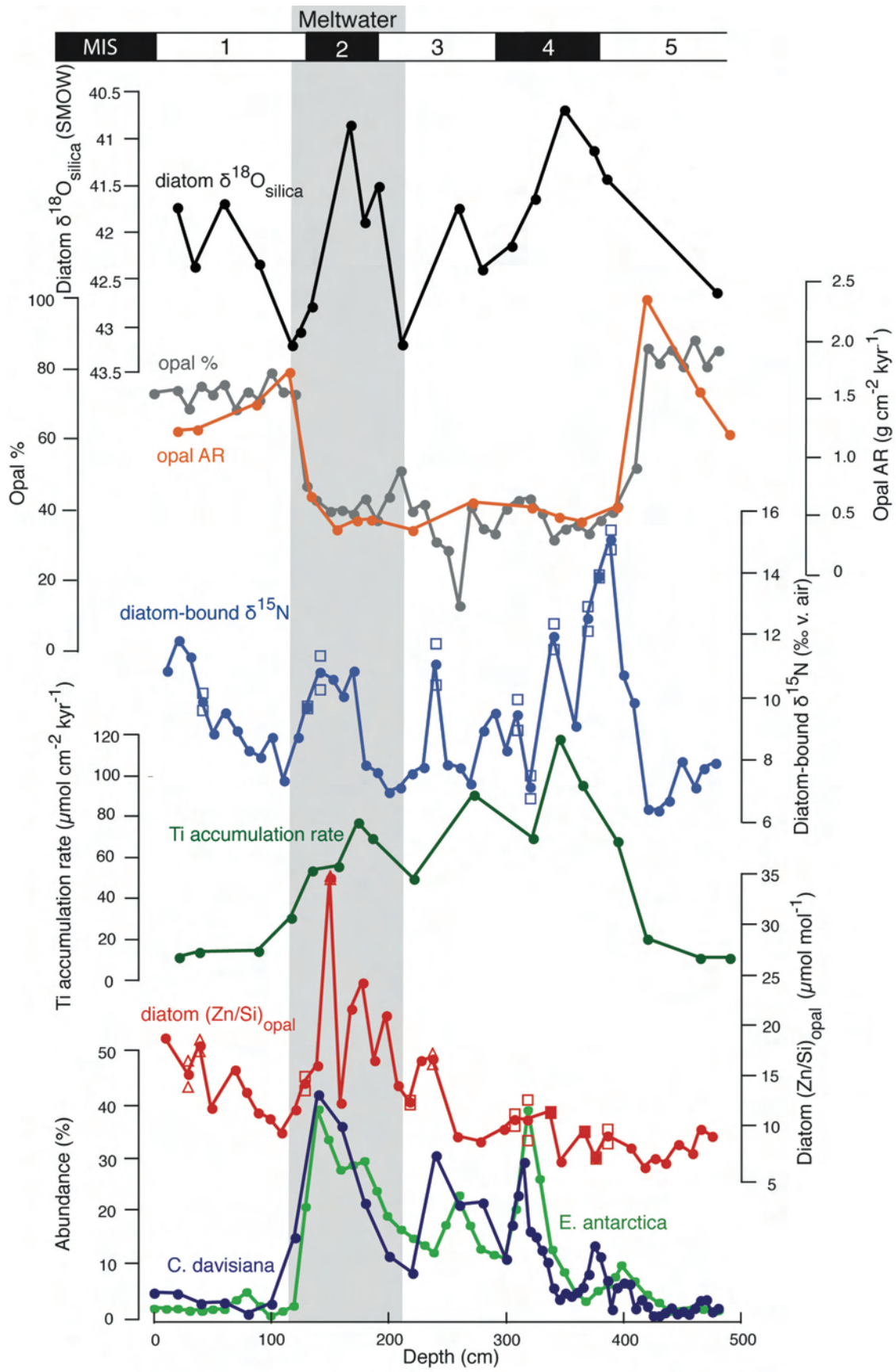
The $(Zn/Si)_{opal}$ values indicate higher bioavailable Zn concentrations in surface waters during the LGM, when both high dust and freshwaters were supplied to surface waters. Since the source of the continental dust deposited to Antarctica was constant over the glacial (Basile et al., 1997), the absence of a $(Zn/Si)_{opal}$ peak during MIS4 and thus a lack of coupling between $(Zn/Si)_{opal}$ and the dust supply over the entire ice age argues for additional mechanisms influencing the availability of Zn to phytoplankton. Since the bioavailability of trace metals is generally related to the free metal ion rather than the total metal concentration (Sunda and Guillard, 1976; Anderson et al., 1978; Hudson and Morel, 1990), chemical speciation in surface waters greatly influences trace metal uptake by phytoplankton. In seawater, a significant fraction of Zn (>98%) is complexed by strong natural organic ligands (Bruland, 1989; Ellwood and Van den Berg, 2000; Ellwood, 2004) - likely resulting from the microbial degradation of microorganisms or from exudation of the organisms themselves. If it is assumed that the organic-Zn complexes are not bioavailable, then, the bioavailability of Zn will be mainly controlled by the quantity of dissolved Zn and the amount of metal-binding ligand. In coastal Antarctica, the $(Zn/Si)_{opal}$ proxy was used to negatively correlate bioavailable Zn concentrations and surface water salinities (Hendry and Rickaby, 2008). This was likely the result of high $Zn^{2+}$ and/or low ligand concentrations in the arriving meltwaters. Nevertheless, the expected simultaneous increase in the concentrations of other metals may have attenuated somewhat the overall effect due to competitive interactions for the same ligands (Xue et al., 1995).

Since the mechanism of Zn supply to surface waters (*i.e.* associated or not with meltwater) is an important parameter for Zn bioavailability, we combined $\delta^{18}O$ data of the planktonic foraminifera, *N. pachyderma*, and diatom $\delta^{18}O_{silica}$ data in order to reconstruct changes in surface water isotopic composition (Charles et al., 1991; Shemesh et al., 1992) (*i.e.* salinity) during last ice age. Because fluxes of *N. pachyderma* have been show to be tied to periods of increasing primary productivity or bloom events (Kohfeld et al., 1996), both $\delta^{18}O$ signals record seasonal growth surface water conditions. Changes in surface water $\delta^{18}O$ show highly depleted values of 2.7‰ and 1.9‰ for respectively the LGM and MIS4 compared to late Holocene values (Fig. 4.3). $\delta^{18}O$ of the deep ocean waters have been shown to be respectively *ca.* 1.1‰ and 0.7‰ heavier during the LGM and MIS4 than during late Holocene (Martinson et al.,

1987). This corresponds roughly to surface water at site RC13-259 being 3.8‰ (LGM) and 2.6‰ (MIS4) lighter than deep ocean value. A simple isotopic mass balance calculation (by taking *ca.* -53‰ for the $\delta^{18}O$ of glacial Antarctic ice (EPICA, 2006)) yields a mixture of 7% freshwater to 93% of seawater during the LGM and 5% freshwater to 95% of seawater during MIS4. Nonetheless, one line of evidence suggests however that these estimations - especially for the LGM - are too conservative. *N. pachyderma* $\delta^{18}O$ records conditions between 40 and 200 m and is thought to reflect surface temperature and salinity conditions in regions with deep surface mixed layer (>300 m) and minimal seasonal temperature changes (Kohfeld et al., 1996).
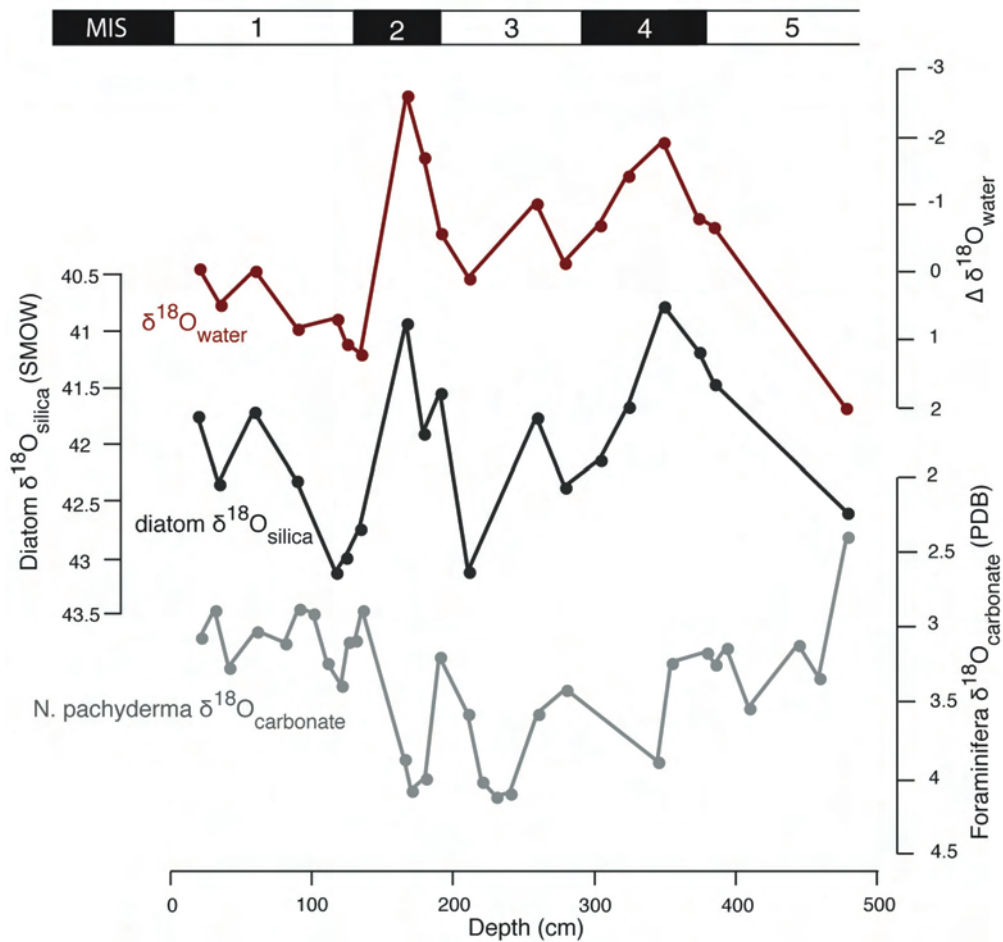


**Figure 4.3** Calculated $\Delta\delta^{18}O_{water}$ (red), diatom $\delta^{18}O_{silica}$ (black), and *N. pachyderma* $\delta^{18}O_{carbonate}$ (grey) (Charles et al., 1991). $\Delta\delta^{18}O_{water}$ was calculated from diatom $\delta^{18}O_{silica}$ and interpolated *N. pachyderma* $\delta^{18}O_{carbonate}$ using the following equation (Shemesh et al., 1992): $\Delta\delta^{18}O_{water} = 0.89 (\delta^{18}O_{silica2} - \delta^{18}O_{silica2}) - 1.9 (\delta^{18}O_{carbonate2} - \delta^{18}O_{carbonate1})$, where the subscript 1 and 2 refer to the lower and upper data point of the interval respectively.

The strong decoupling observed for the diatom $\delta^{18}O_{silica}$ signal and the $\delta^{18}O$ of *N. pachyderma* during the LGM (and to a lesser extent during MIS4) strongly suggests the presence of a shallow mixed layer and indeed an overestimation of the surface water salinity. The depleted $\delta^{18}O$ values can be explained by a regional concentration of icebergs, melting of snow accumulated on sea ice, or by a decrease in surface salinity through ocean/atmosphere freshwater exchange. In addition, surface-water stratification of the glacial Southern Ocean (Francois et al., 1997) may have favored the freshening of surface waters by increasing the residence time of the Antarctic mixed layer (Robinson and Sigman, 2008). The transition from well-mixed interglacial to stratified glacial conditions is consistent with the observed increase of $\delta^{18}O_{silica}$ and $\delta^{18}O_{water}$ from MIS5 to MIS4. If we assume that winter mixing was nearly eliminated in the Antarctic Zone (AZ) during the ice age (Robinson and Sigman, 2008), the subsequent increase in the $\delta^{18}O$ signals might result from lateral mixing with glacial Southern Ocean saline water (Adkins et al., 2002) upwelled further north (likely near the Antarctic Polar Front; APF (Robinson and Sigman, 2008)). The additional - intense - freshening of surface waters during the LGM must however be the result of heavy meltwater discharge.

In order to reconcile the $\delta^{18}O$ and $(Zn/Si)_{opal}$ records we invoke a scenario by which a high regional concentration of icebergs during the LGM may have lead to the entry of significant quantities of freshwater and trace metals (accumulated during several years in the snow) into surface waters during the growth season of the phytoplankton (*i.e.* summer). This would result in a high seasonal and spatial concentration of Zn in the surface waters. The concomitant delivery of Zn (and other trace metals) and freshwater would yield high ratios of $Zn^{2+}$ to Zn-binding ligands ratios and consequently increased Zn bioavailability as reflected by the $(Zn/Si)_{opal}$ ratios in the diatoms. During MIS4, the increased Zn bioavailability and increased freshwater supply may not have been coupled. Rather, due to stratification, a gradual freshening of surface waters may have occurred in the presence of aeolian Zn deposition. Such a scenario would contrast with the punctual massive addition of freshwater and Zn that was observed during the LGM. The resulting stable Zn availability to the diatoms would be consistent with the small variability of the $(Zn/Si)_{opal}$ ratios that were observed during MIS4 in spite of higher $\delta^{18}O_{silica}$ and dust fluxes. Records of Ice Rafted Detritus (IRD) do not show higher

concentrations during the LGM than during MIS 4 (Burckle and Cooke, 1983). However recent data suggest that in the Atlantic sector of the Southern Ocean, glacial-aged IRD were mainly composed of volcanic ashes delivered by sea ice and would consequently not reflect regional concentrations of icebergs calved from the Antarctic ice shelves (Nielsen et al., 2007).

The potential influence of these high micronutrient concentrations on productivity and C-export to the deep sea during the LGM can be addressed through the use of additional indicators. The $^{15}N/^{14}N$ ratio of diatom-bound organic matter (Robinson and Sigman, 2008), a proxy for relative nitrate utilization (Shemesh et al., 1993) shows higher $\delta^{15}N$ during the LGM than during the Holocene with lower values earlier in the glacial (MIS 3) and an increase of $\delta^{15}N$ in the late Holocene. The period of high $(Zn/Si)_{opal}$ corresponds to intense nitrate drawdown. These observations are consistent with a mechanism by which the input of meltwater -and its associated micronutrients- would have favored algal growth. In addition to improve light conditions by reducing the depth of the mixed layer, melting snow would have released bioavailable Zn and other trace metals and indeed likely relieved Fe-limitation.

The opal accumulation rate (Charles et al., 1991) and $^{231}Pa/^{230}Th$ ratios in sediments at this site (Kumar et al., 1993) indicate that export production during ice ages has been lower than during interglacials. Because Fe-fertilization decreases the silicate-to-nitrate uptake ratio in diatoms (Hutchins and Bruland, 1998; Takeda, 1998), carbon export could have been increased in spite of lower opal and particle fluxes. Consistently, concomitant minima in $\delta^{30}Si$ (pointing toward lower $Si(OH)_4$ utilization by diatom) and maxima in $\delta^{15}N_{bulk}$ observed during the LGM have been interpreted to indicate changes in $Si(OH)_4 : NO_3^-$ uptake ratios due to Fe addition (Brzezinski et al., 2002). Fe-fertilization is not thought to greatly affect $(Zn/Si)_{opal}$ since it has been shown to decrease both Si and Zn uptake (Sunda and Huntsman, 2000; Cullen et al., 2003). By examining down-core variations in *Chaetoceros* resting spores, Abelmann et al. (2006), found evidence for extensive blooms and near nutrient exhaustion across the entire Atlantic sector of the AZ. An increased presence of the deep living radiolarian *C. davisiana* in glacial sediments indicated that extensive nutrient drawdown was accompanied by higher carbon export. Because these changes were particularly observed in the seasonal ice zone (SIZ), the authors concluded that Fe released from sea-ice was probably the main

driver of these events. In addition, they interpreted the lower glacial opal fluxes in the Antarctic zone (and higher fluxes in the Subantarctic) to reflect a northward shift in the high opal-low carbon ecosystem associated with *F. kerguelensis*. Based on their study, opal flux would not be a reliable indicator of organic carbon flux.

In RC13-259, the abundance of *C. davisiana* (Shemesh et al., 1994) during MIS 2 strongly suggests a nitrate drawdown that is accompanied by an increased carbon export to the deep sea. Our data agree well with the hypothesis of Abelmann and co-workers (2006), except that for the RC13-259 site, we show strong evidence for meltwater input, and not melting sea-ice as being the main driver of extensive phytoplankton blooms leading to intense nitrate drawdown and increased carbon export. Since, RC13-259 resides in the glacial SIZ (Robinson and Sigman, 2008) - as derived from diatom analyses on the near-cores PS1768 and PS1772 (Frank et al., 2000) - , the release of bioavailable micronutrients from sea ice should indeed result in a correlation between $(Zn/Si)_{opal}$ and the dust flux over the entire glacial and not only during the LGM, as was observed.

## 4.4 Implications

Further work covering a larger area is crucial in order to elucidate whether these local observations correspond to a more general feature of the glacial Southern Ocean. If so, meltwaters and free drifting icebergs may have played a significant role in the pelagic ecosystem of the Southern Ocean during ice ages, with major implications for atmospheric $CO_2$ content. These data may further add to the ongoing debate dealing with the ocean's responses to the increasing discharge of icebergs to the Southern Ocean and associated productivity changes linked to global warming.

## 4.5 References

Abelmann A., Gersonde R., Cortese G., Kuhn G., and Smetacek V. (2006) Extensive phytoplankton blooms in the Atlantic sector of the glacial Southern Ocean. *Paleoceanography* **21**, PA1013, doi:10.1029/2005PA001199.

Adkins J. F., McIntyre K., and Schrag D. P. (2002) The salinity, temperature, and delta $^{18}$O of the glacial deep ocean. *Science* **298**(5599), 1769-1773.

Anderson M. A., Morel F. M. M., and Guillard R. R. L. (1978) Growth limitation of a coastal diatom by low zinc ion activity. *Nature* **276**, 70-71.

Basile I., Grousset F. E., Revel M., Petit J. R., Biscaye P. E., and Barkov N. I. (1997) Patagonian origin of glacial dust deposited in East Antarctica (Vostok and Dome C) during glacial stages 2,4 and 6. *Earth Planet. Sci. Lett.* **146**, 573-589.

Blain S., Queguiner B., Armand L., Belviso S., Bombled B., Bopp L., Bowie A., Brunet C., Brussaard C., Carlotti F., Christaki U., Corbiere A., Durand I., Ebersbach F., Fuda J.-L., Garcia N., Gerringa L., Griffiths B., Guigue C., Guillerm C., Jacquet S., Jeandel C., Laan P., Lefevre D., Lo Monaco C., Malits A., Mosseri J., Obernosterer I., Park Y.-H., Picheral M., Pondaven P., Remenyi T., Sandroni V., Sarthou G., Savoye N., Scouarnec L., Souhaut M., Thuiller D., Timmermans K., Trull T., Uitz J., van Beek P., Veldhuis M., Vincent D., Viollier E., Vong L., and Wagener T. (2007) Effect of natural iron fertilization on carbon sequestration in the Southern Ocean. *Nature* **446**(7139), 1070-1074.

Boyd P. W., Jickells T., Law C. S., Blain S., Boyle E. A., Buesseler K. O., Coale K. H., Cullen J. J., de Baar H. J. W., Follows M., Harvey M., Lancelot C., Levasseur M., Owens N. P. J., Pollard R., Rivkin R. B., Sarmiento J., Schoemann V., Smetacek V., Takeda S., Tsuda A., Turner S., and Watson A. J. (2007) Mesoscale iron enrichment experiments 1993-2005: synthesis and future directions. *Science* **315**(5812), 612-617.

Bruland K. W. (1989) Complexation of zinc by natural organic ligand in the Central North Pacific. *Limnol. Oceanogr.* **34**, 269-285.

Brzezinski M. A., Pride C. J., Franck V. M., Sigman D. M., Sarmiento J. L., Matsumoto K., Gruber N., Rau G. H., and Coale K. H. (2002) A switch from $Si(OH)_4$ to $NO_3$

depletion in the glacial Southern Ocean. *Geophys. Res. Lett.* **29**(12), 1564, doi:10.1029/2001GL014349.

Burckle L. H. and Cooke D. W. (1983) Late pleistocene *Eucampia antarctica* abundance stratigraphy in the Atlantic sector of the Southern Ocean. *Micropaleontology* **29**(1), 6-10.

Charles C. D., Froelich P. N., Zibello M. A., Mortlock R. A., and Morley J. J. (1991) Biogenic opal in Southern Ocean sediments over the last 450,000 years: Implications for surface water chemistry and circulation. *Paleoceanography* **6**, 697-728.

Cullen J. T., Chase Z., Coale K. H., Fitzwater S. E., and Sherrell R. M. (2003) Effect of iron limitation on the cadmium to phosphorus ratio of natural phytoplankton assemblages from the Southern Ocean. *Limnol. Oceanogr.* **48**(3), 1079-1087.

Dierssen H. M., Smith R. C., and Vernet M. (2002) Glacial meltwater dynamics in coastal waters west of the Antarctic peninsula. *Proc. Natl Acad. Sci. USA* **99**(4), 1790-1795.

Ellwood M. J. (2004) Zinc and cadmium speciation in subantarctic waters east of New Zealand. *Mar. Chem.* **87**, 37-58.

Ellwood M. J. and Hunter K. A. (1999) Determination of the Zn/Si ratio in diatom opal: a method for the separation, cleaning and dissolution of diatoms. *Mar. Chem.* **66**(3-4), 149-160.

Ellwood M. J. and Hunter k. A. (2000a) The incorporation of zinc and iron into the frustule of the marine diatom *Thalassiosira pseudonana*. *Limnol. Oceanogr.* **45**(7), 1517-1524.

Ellwood M. J. and Hunter K. A. (2000b) Variations in the Zn/Si record over the last interglacial glacial transition. *Paleoceanography* **15**(5), 506-514.

Ellwood M. J. and Van den Berg C. M. G. (2000) Zinc speciation in the Northeastern Atlantic Ocean. *Mar. Chem.* **68**(4), 295-306.

EPICA. (2006) One-to-one coupling of glacial climate variability in Greenland and Antarctica. *Nature* **444**(7116), 195-198.

Francois R., Altabet M. A., Yu E.-F., Sigman D. M., Bacon M. P., Frank M., Bohrmann G., Bareille G., and Labeyrie L. D. (1997) Contribution of Southern Ocean

surface-water stratification to low atmospheric $CO_2$ concentrations during the last glacial period. *Nature* **389**(6654), 929-935.

Frank M., Gersonde R., Rutgers van der Loeff M., Bohrmann G., Nürnberg C. C., Kubik P. W., Suter M., and Mangini A. (2000) Similar glacial and interglacial export bioproductivity in the Atlantic sector of the Southern Ocean: Multiproxy evidence and implications for glacial atmospheric $CO_2$. *Paleoceanography* **15**(6), 642-658.

Hendry K. R. and Rickaby R. E. M. (2008) Opal (Zn/Si) ratios as a nearshore geochemical proxy in coastal Antarctica. *Paleoceanography* **23**(PA2218), , doi:10.1029/2007PA001576.

Hudson R. J. M. and Morel F. M. M. (1990) Iron transport in marine phytoplankton: Kinetics of cellular and medium coordination reactions. *Limnol. Oceanogr.* **35**, 1002-1020.

Hutchins D. A. and Bruland K. W. (1998) Iron-limited diatom growth and Si:N uptake ratios in a coastal upwelling regime. *Nature* **393**(6685), 561-564.

Jaccard T., Ariztegui D., and Wilkinson K. J. (in review) Incorporation of zinc into the frustule of the freshwater diatom *Stephanodiscus hantzschii*. *Chem. Geol.*

Jaccard T., Ariztegui D., and Wilkinson K. J. (submitted) Incorporation of zinc into the frustule of the freshwater diatom *Stephanodiscus hantzschii*. *Biogeochemistry*.

Knox F. and McElroy M. B. (1984) Changes in atmospheric CO2: Influence of the marine biota at high latitude. *J. Geophys. Res.* **89**, 4629-4637.

Kohfeld K. E., Fairbanks R. G., Smith S. L., and Walsh I. D. (1996) *Neogloboquadrina pachyderma (sinistral coiling)* as paleoceanographic tracers in polar oceans: Evidence from Northeast Water Polynya plankton tows, sediment traps, and surface sediments. *Paleoceanography* **11**(6), 679-699.

Kumar N., Gwiazda R., Anderson R. F., and Froelich P. N. (1993) [231]Pa/[230]Th ratios in sediments as a proxy for past changes in southern ocean productivity. *Nature* **362**, 45-48.

Labeyrie L. D., Pichon J. J., Labracherie M., Ippolito P., Duprat J., and Duplessy J. C. (1986) Melting history of Antarctica during the past 60,000 years. *Nature* **322**(6081), 701-706.

Latimer J. C. and Filippelli G. M. (2001) Terrigenous input and paleoproductivity in the Southern Ocean. *Paleoceanography* **16**(6), 627-643.

Martin J. H. (1990) Glacial-Interglacial $CO_2$ change: The iron hypothesis. *Paleoceanography* **5**(1), 1-13.

Martinson D. G., Pisias N. G., Hays J. D., Imbrie J., Moore T. C., and Shackleton N. J. (1987) Age dating and the orbital theory of the ice ages: Development of a high-resolution 0 to 300,000-year chronostratigraphy. *Quat. Res.* **27**(1), 1-29.

Nielsen S. H. H., Hodell D. A., Kamenov G., Guilderson T., and Perfit M. R. (2007) Origin and significance of ice-rafted detritus in the Atlantic sector of the Southern Ocean. *Geochem. Geophys. Geosyst.* **8**, Q12005, doi:10.1029/2007GC001618.

Orsi A. H., Whitworth T., and Nowlin W. D. (1995) On the meridional extent and fronts of the Antarctic Circumpolar Current *Deep Sea Res.* **42**(5), 641-673.

Petit J. R., Jouzel J., Raynaud D., Barkov N. I., Barnola J.-M., Basile I., Bender M., Chappellaz J., Davis M., Delaygue G., Delmotte M., Kotlyakov V. M., Legrand M., Lipenkov V. Y., Lorius C., PEpin L., Ritz C., Saltzman E., and Stievenard M. (1999) Climate and atmospheric history of the past 420,000 years from the Vostok ice core, Antarctica. *Nature* **399**(6735), 429-436.

Robinson R. S. and Sigman D. M. (2008) Nitrogen isotopic evidence for a poleward decrease in surface nitrate within the ice age Antarctic. *Quat. Sci. Rev.* **27**(9-10), 1076-1090.

Sarmiento J. L. and Toggweiler J. R. (1984) A new model for the role of the oceans in determining atmospheric $pCO_2$. *Nature* **308**(5960), 621-624.

Shemesh A., Charles C. D., and Fairbanks R. G. (1992) Oxygen isotopes in biogenic silica: global changes in ocean temperature and isotopic composition. *Science* **256**, 1434-1436.

Shemesh A., Burckle L. H., and Hays J. D. (1994) Meltwater input to the Southern Ocean during the Last Glacial Maximum. *Science* **266**(5190), 1542-1544.

Shemesh A., Macko S. A., Charles C. D., and Rau G. H. (1993) Isotopic evidence for reduced productivity in the glacial Southern Ocean. *Science* **262**(5132), 407-410.

Siegenthaler U. and Wenk T. (1984) Rapid atmospheric CO2 variations and ocean circulation. *Nature* **308**(5960), 624-626.

Smith K. L., Jr., Robison B. H., Helly J. J., Kaufmann R. S., Ruhl H. A., Shaw T. J., Twining B. S., and Vernet M. (2007) Free-drifting icebergs: hot spots of chemical and biological enrichment in the Weddell Sea. *Science* **317**(5837), 478-482.

Sunda W. G. and Guillard R. R. L. (1976) The relationship between cupric ion activity and the toxicity of copper to phytoplankton. *J. Mar. Res.* **34**, 511-529.

Sunda W. G. and Huntsman S. A. (2000) Effect of Zn, Mn, and Fe on Cd accumulation in phytoplankton: implications for oceanic Cd cycling. *Limnol. Oceanogr.* **45**, 1501-1516.

Takeda S. (1998) Influence of iron availability on nutrient consumption ratio of diatoms in oceanic waters. *Nature* **393**(6687), 774-777.

Xue H. B., Kistler D., and Sigg L. (1995) Competition of copper and zinc for strong ligands in a eutrophic lake. *Limnol. Oceanogr.* **40**(6), 1142-1152.

# Conclusions and outlook

In this work, we evaluated the possibility of using the Zn content of fossil frustules to reconstruct past changes in Zn bioavailable concentrations of surface waters.

Processes behind Zn incorporation into the frustules were evaluated from Zn uptake experiments with the freshwater diatom *Stephanodiscus hantzschii*. Zn concentrations in the frustule were related to the $Zn^{2+}$ concentrations in the growth medium and positively correlated with intracellular concentrations. The data were interpreted to indicate that the presence of Zn in the frustule might reflect encapsulation of a Zn-bearing macromolecule in the silica during frustule formation.

The use of these results to interpret data of fossil frustules isolated from a sedimentary core retrieved from Lake Geneva led to a reliable reconstruction of modern bioavailable Zn concentrations of surface waters. The downcore results indicated that the heavy anthropogenic input of Zn during the sixties and the seventies led to an increase in Zn uptake by phytoplankton. The extrapolated concentrations were nonetheless likely not high enough to have induced adverse effects on the pelagic community.

The same methodology was applied to marine sediments in order to reconstruct past changes in Zn delivery and availability to phytoplankton of the Southern Ocean during the last ice age. The data evidence for the first time a greater availability of micronutrients to phytoplankton during the Last Glacial Maximum (LGM). These changes were consistent with a mechanism by which, during LGM, massive meltwater discharges - resulting from melting icebergs - supplied Zn to surface waters. Additional data indicated that these meltwater events stimulated biological productivity and could consequently contribute to the sequestration of $CO_2$ during ice ages.

According to this study, the zinc content of the frustules of fossil diatoms is likely to be a valuable proxy to reconstruct past concentrations of bioavailable Zn in surface waters. Such a tool would be particularly relevant for assessing the impact of past events of anthropogenic loading of Zn to biological communities and for studying the processes that controlled Zn limitation and delivery in oceanic waters on glacial-interglacial timescales.

Finally, this investigation raises the question of generalizing the conclusion obtained for Zn to other trace metals. In other words, can the presence of other trace metals in the frustule also be indicative of their bioavailable concentration? Although this hypothesis remains to be tested, our data suggest that the presence of Zn in the frustules is likely to reflect an active role for this metal in frustule formation and that consequently the result obtained here cannot be generalized to other metals.

# Appendix1_culture medium

## Modified CHU-10 medium

### Stock solutions

| | | | | | |
|---|---|---|---|---|---|
| $Na_2SiO_3 \cdot 5H_2O$ | 4.4 $gL^{-1}$ | Trace metal mix: | $Na_2EDTA$ | 1 $gL^{-1}$ |
| $Ca(NO_3)_2 \cdot 4H_2O$ | 57.56 $gL^{-1}$ | | $H_3BO_3$ | 2.86 $gL^{-1}$ |
| $K_2HPO_4$ | 10 $gL^{-1}$ | | $MnCl_2 \cdot 4H_2O$ | 1.81 $gL^{-1}$ |
| $MgSO_4 \cdot 7H_2O$ | 25 $gL^{-1}$ | | $NaMoO_4 \cdot 5\,H_2O$ | 0.390 $gL^{-1}$ |
| $Na_2CO_3$ | 20 $gL^{-1}$ | | $CuSO_4 \cdot 5\,H_2O$ | 0.079 $gL^{-1}$ |
| | | | $Co(NO_3)_2 \cdot 6\,H_2O$ | 0.0494 $gL^{-1}$ |
| | | Fe solution: | $FeCl_3 \cdot 6\,H_2O$ | 3.15 $gL^{-1}$ |
| | | | $Na_2EDTA$ | 4.36 $gL^{-1}$ |
| | | F/2 vitamin mix: | $B_{12}$ | 1 $mgL^{-1}$ |
| | | | $B_1$ | 1 $mgL^{-1}$ |
| | | | Biotin | 200 $mgL^{-1}$ |

### For 1L of modified CHU-10 medium

| | |
|---|---|
| $Na_2SiO_3 \cdot 5H_2O$ | 10 mL |
| $Ca(NO_3)_2 \cdot 4H_2O$ | 1 mL |
| $K_2HPO_4$ | 1 mL |
| $MgSO_4 \cdot 7H_2O$ | 1mL |
| $Na_2CO_3$ | 1mL |
| Trace metal mix | 1 mL |
| Fe solution | 0.1 mL |
| F/2 vitamin mix | 1mL |

| | |
|---|---|
| $ZnSO_4 \cdot 7\,H_2O$ | concentrations varied between 77 and 0.077 $\mu mol\ L^{-1}$ |
| $Na_2EDTA$ | concentrations varied between 89 and 12.4 $\mu mol\ L^{-1}$ |

Completed to 1 L and pH adjusted to 6.4

# CHAPTER 2

**Growth rate (see Figure 2.1)**

*Zn uptake experiment*

| pZn$^{2+}$ | specific growth rate (d$^{-1}$) | 95% CI |
|---|---|---|
| 10.62 | 0.580 | 0.032 |
| 9.94 | 0.496 | 0.083 |
| 9.62 | 0.543 | 0.047 |
| 9.34 | 0.635 | 0.119 |
| 9.23 | 0.492 | 0.054 |
| 8.93 | 0.470 | 0.137 |
| 8.62 | 0.523 | 0.107 |
| 8.36 | 0.563 | 0.092 |
| 7.62 | 0.244 | 0.043 |

*Role of Mn$^{2+}$ on Zn incorporation*

| pZn$^{2+}$ | specific growth rate (d$^{-1}$) | 95% CI |
|---|---|---|
| 9.23 | 0.557 | 0.023 |
| 8.93 | 0.394 | 0.062 |

*Role of Si on Zn incorporation*

| pZn$^{2+}$ | specific growth rate (d$^{-1}$) | 95% CI |
|---|---|---|
| 9.23 | 0.425 | 0.059 |
| 8.93 | 0.593 | 0.107 |

## Intracellular zinc concentrations (see Figure 2.2)

*Zn uptake experiment*

| pZn$^{2+}$ | Zn$_{cell}$(mol/cell) | 95% CI |
|---|---|---|
| 10.62 | 1.36E-17 | 4.5E-18 |
| 9.94 | 1.05E-17 | 2.3E-18 |
| 9.62 | 1.21E-17 | 2.9E-18 |
| 9.34 | 1.91E-17 | 6.7E-18 |
| 9.23 | 1.55E-17 | 2.9E-18 |
| 8.93 | 2.11E-17 | 6.1E-18 |
| 8.36 | 3.07E-17 | 9.6E-18 |

## Zinc in the frustule: Zn/Si and Zn$_{frust}$ (see Figures 2.3 and 2.7)

*Zn uptake experiment*

| pZn$^{2+}$ | Zn/Si (mol/mol) | 95% CI | Zn$_{frust}$ (mol/cell) | 95% CI |
|---|---|---|---|---|
| 10.62 | 1.24E-06 | 4.0E-07 | 2.6E-19 | 8E-20 |
| 9.94 | 8.6E-07 | 1.8E-07 | 1.8E-19 | 4E-20 |
| 9.62 | 4.31E-06 | 2.97E-06 | 9.0E-19 | 6.2E-19 |
| 9.34 | 4.84E-06 | 1.16E-06 | 1.02E-18 | 2.4E-19 |
| 9.23 | 2.369E-05 | 8.32E-06 | 4.97E-18 | 1.75E-18 |
| 8.93 | 4.647E-05 | 1.810E-05 | 9.76E-18 | 3.80E-18 |
| 8.62 | 5.730E-05 | 1.466E-05 | 1.203E-17 | 3.08E-18 |
| 8.36 | 2.982E-05 | 2.138E-05 | 6.26E-18 | 4.49E-18 |
| 7.62 | 4.513E-05 | 1.805E-05 | 9.48E-18 | 3.79E-18 |

## Role of Mn$^{2+}$ on Zn incorporation (see Figure 2.5)

*Intracellular Zn and Mn concentrations*

| pZn$^{2+}$ | pMn$^{2+}$ | Zn$_{cell}$ (mol/cell) | 95%CI | Mn$_{cell}$ (mol/cell) | 95%CI |
|---|---|---|---|---|---|
| 9.23 | 6.2 | 1.55E-17 | 2.9E-18 | 4.21E-16 | 8.2E-17 |
| 8.93 | 6.2 | 2.11E-17 | 6.1E-18 | 3.31E-16 | 5.6E-17 |
| 9.23 | 5.2 | 1.41E-17 | 8E-19 | 6.58E-16 | 4.9E-17 |
| 8.93 | 5.2 | 1.95E-17 | 4.4E-18 | 9.50E-16 | 2.01E-16 |

*Frustule Zn/Si and Mn/Si molar ratio*

| pZn$^{2+}$ | pMn$^{2+}$ | Zn/Si (mol/mol) | 95%CI | Mn/Si (mol/mol) | 95%CI |
|---|---|---|---|---|---|
| 9.23 | 6.2 | 2.369E-05 | 8.32E-06 | 1.34E-04 | 6.7E-05 |
| 8.93 | 6.2 | 4.647E-05 | 1.810E-05 | 1.46E-04 | 7.3E-05 |
| 9.23 | 5.2 | 6.77E-06 | 2.62E-06 | 4.41E-04 | 7.4E-05 |
| 8.93 | 5.2 | 1.293E-05 | 9.0E-07 | 4.12E-04 | 1.21E-04 |

## Role of Si on Zn incorporation (see Figure 2.6)

*Intracellular Zn and Mn concentrations*

| pZn$^{2+}$ | [Si(OH)$_4$] mmol/L | Zn$_{cell}$ (mol/cell) | 95%CI | Mn$_{cell}$ (mol/cell) | 95%CI |
|---|---|---|---|---|---|
| 9.23 | 0.21 | 1.55E-17 | 2.9E-18 | 4.21E-16 | 8.2E-17 |
| 8.93 | 0.21 | 2.11E-17 | 6.1E-18 | 3.31E-16 | 5.6E-17 |
| 9.23 | 2.10 | 1.97E-17 | 1.6E-18 | 1.047E-15 | 2.88E-16 |
| 8.93 | 2.10 | 5.53E-17 | 1.32E-17 | 1.056E-15 | 3.21E-16 |

*Frustule Zn/Si and Mn/Si molar ratio*

| pZn$^{2+}$ | [Si(OH)$_4$] mmol/L | Zn/Si (mol/mol) | 95%CI | Mn/Si (mol/mol) | 95%CI |
|---|---|---|---|---|---|
| 9.23 | 0.21 | 2.369E-05 | 8.32E-06 | 1.34E-04 | 6.7E-05 |
| 8.93 | 0.21 | 4.647E-05 | 1.810E-05 | 1.46E-04 | 7.3E-05 |
| 9.23 | 2.10 | 2.625E-05 | 6.46E-06 | 2.07E-04 | 6.8E-05 |
| 8.93 | 2.10 | 1.2578E-04 | 4.217E-05 | 1.14E-04 | 5.4E-05 |

# CHAPTER 3

**Analyses performed on the first half of the LeBC-3-06 core**

| Depth (cm) | magnetic susceptibility (SI x 10^5) | Min C (%) | TOC (%) | HI (mg HC / g TOC) | Si/Al (mol/mol) | $^{137}$Cs (Bq/kg) |
|---|---|---|---|---|---|---|
| 0.5 | 1.06 | 3.89 | 2.07 | 411 | 3.85 | 31.9 |
| 1.5 | 1.22 | 2.57 | 1.34 | 425 | 3.31 | 38.6 |
| 2.5 | 1.13 | 5.97 | 3.31 | 389 | 3.14 | 52.5 |
| 3.5 | 1.07 | 5.82 | 3.17 | 376 | 2.65 | 56.6 |
| 4.5 | 0.89 | 5.97 | 2.91 | 375 | 2.65 | 126.0 |
| 5.5 | 0.60 | 6.14 | 2.58 | 378 | 2.91 | 160.6 |
| 6.5 | 0.65 | 6.13 | 2.55 | 367 | 2.52 | 79.4 |
| 7.5 | 0.58 | 5.88 | 2.63 | 363 | 3.25 | 61.1 |
| 8.5 | 0.52 | 5.57 | 2.88 | 369 | 2.83 | 56.3 |
| 9.5 | 0.67 | 5.75 | 2.54 | 348 | 2.55 | 79.4 |
| 10.5 | 0.71 | 5.79 | 2.60 | 367 | 2.71 | 77.4 |
| 11.5 | 0.86 | 5.59 | 2.33 | 310 | 2.50 | 145.4 |
| 12.5 | 1.22 | 5.41 | 2.18 | 283 | 2.36 | 132.4 |
| 13.5 | 1.49 | 5.56 | 2.07 | 266 | 2.35 | 91.3 |
| 14.5 | 1.92 | 5.61 | 1.71 | 230 | 2.48 | 29.6 |
| 15.5 | 2.43 | 5.40 | 1.44 | 188 | 2.14 | 7.7 |
| 16.5 | 2.83 | 5.37 | 1.37 | 176 | 2.38 | 5.2 |
| 17.5 | 3.49 | 4.70 | 1.71 | 103 | 2.34 | 3.0 |
| 18.5 | 3.72 | 4.94 | 1.17 | 173 | 2.47 | 3.6 |
| 19.5 | 3.90 | 4.59 | 1.25 | 98 | 2.51 | |
| 20.5 | 4.02 | 4.90 | 0.89 | 111 | 2.75 | |
| 21.5 | 3.94 | 4.55 | 0.78 | 99 | 2.41 | |
| 22.5 | 3.79 | 4.70 | 0.90 | 110 | 2.25 | |
| 23.5 | 3.75 | 4.86 | 0.68 | 98 | 2.03 | |
| 24.5 | 3.71 | 4.90 | 0.75 | 105 | 2.05 | |
| 25.5 | 3.88 | 4.96 | 0.79 | 87 | 2.00 | |
| 26.5 | 4.07 | | | | | |
| 27.5 | 4.25 | 4.58 | 0.72 | 80 | 1.94 | |
| 28.5 | 4.80 | | | | | |
| 29.5 | 4.48 | 4.98 | 0.68 | 82 | 2.20 | |
| 30.5 | 4.06 | | | | | |
| 31.5 | 3.98 | 4.98 | 0.77 | 96 | 1.97 | |
| 32.5 | 4.02 | | | | | |
| 33.5 | 4.08 | 4.90 | 0.70 | 92 | 2.05 | |
| 34.5 | 4.30 | | | | | |
| 35.5 | 4.33 | 4.92 | 0.73 | 106 | 2.03 | |
| 36.5 | 4.17 | | | | | |
| 37.5 | 4.13 | 4.84 | 0.66 | 90 | 1.96 | |
| 38.5 | 4.15 | | | | | |
| 39.5 | 4.73 | 4.95 | 0.77 | 133 | 1.93 | |
| 40.5 | 4.03 | | | | | |
| 41.5 | 3.95 | 4.71 | 0.65 | 90 | 1.91 | |
| 42.5 | 3.87 | | | | | |
| 43.5 | 3.92 | 5.03 | 0.65 | 94 | 1.83 | |

# Analyses performed on the second half of the LeBC-3-06 core

| Depth (cm) | $Zn_{sed}$ (mg/kg) | $(Zn/Si)_{opal}$ (mol/mol) |
|---|---|---|
| 0.25 | 83.4 | 5.50E-06 |
| 0.75 | 80.8 | 7.19E-06 |
| 1.25 | 108.9 | 8.1E-07 |
| 1.75 | 111.0 | 3.56E-06 |
| 2.25 | 124.5 | 2.94E-06 |
| 2.75 | 109.2 | 2.27E-06 |
| 3.25 | 122.3 | 2.57E-06 |
| 3.75 | 125.6 | 1.21E-06 |
| 4.25 | 118.2 | 1.08E-06 |
| 4.75 | 111.1 | 2.47E-06 |
| 5.25 | 136.2 | 4.20E-06 |
| 5.75 | 136.4 | 1.55E-06 |
| 6.25 | 129.0 | 5.50E-06 |
| 6.75 | 129.8 | 5.30E-06 |
| 7.25 | 142.4 | |
| 7.75 | 154.1 | 5.16E-06 |
| 8.25 | 140.6 | |
| 8.75 | 149.4 | 5.12E-06 |
| 9.25 | 139.2 | |
| 9.75 | 131.5 | 7.09E-06 |
| 10.25 | 137.8 | |
| 10.75 | 134.2 | 4.63E-06 |
| 11.25 | 155.1 | |
| 11.75 | 141.9 | 9.80E-06 |
| 12.25 | 142.5 | |
| 12.75 | 134.7 | 3.89E-06 |
| 13.25 | 129.3 | |
| 13.75 | 127.5 | 1.87E-06 |
| 14.25 | 100.1 | |
| 14.75 | 94.8 | |
| 15.5 | 78.1 | 1.03E-06 |
| 16.5 | 86.4 | 6.507E-07 |
| 17.5 | 70.3 | |
| 18.5 | 58.8 | |
| 19.5 | 56.7 | |
| 20.5 | 53.1 | |
| 21.5 | 58.0 | |
| 22.5 | 59.6 | |
| 23.5 | 60.6 | |
| 24.5 | 60.7 | |
| 25.5 | 55.0 | |
| 27.5 | 61.9 | |
| 29.5 | 57.8 | |
| 31.5 | 64.5 | |
| 33.5 | 64.4 | |
| 35.5 | 50.3 | |
| 37.5 | 58.8 | |
| 39.5 | 53.1 | |
| 41.5 | 57.1 | |
| 43.5 | 58.0 | |

<em>Reliability test (samples 34 and 40; see section 3.3)</em>

| Depth (cm) | $(Zn/Si)_{opal}$ (mol/mol) | Mean | 95%CI |
|---|---|---|---|
| 36.5 | 1.33E-06 | | |
| 36.5 | 9.1E-07 | 1.13E-06 | 1.8E-07 |
| 36.5 | 1.08E-06 | | |
| 36.5 | 1.21E-06 | | |

# CHAPTER 4

## Core RC13-259

| Depth (cm) | $(Zn/Si)_{opal}$ (mol/mol) | $(Zn/Si)_{opal}$ (mol/mol) "full replicates"* | $(Zn/Si)_{opal}$ (mol/mol) "partial replicates"* |
|---|---|---|---|
| 10 | 1.852E-05 | | |
| 30 | 1.494E-05 | | 1.623E-05 1.366E-05 |
| 40 | 1.776E-05 | | 1.835E-05 1.717E-05 |
| 50 | 1.159E-05 | | |
| 70 | 1.535E-05 | | |
| 80 | 1.316E-05 | | |
| 90 | 1.111E-05 | | |
| 100 | 1.054E-05 | | |
| 110 | 9.13E-06 | | |
| 122 | 1.142E-05 | | |
| 130 | 1.404E-05 | 1.334E-05 1.474E-05 | |
| 141 | 1.578E-05 | | |
| 152 | 3.436E-05 | | 3.420E-05 3.452E-05 |
| 161 | 1.208E-05 | | |
| 170 | 2.137E-05 | | |
| 180 | 2.399E-05 | | |
| 190 | 1.630E-05 | | |
| 200 | 2.074E-05 | | |
| 210 | 1.382E-05 | | |
| 220 | 1.218E-05 | 1.240E-05 1.196E-05 | |
| 230 | 1.627E-05 | | |
| 240 | 1.644E-05 | | 1.590E-05 1.698E-05 |

| | | |
|---|---|---|
| 261 | 8.77E-06 | |
| 281 | 8.23E-06 | |
| 301 | 9.49E-06 | |
| 310 | 1.043E-05 | 1.102E-05 |
| | | 9.84E-06 |
| 321 | 1.041E-05 | 8.40E-06 |
| | | 1.243E-05 |
| 341 | 1.118E-05 | 1.109E-05 |
| | | 1.126E-05 |
| 350 | 6.28E-06 | |
| 370 | 9.27E-06 | 9.31E-06 |
| | | 9.22E-06 |
| 380 | 6.68E-06 | 6.77E-06 |
| | | 6.58E-06 |
| 390 | 8.81E-06 | 9.53E-06 |
| | | 8.10E-06 |
| 410 | 7.61E-06 | |
| 422 | 5.69E-06 | |
| 431 | 6.60E-06 | |
| 440 | 6.13E-06 | |
| 451 | 7.99E-06 | |
| 463 | 7.08E-06 | |
| 470 | 9.49E-06 | |
| 480 | 8.77E-06 | |

- see section 4.2 fore more informations about the replication procedure.
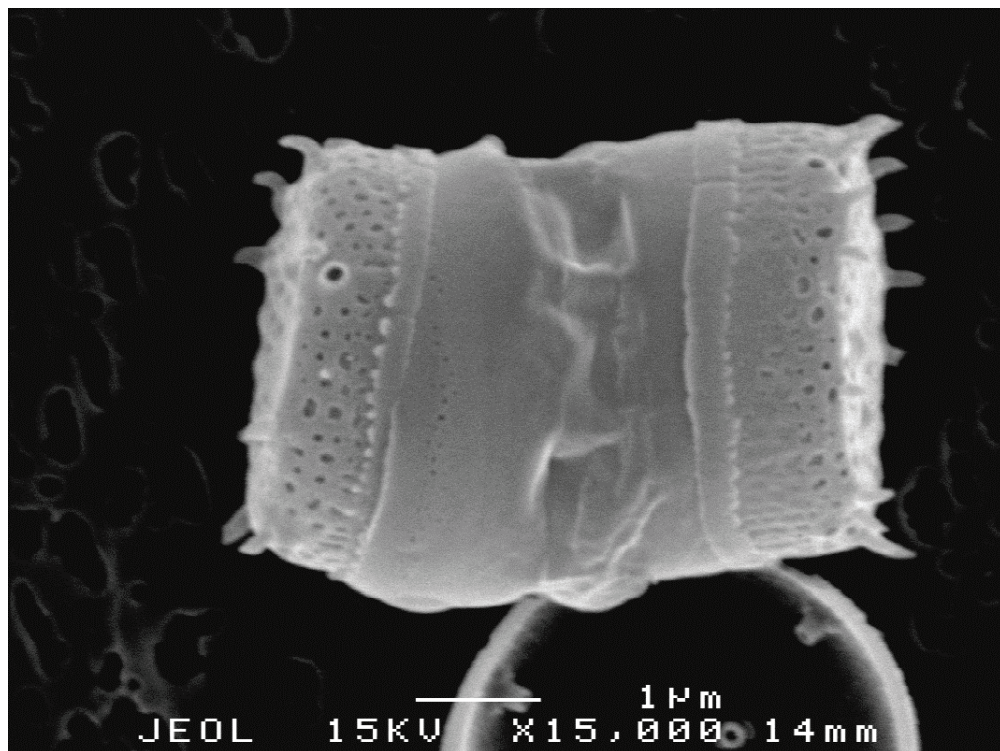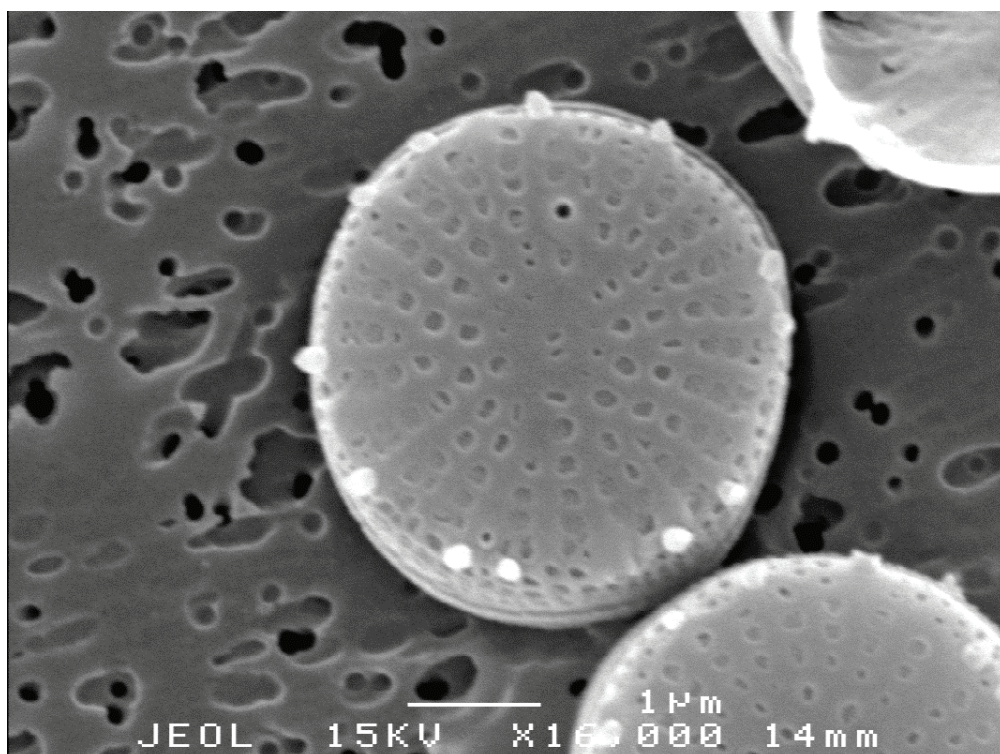
**Plate 1** SEM microphotographs of the diatom *Stephanodiscus hantzschii* used for the Zn uptake experiments discribed in Chapter 2.
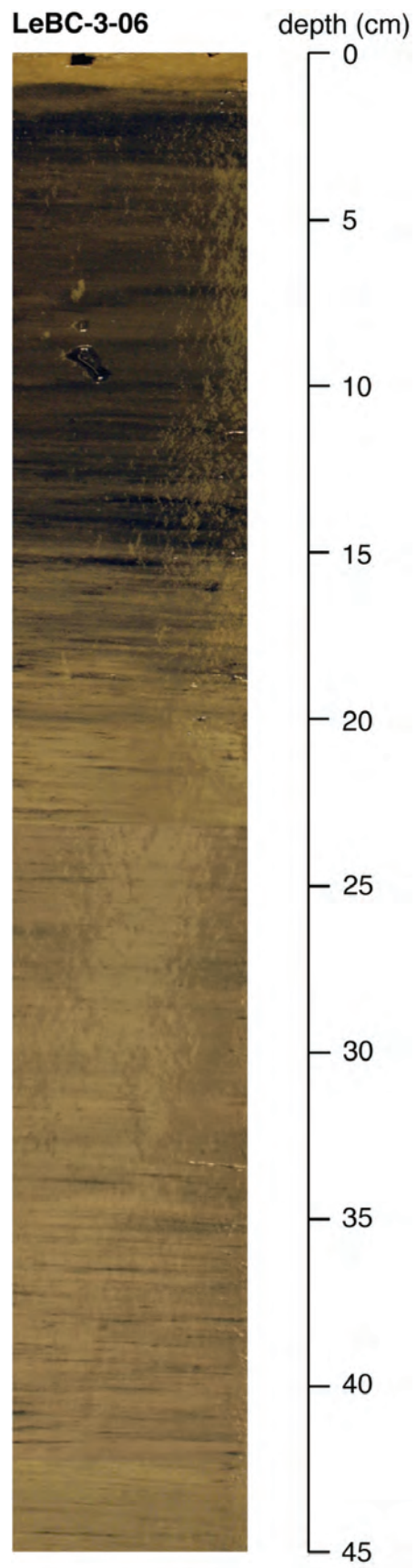
**Plate 2** Photography of Lake Geneva core LeBC-3-06 used in Chapter 3.
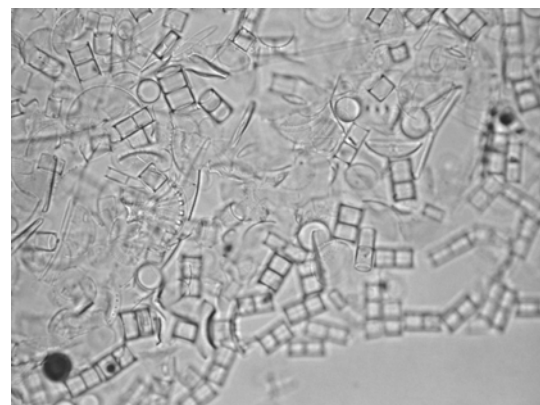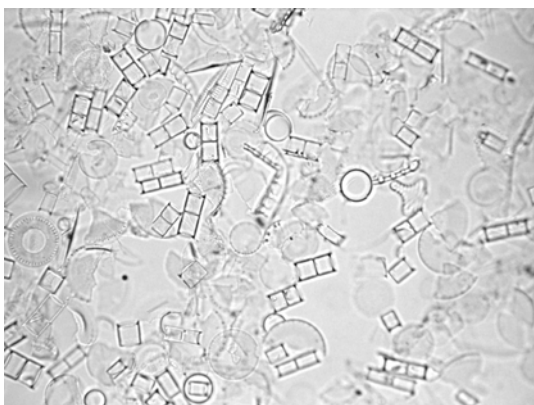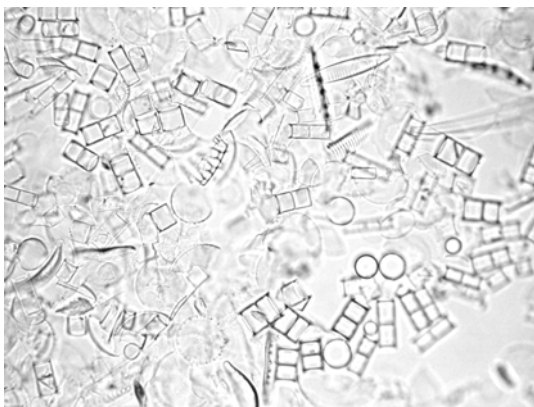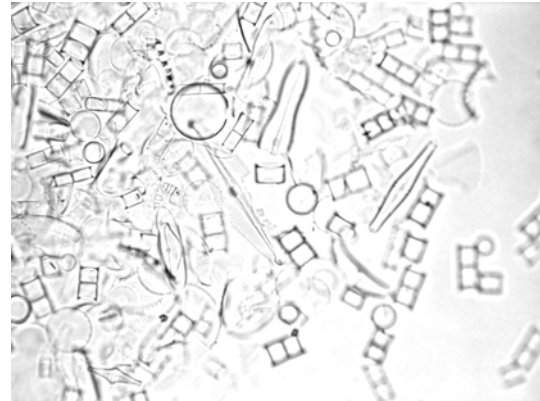
——— 50 µm

**Plate 3** Microscopic photographs under natural light of the extracted fossil diatoms from Lake Geneva used in Chapter 3.
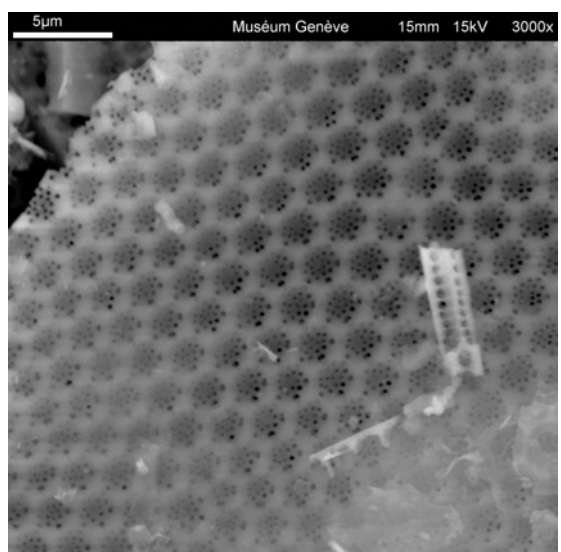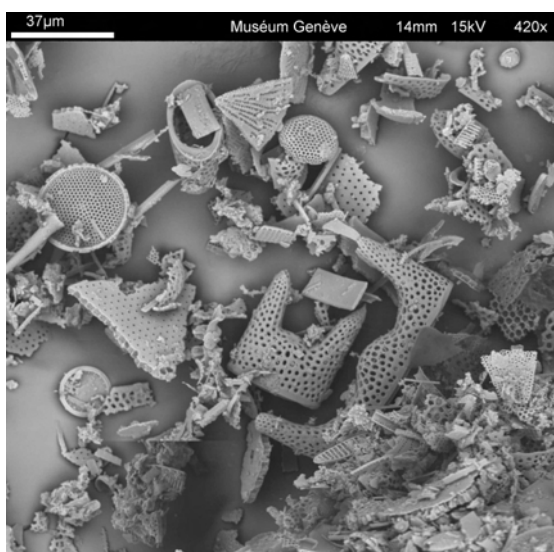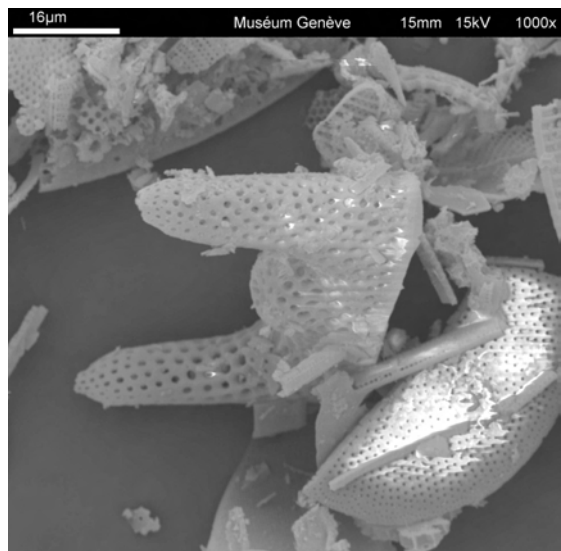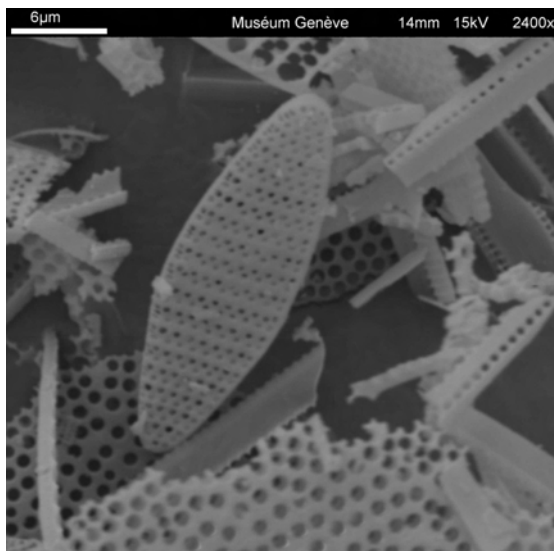
**Plate 4** SEM microphotographs of the extracted fossil diatoms from the South Atlantic samples used in Chapter 4.

# Remerciements/Acknowledgements